Dissertation

Cellular and molecular mechanisms of non-coding RNAs in gastrointestinal malignancies

submitted by

Felix PRINZ, BSc MSc

for the Academic Degree of

Doctor of Philosophy (PhD)

at the

Medical University of Graz

Department of Internal Medicine, Division of Oncology

under the supervision of

Assoc. Prof. Dr. Martin PICHLER

2024

Statutory Declaration

I, Felix Prinz, hereby declare that this dissertation titled “Cellular and molecular mechanisms of non-coding RNAs in gastrointestinal malignancies” is my own original work.

I have fully acknowledged by name all individuals and organizations that have contributed to the research presented in this dissertation. All sources of information and material used in the preparation of this dissertation have been acknowledged in the text.

Throughout this dissertation and in all associated publications, I have followed the “Standards of Good Scientific Practice and Ombuds Committee at the Medical University of Graz”.

During the writing and revision process, ChatGPT (GPT-4, OpenAI, content generated between 01.08.24 – 27.09.24, https://chatgpt.com) was used exclusively for grammatical and semantic improvements. This usage adhered strictly to the guidelines outlined in the “Orientierungshilfe zur Verwendung von KI-Systemen für die Erstellung von schriftlichen Abschlussarbeiten an der Medizinischen Universität Graz“, published by Kirnbauer B., Bornemann-Cimenti H., and Rehatschek H. on 08.05.2024.

e.h. Felix Prinz
Graz, 27.09.2024

Disclosures

Parts of this dissertation have been published in the following two manuscripts:

- Prinz Felix[1,2], Jonas Katharina[1,2], Balihodzic Amar[1,2], Klec Christiane[1,2], Reicher Andreas[1,2], Barth Dominik A[1], Riedl Jakob[1], Gerger Armin[1], Kiesslich Tobias[3,4], Mayr Christian[3,4], Rinner Beate[5], Kargl Julia[6], Pichler Martin[1,2,7]. **MicroRNA mimics can distort physiological microRNA effects on immune checkpoints by triggering an antiviral interferon response.** RNA Biol. 2022 Jan;19(1):1305-1315. doi: 10.1080/15476286.2022.2152978. PMID: 36469564; PMCID: PMC9728468. (1)

- Posch Florian[1], Prinz Felix[1,2], Balihodzic Amar[1,2], Mayr Christian[3,4], Kiesslich Tobias[3,4], Klec Christiane[1,2], Jonas Katharina[1,2], Barth Dominik A[1,2,7], Riedl Jakob M[1], Gerger Armin[1], Pichler Martin[1,2,7]. **MiR-200c-3p Modulates Cisplatin Resistance in Biliary Tract Cancer by ZEB1-Independent Mechanisms.** Cancers (Basel). 2021 Aug 8;13(16):3996. doi: 10.3390/cancers13163996. PMID: 34439151; PMCID: PMC8392278. (2)

Additionally, this dissertation contains data, which are part of an ongoing project and will likely be included in the following unpublished manuscript (in preparation):

- Prinz Felix[1,2], Jonas Katharina[1,2], Kiesslich Tobias[3,4], Mayr Christian[3,4], Pichler Martin[1,2,7,8], Noeparast Maxim[8]. **Cisplatin modulates immune checkpoint expression through the activation of innate immunity.** *(in preparation; variations in author list and title might occur)*

[1] Division of Oncology, Department of Internal Medicine, Medical University of Graz, Graz, Austria

[2] Research Unit for Non-Coding RNA and Genome Editing, Medical University of Graz, Graz, Austria

[3] Center for Physiology, Pathophysiology and Biophysics, Institute for Physiology and Pathophysiology Salzburg, Paracelsus Medical University, Salzburg, Austria

[4] Department of Internal Medicine I, University Hospital Salzburg, Paracelsus Medical University, Salzburg, Austria

[5] Division of Biomedical Research, Medical University of Graz, Graz, Austria

[6] Division of Pharmacology, Otto Loewi Research Center, Medical University of Graz, Graz, Austria

[7] Department of Experimental Therapeutics, The University of Texas MD Anderson Cancer Center, Houston, TX, USA

[8] Translational Oncology, II. Med Clinics University of Augsburg, Augsburg, Germany

All coauthors have agreed to the use of their data in this dissertation.

Acknowledgements

I am grateful for the financial support from the Austrian Science Fund (FWF; DK-MCD W1226 to Martin Pichler) and the Medical University of Graz through the PhD program “Metabolic and Cardiovascular Diseases (DK-MCD)”.

I would like to sincerely thank my supervisor and mentor, Assoc. Prof. Dr. Martin Pichler, for finding a perfect balance between guidance and independence. Your support during challenging times and your trust in my ability to pursue my own ideas and hypotheses have been invaluable to my development as an independent researcher. Despite your demanding role as oncologist, you were always accessible and open to scientific discussions, which I found truly impressive. I value the positive and almost friendship-like relationship we have built over these years.

I am also thankful to my thesis committee members, Assoc. Prof. Dr. Beate Rinner and Assoc. Prof. Dr. Julia Kargl, for their critical and insightful evaluations of my work. Your constructive feedback provided new perspectives and was essential to advancing my research projects.

Finally, I would like to thank all the current and former lab members and colleagues who have been part of my PhD journey. I am grateful for our enriching scientific and non-scientific discussions, the unwavering support, our shared achievements and frustrations, and the collective drive to progress.

Table of Contents

Abbreviations

AGO	Argonaute protein
AGO2	Argonaute RISC Catalytic Component 2
AHR	Aryl Hydrocarbon Receptor
APC	antigen-presenting cell
ARIH1	Ariadne RBR E3 Ubiquitin-protein Ligase 1
B7H2	B7 Homolog 2
B7H3	B7 Homolog 3
BAP1	BRCA1-associated protein 1
Bcl-2	B-Cell CLL/Lymphoma 2
BIN1	Bridging Integrator-1
BMP	Bone Morphogenetic Protein
BSA	bovine serum albumin
BTC	biliary tract cancer
CD28	Cluster of Differentiation 28
CD47	Cluster of Differentiation 47
CD80	Cluster of Differentiation 80
CD86	Cluster of Differentiation 86
CDC25A	Cell Division Cycle 25A
CDH1	E-Cadherin
cDNA	complementary DNA
CEACAM1	Carcinoembryonic Antigen-Related Cell Adhesion Molecule 1
cGAS	Cyclic GMP-AMP Synthase
c-Myc	MYC proto-oncogene
CTLA-4	Cytotoxic T-Lymphocyte Associated Protein 4
DAMP	damage-associated molecular pattern
DAPI	4',6-Diamidino-2-Phenylindole
DDX3X	DEAD-box RNA helicase 3X
DGCR8	DiGeorge Syndrome Critical Region 8
DMEM	Dulbecco’s Modified Eagle Medium
DMSO	dimethyl sulfoxide
DNA-PKcs	DNA-dependent protein kinase catalytic subunit
DSMZ	German Collection of Microorganisms and Cell Cultures GmbH
dsRNA	double-stranded RNA
ECC	extrahepatic cholangiocarcinoma
EGFR	Epidermal Growth Factor Receptor
ELISA	Enzyme-linked Immunosorbent Assay
EMT	epithelial-mesenchymal transition
EMT-TF	EMT-promoting transcription factor
ENCODE	Encyclopedia of DNA Elements
ENSCCA	European Network for the Study of Cholangiocarcinoma
ERBB2/HER2	Erb-B2 Receptor Tyrosine Kinase 2
ERV	endogenous retroviral element
EV	extracellular vesicle
FACS	Fluorescence-Activated Cell Sorting

FBS	fetal bovine serum
FDA	Food and Drug Administration
FGFR2	Fibroblast Growth Factor Receptor 2
GBC	gallbladder carcinoma
GCN2	General Control Non-depressible 2
GemCis	gemcitabine plus cisplatin combination therapy
GFP	green fluorescent protein
GI	gastrointestinal
HLA-DPA1	Major Histocompatibility Complex, Class II, DP Alpha 1
HMGB1	High Mobility Group Box 1 Protein
HRP	horse radish peroxidase
IARC	International Agency for Research on Cancer
IC	immune checkpoint
ICC	intrahepatic cholangiocarcinoma
ICI	immune checkpoint inhibitor
IDH1	Isocitrate Dehydrogenase 1
IDO1	Indoleamine 2,3-dioxygenase 1
IFIT1	Interferon-induced Protein with Tetratricopeptide Repeats 1
IFNAR1	Interferon-Alpha/Beta Receptor Alpha Chain
IFNAR2	Interferon-Alpha/Beta Receptor Beta Chain
IFN-β	Interferon Beta
IFN-γ	Interferon Gamma
IFN-λ1	Interferon Lambda 1
IFN-λ2	Interferon Lambda 2
IRF1	Interferon Regulatory Factor 1
IRF3	Interferon Regulatory Factor 3
IRF7	Interferon Regulatory Factor 7
JAK/STAT	Janus Kinase/Signal Transducer and Activator of Transcription
JAK1	Janus Kinase 1
JAK2	Janus Kinase 2
JCRB	Japanese Collection of Research Bioresources Cell Bank
KRAS	Kirsten Rat Sarcoma Viral Proto-Oncogene
KRT8	Keratin 8
LGALS3	Galectin-3
LGALS9	Galectin-9
lncRNA	long non-coding RNA
LSD1	Lysine-specific Histone Demethylase 1A
MAVS	Mitochondrial Antiviral-signaling Protein
MCL1	Myeloid Cell Leukemia 1
MDA5	Melanoma Differentiation-Associated Protein 5
MDSC	myeloid-derived suppressor cell
MET	mesenchymal-epithelial transition
METTL3	N6-Adenosine-Methyltransferase 70 KDa Subunit
MHC-I	Major Histocompatibility Complex I
MHC-II	Major Histocompatibility Complex I
miRNA	microRNA
MLKL	Mixed Lineage Kinase Domain-like Protein

MMR	mismatch repair
mOS	median overall survival
mRNA	messenger RNA
MX1	MX Dynamin like GTPase 1
MyD88	Myeloid Differentiation Primary Response Protein 88
ncRNA	non-coding RNA
NER	nucleotide-excision repair
NF-κB	Nuclear Factor Kappa-light-chain-enhancer of Activated B Cells
NK	natural killer
NSCLC	non-small cell lung cancer
nt	nucleotide
NTC	no template control
OAS1	2'-5'-oligoadenylate synthetase 1
ORR	objective response rate
OS	overall survival
p53	Tumor Protein P53
PAMP	pathogen-associated molecular pattern
PBRM1	Polybromo 1
PBS	phosphate-buffered saline
PD-1	Programmed Cell Death 1
PDCD4	Programmed Cell Death 4
PD-L1	Programmed Cell Death 1 Ligand 1
PD-L2	Programmed Cell Death 1 Ligand 2
piRNA	Piwi-interacting RNA
PKR	Protein Kinase R
Poly(I:C)	polyinosinic:polycytidylic acid
pre-miRNA	precursor microRNA
pri-miRNA	primary microRNA
PRR	pattern recognition receptor
PTEN	Phosphatase and Tensin Homolog
Ran-GTP	RAS-related Nuclear Protein with bound Guanosine Triphosphate
RIG-I	Retinoic Acid-Inducible Gene 1 Protein
RIPK1	Receptor-interacting Protein Kinase 3
RIPK3	Receptor-interacting Protein Kinase 3
RISC	RNA-induced Silencing Complex
RNA pol II	RNA polymerase II
RNA pol III	RNA polymerase III
ROS	reactive oxygen species
rRNA	ribosomal RNA
RT	room temperature
RT- control	control without reverse transcriptase
RT-qPCR	Reverse transcription quantitative PCR
SD	standard deviation
SDS	sodium dodecyl sulfate
SIDT2	SID1 Transmembrane Family Member 2
siRNA	short-interfering RNA
SNAI1	Snail Family Transcriptional Repressor 1

SNAI2	Snail Family Transcriptional Repressor 2
sncRNA	small non-coding RNA
snoRNA	small nucleolar RNA
snRNA	small nuclear RNA
SR-A	Class A Scavenger Receptor
Src	Proto-oncogene Tyrosine-protein Kinase
ssRNA	single-stranded RNA
STAT1	Signal Transducer And Activator Of Transcription 1
STAT2	Signal Transducer And Activator Of Transcription 2
STAT3	Signal Transducer And Activator Of Transcription 3
STING	Stimulator of Interferon Genes
TBS-T	Tris-buffered saline containing 0.1% Tween® 20
TCR	T cell receptor
TGFBR2	Transforming Growth Factor Receptor II
TGF-β	Transforming Growth Factor Beta
TIL	tumor-infiltrating lymphocyte
TIM-3	T-cell Immunoglobulin and Mucin-domain containing-3
TLR3	Toll-like Receptor 3
TME	tumor microenvironment
TNFSF4	Tumor Necrosis Factor Ligand Superfamily Member 4
TNFSF9	Tumor Necrosis Factor Ligand Superfamily Member 9
T_{reg}	regulatory T cell
TRIF	TIR Domain-containing Adaptor Protein inducing IFN-β
tRNA	transfer RNA
TWIST1	Twist Family BHLH Transcription Factor 1
TYK2	Tyrosine Kinase 2
ZBP1	Z-DNA-binding Protein 1
ZEB1	Zinc Finger E-Box Binding Homeobox 1
ZEB2	Zinc Finger E-Box Binding Homeobox 2

Zusammenfassung

Krebserkrankungen der Gallenwege (BTC) zeichnen sich durch eine hohe Sterblichkeitsrate und begrenzte Behandlungsmöglichkeiten aus, was den Bedarf an neuen molekularen Zielen für die Entwicklung therapeutischer Strategien unterstreicht. Um regulatorische Netzwerke mit Beteiligung nicht-kodierender RNAs zu identifizieren, konzentrierten wir uns auf die miR-200 Familie mit ihrem Einfluss auf die epithelial-mesenchymale Transition (EMT) und ihrer kürzlich beschriebenen Rolle in Immunevasions-Mechanismen, wie der Expression von Immuncheckpoints (ICs). Unser Ziel war es, die Beziehung zwischen EMT und Immunevasion in BTC zu untersuchen, mit der miR-200 Familie als potenzielle regulatorische Schnittstelle.

Anfängliche Analysen zeigten einen vielversprechenden Zusammenhang zwischen der Überexpression von miR-200c-3p mittels microRNA-Mimics und der Hochregulierung wichtiger ICs wie LGALS9, PD-L1 und IDO1. Als wir jedoch feststellten, dass weder der Knockdown von miR-200c-3p, noch die stabile Überexpression von miR-200c-3p oder die Verwendung eines miR-200c-3p-Mimics eines anderen Herstellers Auswirkungen auf ICs hatten, hinterfragten wir unsere ursprünglichen Ergebnisse. Wir vermuteten, dass die beobachtete Hochregulierung von ICs nicht durch physiologische Effekte von miR-200c-3p, sondern durch unerwartete Effekte des miR-200c-3p-Mimics verursacht wurde.

Im Rahmen der Untersuchung möglicher unspezifischer Effekte identifizierten wir eine doppelsträngige (ds)RNA-abhängige angeborene Immunantwort als Hauptursache. Der miScript miR-200c-3p-Mimic, nicht aber miR-200c-3p selbst, führte zu einer Hochregulierung von dsRNA-Sensoren, Interferonen (IFNs) und antiviralen Effektoren. Weitere Analysen mit dem dsRNA-Analog Poly(I:C) zeigten das Vorhandensein von auto- und parakrinen IFN-β Signalen, die zu einer Aktivierung des Janus-Kinase/Signaltransducer und Aktivator der Transkription (JAK/STAT)-Signalweg führten. JAK/STAT Inhibierung hob die Auswirkungen der dsRNA-abhängigen Immunantwort auf die Hochregulierung von ICs auf, wodurch dieser Signalweg als wesentliche Verbindung zwischen einer angeborenen Immunantwort und der Expression von ICs wie LGALS9, PD-L1 und IDO1 identifiziert werden konnte.

Interessanterweise wurden manche dieser dsRNA-vermittelten Effekte auch bei der Behandlung von BTC Zellen mit Cisplatin beobachtet. Während die Mechanismen, die hinter der Cisplatin-vermittelten IC-Hochregulierung stehen, noch weitgehend ungeklärt sind, deuten unsere Daten auf eine mögliche Beteiligung der dsRNA-vermittelten angeborenen Immunität hin - ein Thema, mit dem sich zukünftige Forschungsprojekte befassen werden.

Abstract

Biliary tract cancers (BTC) stand out among gastrointestinal malignancies for their high mortality rates and limited treatment options, emphasizing the need for new molecular targets to guide the development of therapeutic strategies. In an effort to uncover novel regulatory networks involving non-coding RNAs, we focused on the miR-200 family, with its impact on the epithelial-mesenchymal transition (EMT) and its more recently described role in immune evasion mechanisms like immune checkpoint (IC) expression. We aimed to investigate the relationship between EMT and immune evasion in BTC, with the miR-200 family as potential regulatory interface.

Initial analyses suggested a promising link between microRNA mimic-mediated miR-200c-3p overexpression and the upregulation of key ICs like LGALS9, PD-L1, and IDO1. However, when we noticed that neither miR-200c-3p knockdown, nor stable miR-200c-3p overexpression, or transient overexpression using a miR-200c-3p mimic from a different manufacturer had any effects, we questioned our original findings. This led to the hypothesis that the upregulation of ICs was not driven by the physiological action of miR-200c-3p, but rather by unspecific effects of the miR-200c-3p mimic itself.

Shifting our research focus towards understanding the unintended miR-200c-3p mimic effect on ICs, we identified a strong involvement of double-stranded (ds)RNA-dependent innate immune responses. The miScript miR-200c-3p mimic, but not miR-200c-3p itself, lead to an upregulation of dsRNA sensors, interferons (IFNs), and antiviral effectors. Further analyses using a dsRNA analog poly(I:C) revealed the presence of IFN-β-mediated auto- and paracrine signaling involving Janus Kinase/Signal Transducer and Activator of Transcription (JAK/STAT) signaling pathway. Inhibiting JAK/STAT abrogated the effects of dsRNA-mediated immune responses on the upregulation of ICs, establishing this pathway as essential link between innate immune responses and the expression of ICs like LGALS9, PD-L1, and IDO1.

Intriguingly, parts of these dsRNA-mediated effects were also observed when treating BTC cells with cisplatin. While the mechanisms behind the cisplatin-mediated IC upregulation remain mostly elusive, our data suggest a potential involvement of dsRNA-mediated innate immunity – a topic that will be addressed in future research.

1. Introduction

1.1. Gastrointestinal malignancies

Gastrointestinal (GI) cancer refers to a range of malignancies affecting the GI tract and associated digestive organs. These include cancers of the upper digestive tract including the esophagus, stomach, liver, gallbladder, biliary ducts, and pancreas, as well as the lower digestive tract including the small intestine, rectum, and anus. According to the current GLOBOCAN database from the International Agency for Research on Cancer (IARC), GI cancers accounted for 26.2% of the global cancer incidence with a total of 4,905,882 new cases in 2022 (3,4). Colorectal cancer (9.6%) and gastric cancer (4.9%) were the third and fifth most commonly diagnosed malignancies, respectively (4). In 2022, GI cancers caused 332,774 deaths, representing approximately 34.4% of cancer-related mortality worldwide (3). Among these, colorectal cancer (9.3%), liver cancer (7.8%), and gastric cancer (6.8%) were the second, third, and fifth leading causes of cancer deaths, respectively (4).

1.2. Biliary tract cancers (BTC)

1.2.1. Incidence and epidemiology

Among GI cancers, biliary tract cancers (BTC) deserve special attention despite their low overall incidence, accounting for less than 1% of all human cancers. However, their global incidence and mortality rates have been rising in recent decades (5–7). BTCs are often asymptomatic in their early stages and are known for their aggressive nature and high recurrence rates after chemotherapy, contributing to a concerning mortality rate of approximately 2% of all cancer-related deaths worldwide annually (8). The overall survival (OS) rate is low, with a five-year survival rate of less than 20% across all BTC subtypes (9).

Geographical differences in BTC incidence are notable. Rates are relatively low in Western, high-income countries, but significantly higher in parts of China and Southeast Asia mostly due to the presence of endemic liver flukes (5,10–12). In addition to these region-specific risk factors, global risk factors for BTC include primary sclerosing cholangitis, hepatitis B and C infections, obesity-related liver disease, diabetes, liver cirrhosis, choledochal cysts, and cholelithiasis (13–16). Despite the variability of risk factors, chronic inflammation of the biliary epithelium is a common underlying feature (7).

1.2.2. Classification

Malignancies of the biliary tract are a heterogeneous group of invasive tumors historically classified by their anatomical location into intrahepatic cholangiocarcinoma (ICC), extrahepatic cholangiocarcinoma (ECC), and gallbladder carcinoma (GBC) (5).

ICC originates from the right and left hepatic ducts and the upper part of the common bile duct within the liver (5). In contrast, ECC arises from bile ducts outside the liver and can be further subdivided into perihilar cholangiocarcinoma, which starts at the liver hilum where the left and right hepatic ducts merge, and the distal bile duct cancers, which originate further down the biliary tree, including the common bile duct (5). Ampullary cancer, originating from the ampulla of Vater located where the bile duct and the pancreatic duct join and empty into the small intestine, is another anatomical subtype (5). GBC arises from the gallbladder or the cystic duct (5).

Besides their anatomical diversity, advances in high-throughput sequencing technologies have revealed significant molecular heterogeneity across BTC subtypes (5). Specific molecular alterations are often linked to the tumor's anatomical origin (17–19). For instance, gain-of-function mutations in genes like Isocitrate Dehydrogenase 1 (*IDH1*), BRCA1-associated protein 1 (*BAP1*), and Polybromo 1 *(PBRM1*), as well as genetic translocations and fusions of Fibroblast Growth Factor Receptor 2 (*FGFR2*), are predominantly found in ICC (5,20–22). In contrast, Kirsten Rat Sarcoma Viral Proto-Oncogene (*KRAS*) mutations and Erb-B2 Receptor Tyrosine Kinase 2 (*ERBB2/HER2*) amplifications are more commonly observed in ECC (5,21,22). GBC is associated with increased rates of *ERBB2/HER2* amplifications and homologous repair deficiencies (22).

However, Jusakul *et al.* argue that the anatomical site alone does not define molecular characteristics of BTC (17). Genetic alterations, while often associated with specific tumor origins, can occur across multiple anatomical subtypes (17). Additionally, tumors from the same origin may exhibit significant molecular differences, while tumors from different origins can share genetic similarities (17). This suggests that anatomical classification alone is insufficient to capture the full molecular diversity of BTC (17). Supporting this idea, an independent gene expression profiling study identified two molecular clusters within ICC patients: the "inflammation class" and the "proliferation class" (19). The inflammation class, comprising 38% of analyzed ICCs, was characterized by active inflammatory signaling pathways, increased cytokine expression, and Signal Transducer And Activator Of Transcription 3 (STAT3) activation (19). The proliferation class, representing 62% of analyzed

ICCs, was associated with activated oncogenic signaling pathways and displayed a worse prognosis (19). Similarly, Andersen *et al.*, identified two subclasses of cholangiocarcinoma, independent of anatomical origin, with one subgroup showing genetic alterations in *KRAS* and activation of oncogenic pathways including HER2, and Epidermal Growth Factor Receptor (EGFR) signaling, characterized by a poor prognosis (18).

1.3. Clinical management of BTC

Treatment of BTC remains challenging, with surgical resection being the only potentially curative approach (7). However, according to data of the European Network for the Study of Cholangiocarcinoma (ENSCCA) registry, which includes information from 26 healthcare centers across 11 European countries, including Austria, only 50.3% of BTC patients were eligible for surgical resection in 2022 (23). Even with surgery, treatment outcomes were only moderate. Patients who underwent surgical resection with a negative-resection margin (R0) had a median overall survival (mOS) of 45.1 months and a 5-year survival rate of 43.3% (23). In contrast, patients with microscopic residual disease (R1), had a mOS of 24.7 months with a 5-year survival rate of 13.7% (23). Postoperative recurrence is not uncommon (24).

For patients ineligible for surgical resection, often due to advanced stages of disease at diagnosis, 29% received active palliative treatment and 20.6% received best supportive care (23). Most patients receiving active palliative care underwent chemotherapy, but their prognosis remained dismal, with a mOS of 10.6 months and a 5-year survival rate of 1.8% (23). Patients on best supportive care had an mOS of 4.0 months and a 5-year survival of just 0.5% (23).

1.3.1. Chemotherapy

Most patients with unresectable or recurrent BTC are treated with chemotherapy, which, while improving quality of life, does not cure the disease (18). As of 2021, the global standard first-line chemotherapy regimen for unresectable, advanced BTC is a combination of gemcitabine and cisplatin (GemCis) (24). Clinical studies from 2009 and 2010 demonstrated that GemCis provided survival benefits over single-agent gemcitabine, leading to its widespread use in clinical practice (25–27).

Mechanistically, both gemcitabine and cisplatin are cytotoxic agents that induce cell death through various molecular mechanisms. Gemcitabine, a deoxycytidine analog, is activated within the cell through various phosphorylation steps and is incorporated into nascent DNA

strands, leading to masked chain termination and subsequent inhibition of DNA synthesis and apoptosis (28,29).

Cisplatin's cytotoxicity arises mainly from its ability to bind to DNA (30). Once inside the cell, cisplatin becomes activated and forms intra-strand DNA adducts, resulting in single- and double-strand DNA breaks and triggering several cellular responses. These responses include activation of DNA damage repair mechanisms, induction of oxidative stress, inhibition of DNA replication, cell cycle arrest, and the induction of apoptosis (30–32). Cisplatin-induced necrosis has also been observed in addition to classical apoptosis (33).

Despite these effects, the effectiveness of gemcitabine and cisplatin is frequently diminished by intrinsic or acquired resistance mechanisms. For cisplatin, resistance mechanisms include altered drug uptake dynamics due to increased efflux and reduced cellular uptake, inactivation by binding to glutathione or metallothionein, enhanced DNA repair, and adaptive phenotypic processes like epithelial-mesenchymal transition (EMT) (31,34). Similarly, Gemcitabine resistance is associated increased drug efflux, inactivation of apoptosis pathways, induction of EMT, and alterations in deoxynucleotide metabolism (28,35). Additionally, reactivation of crucial signaling pathways such as Hedgehog, Wnt, Notch, or Nuclear Factor Kappa-light-chain-enhancer of Activated B Cells (NF-kB) pathways, has been implicated in gemcitabine resistance (28,35).

Thus, while GemCis has demonstrated improved effectiveness as first-line treatment for advanced BTC, resistance frequently occurs, leading to disease progression and contributing to the poor prognosis of patients undergoing chemotherapy (5).

The still underwhelming results from current BTC treatment prompted numerous clinical studies to investigate additional strategies, including triple-agent chemotherapy regimens like FOLFIRINOX (leucovorin calcium, 5-fluorouracil, irinotecan, and oxaliplatin), combinations of cisplatin, gemcitabine, and nab-paclitaxel, and the addition of S-1 to GemCis chemotherapy (36–39). Although these approaches generally improved treatment outcomes, with ongoing phase III trials still pending in some cases, OS benefits were mostly moderate (40,41).

1.3.2. Targeted therapy

A promising approach involves targeted therapies based on the molecular profiles of BTC. Thereof, inhibition of gain-of-function IDH1 mutations or activating FGFR2 translocations are especially notable strategies (5). In a phase I trial, ivosidenib, a reversible inhibitor of mutant IDH1, improved OS to 13.8 months in advanced cholangiocarcinoma patients who were

refractory to chemotherapy, surpassing the expected survival with standard treatment in similar cohorts (5,42). This clinical benefit was confirmed in a subsequent phase III trial (43). Similarly, FGFR inhibitors such as infigratinib or pemigatinib have demonstrated clinical antitumor activity against chemotherapy-refractory cholangiocarcinoma with FGFR2 fusions (44,45). The value of molecular testing in guiding treatment decisions was further underlined by a study of an Austrian cohort of BTC patients, which found that molecularly matched targeted treatments led to a significant OS benefit compared to unmatched cytotoxic chemotherapy (9).

1.3.3. Immune checkpoint inhibition

Over the past decade, immunotherapy has transformed the therapeutic management of numerous solid tumors, particularly through targeting immune checkpoints (ICs) (46). ICs are immunosuppressive molecules either expressed on the cell surface or linked to intracellular biochemical processes that result in the accumulation of immunosuppressive metabolites. Two prominent immune checkpoint pathways involve CTLA-4 and PD-1 (47,48). CTLA-4, a negative co-receptor expressed by T cells, interferes with the binding of Cluster of Differentiation 28 (CD28) to CD80 or CD86, thereby preventing full T cell activation and leading to T cell anergy (48–50). Similarly, PD-1, primarily expressed on T cells after T cell receptor (TCR) engagement and on further immune cells like B cells, NK cells, and macrophages, binds to its ligands PD-L1 or PD-L2 on antigen-presenting cells (APCs) or tumor cells, thereby inhibiting T cell activation and proliferation, which leads to T cell exhaustion (51–53).

Galectin-9 (LGALS9) and Indoleamine 2,3-dioxygenase 1 (IDO1) are two additional examples of immunomodulatory molecules (54,55). Similar to CTLA-4 and PD-1, LGALS9 exerts immunosuppressive effects primarily by interacting with its receptor, T-cell Immunoglobulin and Mucin-domain containing-3 (TIM-3). This interaction triggers a number of downstream effects that promote an immunosuppressive TME, leading to exhaustion or apoptosis of effector T cells and the differentiation into T_{regs} (56–60). IDO1, on the other hand, plays a pivotal role as a rate-limiting enzyme in the catabolism of the essential amino acid tryptophan into kynurenine (61). This has a twofold immunosuppressive impact. First, tryptophan depletion in the TME induces T cell anergy and promotes T_{reg} differentiation through the activation of the amino acid starvation sensor General Control Non-depressible 2 (GCN2) (62–64). Second, kynurenine itself has immunoinhibitory effects, activating the Aryl Hydrocarbon Receptor (AHR) on immune cells, which further drives T_{reg} differentiation and activation (65,66).

The discovery of ICs such as CTLA-4 and PD-1 with their important roles in tumor immune evasion has led to the development of immune checkpoint inhibitors (ICIs), marking a

significant advancement in the field of onco-immunology (67–69). ICIs work by blocking the immunosuppressive interactions between ICs and their receptors, thus limiting inhibitory signals to effector immune cells and countering an immunosuppressive TME (70). Therapeutic antibodies targeting CTLA-4 (anti-CTLA-4) and the PD-1/PD-L1 axis (anti-PD-1, anti-PD-L1) were among the first approved ICIs and delivered remarkable therapeutic benefits across various cancers, including non-small cell lung cancer (NSCLC), melanoma, and urothelial cancer (71–74).

BTCs are considered as tumors with a general immunosuppressive tumor microenvironment (TME), likely due to the anatomical proximity to the liver, which has a high capacity of immunotolerance, given its constant exposure to antigens from the intestinal flora (75). Therefore, several clinical trials have attempted applying the success of PD-1/PD-L1 blockade or CTLA-4 blockade in other solid tumors to the treatment of BTC. However, early studies concluded that ICI monotherapies provided limited benefit as second-line treatments (46). Neither pembrolizumab (anti-PD-1) monotherapy in the phase Ib KEYNOTE-028 and phase II KEYNOTE-158 trials, nivolumab (anti-PD-1) monotherapy in a phase II trial, nor durvalumab (anti-PD-L1) monotherapy in a phase I trial demonstrated significant improvements in response and survival rates (76–78).

The limited success of ICI monotherapies in BTC may be partly attributed to the cellular composition of the TME. The TME of BTC contains endothelial and lymphatic cells, cancer-associated fibroblasts, acellular components such as the extracellular matrix, and various immune cells including tumor-infiltrating lymphocytes (TILs) like B cells, $CD4^+$ helper T cells, $CD8^+$ cytotoxic T cells, regulatory T cells (T_{regs}), natural killer (NK) cells, tumor-associated macrophages, and tumor-associated neutrophils (79,80). Nevertheless, up to 45% of 368 ICCs analyzed by Job *et al.* were identified as immune deserts, completely lacking an immune cell infiltrate that could potentially be reactivated by ICIs (81). Additionally, the effectiveness of ICIs may be influenced by the expression of targetable ICs such as PD-1 or PD-L1 within the tumors. Without these targets, there is no mechanism for ICIs to block, limiting their therapeutic potential.

The differences between the KEYNOTE-028 and KEYNOTE-158 trials highlight the impact of PD-L1 expression on ICI treatment outcomes. In the KEYNOTE-028 trial, only advanced BTC patients with positive PD-L1 expression were included, resulting in an objective response rate (ORR) of 13.0% (76). In contrast, the KEYNOTE-158 trial, which included patients regardless

of their PD-L1 expression status, reported a much lower ORR of 5.8%, suggesting that PD-L1 presence enhances the effectivity of anti-PD-1 therapy (76).

However, a meta-analysis of 30 clinical trials investigating the prognostic value of PD-L1 expression in BTC found that PD-L1 expression alone is not a strong predictor of response to anti-PD-1/PD-L1 blockade (82). Nevertheless, the study noted that the cut-off for PD-L1 positivity plays a role, with higher PD-L1 expression being a better predictor of treatment response compared to with lower cut-offs (82). This suggests that while PD-L1 presence alone may not be sufficient to predict response, higher expression levels may be indicative of better outcomes.

This is supported by a study by Ahn *et al.*, which screened 175 advanced BTC patients for tumoral PD-L1 expression before treatment with pembrolizumab (83). Among 26 PD-L1-positive patients, those with high PD-L1 expression levels had an overall response rate of 56% (5/9 patients), compared to a 6% response rate (1/17 patients) in those with low PD-L1 expression, suggesting that PD-L1 expression levels matter (83).

1.3.4. Combination therapies

To address these challenges of a deficient immune cell compartment and the limited expression of targetable ICs, combination strategies are being explored to enhance ICI efficacy in BTC.

For instance, cisplatin and GemCis have demonstrated immunomodulatory properties, contributing to a less immunosuppressive TME (84,85). Cisplatin has been shown to increase the recruitment and proliferation of effector immune cells, upregulate major histocompatibility complex I (MHC-I) expression to promote tumor neoantigen presentation, boost the lytic activity by cytotoxic T cells, and reduce the immunosuppressive populations such as myeloid-derived suppressor cells (MDSCs) and T_{regs} (84). Similarly, GemCis treatment has been associated with reduced levels of suppressive immune cells and increased levels of proinflammatory cytokines (85). However, many cytotoxic agents, including gemcitabine and cisplatin, have also been described to upregulate PD-L1 expression, primarily by generating danger signals, as shown in ovarian and bladder cancers (86–88). These dual immunomodulatory effects provide a rationale for combining chemotherapy with immunotherapy (86).

A phase II clinical trial testing different combinations of GemCis with durvalumab (anti-PD-L1) and trememilumab (anti-CTLA-4) in advanced BTC patients reported an ORR of 72% for the

GemCis + durvalumab combination and 70% for GemCis + dual immunotherapy combination (89). Based on these promising results, the phase III TOPAZ-1 trial compared GemCis + durvalumab with GemCis + placebo as first-line treatment (90). The chemoimmunotherapy showed an ORR of 26.7% compared to the ORR of 18.7% of chemotherapy alone (90). Interestingly, a subgroup analysis found no difference in benefit difference between patients with or without baseline PD-L1 expression, indicating that pre-treatment PD-L1 status might not predict response to chemoimmunotherapy (90). However, changes of PD-L1 expression levels during treatment were not evaluated, leaving open the possibility that GemCis may have upregulated PD-L1 expression over the course of treatment, which in turn enhanced the efficacy of anti-PD-L1 therapy. These positive results led to the approval of GemCis + durvalumab by the Food and Drug Administration (FDA) as first-line treatment for advanced BTC in September 2022. Similarly, the phase III KEYNOTE-966 trial tested GemCis with pembrolizumab (anti-PD-1) as first-line treatment for advanced BTC, showing comparable benefits to TOPAZ-1 (91). Again, baseline PD-L1 status did not appear to influence treatment responses (91).

In addition to therapeutic interventions with immunomodulatory effects, BTC cells themselves can influence the immune compartment of the TME. Recent advances in molecular profiling have not only identified actionable targets but also revealed how oncogenic variants in BTC cells can modulate the immune microenvironment (46). Genetic alterations in oncogenes relevant to BTC, such as *IDH1*, *FGFR2*, *KRAS*, and *HER2*, have been shown to induce immunomodulatory effects, potentially impacting responses to immunotherapy (46).

For instance, in glioma, gain-of-function mutations in IDH1 were found to promote an immunosuppressive TME by suppressing T cell activity through an extracellular accumulation of the oncometabolite *(R)*-2-hydroxyglutarate (92,93). Aberrant FGFR signaling has also been reported to have profound immunoinhibitory effects, including reduced T cell activity via increased PD-1 expression, decreased secretion of Interferon Gamma (IFN-γ) and cytotoxic mediators like granzyme B, and stabilization of T_{regs} (94). Furthermore, deregulated FGFR signaling has been connected to a decreased MHC-I and Major Histocompatibility Complex II (MHC-II) expression and altered PD-L1 expression of tumor cells (94). However, the directionality of PD-L1 expression changes as consequence of deregulated FGFR signaling appears to be context-dependent. In colorectal cancer cells, FGFR2 has been shown to promote PD-L1 expression via activation of Janus Kinase/Signal Transducer and Activator of Transcription (JAK/STAT) signaling (95). In contrast, FGFR2 fusion-positive cholangiocarcinoma cells were mostly negative for PD-L1 expression (96). In addition to direct

cellular consequences, FGFR signaling was also shown to impact tumor vasculature, thereby influencing the infiltration of peripheral immune cells into the tumor (94).

Given the growing appreciation of molecularly targeted therapies in BTC and their potential to modulate the immune environment, ongoing clinical trials are exploring the efficacy of combining targeted therapy with immunotherapy. For example, combining ivosidenib with nivolumab and ipilimumab may yield promising results in *IDH1*-mutated nonresectable or metastatic cholangiocarcinoma (97,98).

It is becoming increasingly evident that immunotherapies can be enhanced by modulating molecular processes that shape the TME, as demonstrated by IDH1- and FGFR2-targeted approaches. This highlights the need for a deeper understanding of genetic alterations and molecular mechanisms driving the establishment of an immunosuppressive environment in BTC. While research has primarily focused on changes in the coding genome, the role of non-coding RNAs (ncRNAs) in BTC requires further exploration. Given their extensive regulatory functions across virtually all cellular processes, ncRNAs are likely to impact immunomodulatory mechanisms within BTC cells, presenting new molecular targets that may be leveraged to improve immunotherapeutic strategies.

1.4. Non-coding RNAs (ncRNAs)

Approximately six decades ago, Francis Crick proposed the central dogma of molecular biology, suggesting an unidirectional flow of genetic information from DNA to RNA to protein synthesis, with proteins serving as final functional effectors (99,100). This protein-centric view initially implied that the primary role of RNA was merely to serve as a temporary mediator for transferring genetic information. However, this concept was later challenged by discoveries of RNA transcripts that were not translated into proteins. Initially considered as evolutionary transcriptional noise without biological relevance, discoveries of transcripts like *lin-4* or *let-7* revealed that RNAs, without coding for proteins, are crucial for cellular processes such as development in *Caenorhabditis elegans* (101,102).

These early findings sparked a surge in scientific interest in understanding these non-coding RNAs (ncRNAs). The subsequent revelations from the Encyclopedia of DNA Elements (ENCODE) project revealed that between 62-75% of the human genome is transcribed into RNA, whereas protein-coding genes account for only about 2-3% of the genome (103). This underscored the functional significance of transcripts from regions initially considered “junk” DNA (104). Since then, numerous studies have confirmed the existence and importance of

ncRNAs across different species and conditions with key roles in the maintenance of physiological processes such as development, hematopoiesis, and aging (105–108).

There are several classes of ncRNAs. They can be roughly classified based on their length into small non-coding RNAs (sncRNAs), which are shorter than 200 nucleotides, and long non-coding RNAs (lncRNAs), which are longer than 200 nucleotides. Conventionally, lncRNAs are further categorized according to their genomic localization into intergenic lncRNAs (lincRNAs), intronic lncRNAs, antisense lncRNAs, bidirectional lncRNAs, or enhancer lncRNAs (105,109).

SncRNAs, on the other hand, are subdivided based on their functionality. Structural "housekeeping" ncRNAs such as ribosomal RNAs (rRNAs), transfer RNAs (tRNAs), small nuclear RNAs (snRNAs), and small nucleolar RNAs (snoRNAs), are involved in key cellular processes ranging from genomic maintenance to protein synthesis (110). Regulatory sncRNAs including endogenous short interfering RNAs (siRNAs), microRNAs (miRNAs), and Piwi-interacting RNAs (piRNAs), primarily act by binding to and regulating DNA or RNA molecules through the RNA interference pathway, thereby modulating gene expression (111).

1.5. MicroRNAs (miRNAs)

Among the various ncRNAs, miRNAs are one of the most extensively investigated classes.

1.5.1. Biogenesis and maturation

To become biologically active, miRNAs undergo a multistep biogenesis and maturation process, which varies depending on their genomic context. Biogenesis of intergenic miRNAs, transcribed from their individual promoters, differs slightly from the processing of intronic or exonic miRNAs, which follow the transcriptional dynamics of the host gene they are embedded in.

Intergenic miRNAs are transcribed by RNA polymerase II (RNA pol II) or RNA polymerase III (RNA pol III) into primary miRNAs (pri-miRNAs), which have a hairpin structure with single-stranded RNA extensions at both their 5' and 3' ends (112,113). During the first maturation step, the microprocessor complex, which consists of DiGeorge Syndrome Critical Region 8 (DGCR8) and the RNase III endonuclease Drosha, cleaves the pri-miRNA at the base of the hairpin, forming precursor miRNAs (pre-miRNAs) of approximately 60-70 nucleotides (nts) with characteristic 3' overhangs (114).

Intronic and exonic miRNAs follow an alternative processing pathway. These miRNAs are co-transcribed with their host genes by RNA pol II as part of the pre-mRNA and depend on splicing and debranching by spliceosomal components (115,116). This results in structures that resemble either pri-miRNAs, which then undergo the same maturation process as intergenic miRNAs, or pre-miRNAs that bypass DGCR8/Drosha processing (117,118).

Regardless of the initial processing pathway, pre-miRNAs are exported from the nucleus to the cytoplasm by an exportin-5/Ran-GTP complex (119). In the cytoplasm, the RNase III endonuclease Dicer cleaves the terminal loop of pre-miRNAs, generating double-stranded miRNA duplexes consisting of a 3' (-3p) strand and a 5' (-5p) strand (120). Once incorporated into an Argonaute protein (AGO) to form the RNA-induced silencing complex (RISC), one strand – known as the guide or active strand – is selected, while the second "passenger strand" is released and subsequently degraded (120,121). The selection of the guide strand is typically determined by the thermodynamic asymmetry of the miRNA duplex, with the strand less stable at its 5' end generally being favored (121). In their mature form, miRNAs average a length of 22 nts (122).

1.5.2. Function

The mature miRNA directs the RISC to messenger RNA (mRNA) targets in a sequence-specific manner, facilitating their post-transcriptional repression (122). Typically, miRNAs bind to the 3' untranslated region (3' UTR) of their target transcripts, although binding sites in the 5' UTR or coding regions have also been observed (123). In humans, miRNAs generally bind with imperfect complementarity to their targets, but a perfect match between bases 2-8 of the miRNA, known as the "seed sequence", is critical for effective interaction (124).

Upon miRNA-mRNA interaction, two primary mechanisms have been well described: translational repression and mRNA degradation (122). To achieve translational repression, the RISC complex disrupts the translation process through various mechanisms, such as preventing the recruitment of initiation factors, blocking ribosome subunit joining, or interfering with post-initiation steps (124).

Alternatively, miRNA binding can directly decrease levels of targeted mRNAs through destabilization or degradation. This process may involve a progressive shortening of the transcript's poly(A) tail, followed by a cytoplasmic exosome-mediated 3' to 5' decay, or the removal of the 7-methylguanosine cap structure, resulting in exonuclease-mediated 5' to 3'

degradation (124,125). In either case, the miRNA-directed binding of the RISC to the target transcript reduces functional protein levels, thereby fine-tuning gene expression within the cell.

Importantly, one miRNA can target multiple transcripts and a single transcript can be targeted by several miRNAs, highlighting the enormous complexity of the miRNA regulatory network within cells (126).

1.6. MicroRNAs in Cancer

Given their crucial role in fine-tuning gene expression to maintain cellular integrity, it lies near that any deregulation of the typically tightly controlled miRNA expression profile is closely linked to various human diseases, marking miRNAs as pivotal contributors to disease onset and progression, especially in cancer (127–132).

1.6.1. Deregulation of microRNA levels

Over the past decades, miRNA levels have been found to be deregulated in human malignancies as a consequence to genetic abnormalities, epigenetic alterations, or changes affecting either the transcriptional control or the biogenesis and maturation machinery (127).

Amplifications or deletions of genetic loci containing miRNA genes or miRNA host genes often lead to aberrant miRNA expression. For instance, miR-15a and miR-16-1, were found to be commonly downregulated in B-cell chronic lymphocytic leukemia cells due to the deletions of their genetic origin on chromosome 13q14 region (133). On the other hand, overexpression of seven miRNAs from the miR-17-92 cluster has been observed across several cancer types, driven by increased copy numbers or translocations of the gene encoding the polycistronic miRNA transcript (134–136).

In addition to genetic abnormalities, alterations in the expression of transcriptional regulators or proteins involved in the miRNA biogenesis have been reported to affect miRNA expression levels (127). Especially transcription factors frequently dysregulated in cancer, such as MYC proto-oncogene (c-Myc) or Tumor Protein P53 (p53), have been associated with changed miRNA expression patterns (127). Interestingly, the oncogenic c-Myc seems to exert dual effects on miRNA regulation. O'Donnell *et al.* discovered that c-Myc induced the expression of miR-17-92 cluster by direct promoter engagement, while other studies have shown that c-Myc represses transcription of a broad range of miRNAs, many of which are typically downregulated in cancer (137,138). Furthermore, c-Myc has been found to upregulate Drosha expression, which suggests a broader impact on miRNA regulation (139).

Moreover, the downregulation of key endonucleases involved in the miRNA maturation process, such as Drosha and Dicer, was observed in multiple cancers, including lung cancer, ovarian cancer, or chronic lymphocytic leukemia, leading to decreased miRNA expression levels (140–142). Deregulation of other enzymes involved in miRNA biogenesis, like Argonaute RISC Catalytic Component 2 (AGO2), has also been implicated in cancer, further disrupting miRNA expression (143).

1.6.2. Oncogenic or tumor suppressive?

Deregulated miRNA levels are known to influence a broad spectrum of cellular processes, contributing to the development of key cancer hallmarks such as abnormal cell proliferation, resistance to cell death, adapted cellular metabolism, promotion of metastasis via EMT, and immune evasion (144–146).

In the context of cancer, miRNAs are typically classified as either oncogenic or tumor suppressive, mostly depending on their cellular targets (147). Oncogenic miRNAs limit the expression of tumor suppressors, thereby promoting an expressional profile favoring carcinogenesis (147). In contrast, tumor suppressive miRNAs downregulate the expression of oncogenes to counteract tumorigenesis (147). However, while this binary classification provides a generally useful framework, the inherent flexibility of miRNA-mRNA interaction networks requires careful consideration of context (148). Disparate and conflicting results observed in different settings emphasize the risk of generalizing miRNA functions within such a dynamic and interconnected regulatory network (148).

Nevertheless, multiple oncogenic and tumor suppressive miRNAs have been identified across various cancers. For example, the oncogenic miR-663 has been found to be upregulated in nasopharyngeal cancer cells, where it promotes cell proliferation by directly targeting $p21^{CIP1}$, thus releasing cells from G1/S arrest (149). Another prominent oncogenic miRNA is miR-21, which is overexpressed in many solid cancers (150,151). miR-21 targets and downregulates several tumor suppressors including Phosphatase and Tensin Homolog (PTEN), Transforming Growth Factor Receptor II (TGFBR2), Cell Division Cycle 25A (CDC25A), and Programmed Cell Death 4 (PDCD4) (152–154). This activity has been linked to an aggressive tumor phenotype by enhancing cell proliferation, metastasis, resistance to cell death, and immune evasion (152–154).

On the other hand, numerous examples illustrate the tumor suppressive roles of miRNAs with wide-ranging effects on cancer cells. For instance, the miR-15/16 family is frequently

downregulated in various solid tumors, including melanoma, colorectal cancer, and bladder cancer (147,155). The tumor suppressive function of miR-15/16 primarily involves the induction of apoptosis by downregulating B-Cell CLL/Lymphoma 2 (Bcl-2), as well as targeting other oncogenes involved in cancer progression, such as cyclin D1 and Myeloid Cell Leukemia 1 (MCL1) (147,155). Another notable example of miRNAs exerting tumor suppressive functions is the interaction between p53 and the miR-34 family (156). p53 induces the expression of miR-34 family members, which in turn contribute to p53's extensive tumor suppressive effects by promoting of cell cycle arrest, senescence, and apoptosis (157,158). Additionally, the miR-34 family has been identified as crucial coordinator of EMT (159).

1.7. Epithelial-mesenchymal transition (EMT)

EMT and its reverse process mesenchymal-epithelial transition (MET) are fundamental and highly conserved biological processes involved in embryonic development, organogenesis, and tissue repair and homeostasis (160). During EMT, epithelial cells undergo a series of changes: they gradually lose their apical-basal polarity, downregulate adhesion molecules critical for maintaining junctions with the basement membrane and adjacent cells, and reorganize their actin cytoskeleton (160,161). These changes enhance their invasive and migratory capabilities, allowing them to leave their tissue of origin and migrate to distant sites, which facilitates tissue remodeling (160,161). However, while EMT supports normal physiological processes, it also plays a crucial role in carcinogenesis. By facilitating the intravasation of originally epithelial cancer cells into lymphatic or blood vessels, it enables their dissemination to distant tissues, thereby promoting metastasis (162). Upon reaching distant secondary sites, mesenchymal cancer cells might undergo MET, reverting to an epithelial phenotype to establish a new tumor (162).

Although EMT and MET are often considered as binary processes resulting in either epithelial or mesenchymal cells, accumulating evidence suggests a spectrum of EMT states (161,163,164). Recent studies have reported the coexistence of epithelial and mesenchymal markers within cells, indicating the presence of intermediate or partial EMT states rather than fixed endpoints (163,165–170).

1.7.1. Regulation of EMT

At the molecular level, EMT and MET are tightly controlled by complex signaling networks, including Transforming Growth Factor Beta (TGF-β), Bone Morphogenetic Protein (BMP), and Notch signaling, as well as environmental conditions like hypoxia (171–174). Kinase cascades

activated by these signals lead to the expression or activation of various transcription factors that drive either epithelial or mesenchymal phenotypes. For instance, pro-epithelial processes promote the expression of epithelial markers like E-cadherin (CDH1) and Keratin 8 (KRT8), while pro-mesenchymal transcription factors induce the expression of mesenchymal markers such as Vimentin or N-cadherin (161,175).

Several key EMT-promoting transcription factors (EMT-TFs) contribute to the initiation and progression of EMT. These include Zinc Finger E-Box Binding Homeobox 1 (ZEB1), Zinc Finger E-Box Binding Homeobox 2 (ZEB2), Snail Family Transcriptional Repressor 1 (SNAI1), Snail Family Transcriptional Repressor 2 (SNAI2), or Twist Family BHLH Transcription Factor 1 (TWIST1) (161). For example, SNAI1 and SNAI2 have been shown to repress CDH1 transcription, thereby promoting a mesenchymal phenotype (176,177). Similarly, overexpression of TWIST1 has been reported to reduce CDH1-mediated cell-cell adhesion and enhance EMT in breast cancer cells (178).

1.7.2. The miR-200 family

MiRNAs have also been identified as crucial regulators of EMT, with the miR-200 family being particularly central to this regulatory network (163,179,180). This miRNA family consists of five closely related miRNAs: miR-141-3p, miR-200a-3p, miR-200b-3p, miR-200c-3p, and miR-429. These miRNAs can be organized according to their genetic location, with the polycistronic gene coding for mir-200a, miR-200b, and miR-429 found on chromosome 1p36.33, while miR-200c and miR-141 are encoded within a gene located on chromosome 12p13.31 (181). Functionally, these miRNAs can also be categorized based on a single-nucleotide variation within their otherwise identical seed sequences. Specifically, miR-141-3p and miR-200a-3p contain a cytosine at the third position of the seed sequence, while other members have an uracil instead (182).

The miR-200 family plays a key role in EMT by post-transcriptionally regulating ZEB1 and ZEB2, which reduces their intracellular abundance and counteracts their repression of CDH1, thus maintaining an epithelial phenotype (183–185). Conversely, high levels of ZEB1 and ZEB2 in mesenchymal cells can transcriptionally repress miR-200 family members, establishing a double-negative loop that affects CDH1 expression (186). In this context, overexpression of miR-200 family members has been shown to induce MET connected to an upregulation of CDH1, while reduced levels of miR-200 family members has been demonstrated to increase ZEB1 levels and the expression of mesenchymal markers (183–185). The miR-200/ZEB axis has been identified as a major regulator of both EMT and MET

across various cancer types, underscoring its importance in these processes (187). Furthermore, miR-200 family members have been reported to induce MET through alternative mechanisms, such as regulating the expression of SNAI1 and other EMT-TFs (188,189).

The significance of the miR-200 family and its regulation of EMT in BTC has been highlighted in several studies. For instance, Urbas *et al.* found that high expression levels of miR-200 family members and CDH1 were associated with improved survival of BTC patients (190). Conversely, low miR-200 family expression and high expression of the mesenchymal marker vimentin were linked to poorer survival outcomes (190). Similarly, overexpression of miR-200c has been described to reduce migrative and invasive capabilities in ICC cells, supporting its role in promoting an epithelial phenotype in BTC (191). Consistent with these findings, overexpression of miR-200b/c has been confirmed to limit migration and invasion of cholangiocarcinoma cells both *in vitro* and *in vivo* (192).

1.8. Connection between EMT and immune evasion

Unsurprisingly, the impact of EMT extends beyond its role in metastasis, influencing a wide range of additional cellular processes critical to cancer progression, including stemness, apoptosis, proliferation, drug resistance, and tumor immune evasion (193,194). Among these, EMT's immunomodulatory effects are particularly intriguing.

Several studies have established connections between EMT and immunosuppression within the TME of various cancer types (193). In NSCLC, EMT was associated with increased expression of ICs such as PD-L1, PD-L2, PD-1, TIM-3, and CTLA-4, along with greater infiltration of $CD4^+$ $FoxP3^+$ T_{regs} (195). In sarcomatoid urothelial bladder cancer, a dysregulated EMT network contributed to an immune infiltration phenotype marked by elevated PD-L1 levels (196). In the context of melanoma, tumors that were non-responsive to anti-PD-1 therapy showed an overexpression of genes associated with a mesenchymal state and a downregulation of CDH1, suggesting a mesenchymal tumor phenotype may be linked to innate anti-PD-1 resistance (197). In breast cancer, epithelial tumor cells displayed high levels of MHC-I, low PD-L1 expression, and moderate infiltration of $CD8^+$ T cells and anti-tumor M1 macrophages (198). In contrast, tumor cells with mesenchymal origin had low MHC-I levels, high PD-L1 expression, exhausted $CD8^+$ cells, and pro-tumor M2 macrophages, indicating that EMT drives an immunosuppressive phenotype (198). Furthermore, Chen *et al.* reported that miR-200 directly targets PD-L1, leading to its downregulation in NSCLC cells (199). ZEB1-mediated repression of miR-200 resulted in elevated PD-L1 expression, which inhibited $CD8^+$ T cells in the TME while also promoting cancer cell metastasis, suggesting the miR-200/ZEB

axis as promising molecular link between EMT and IC expression (199). In line with this, ZEB1 was shown to induce PD-L1 and CD47 expression on invading cell clusters in a KRAS-driven lung adenocarcinoma mouse model, remodeling the immune microenvironment to exclude $CD8^+$ cells and M1-like macrophages (200). Moreover, miR-200 overexpression or siRNA-mediated ZEB1 downregulation reduced PD-L1 expression in a number of breast cancer cell lines (201). Adding to this, Ricciardi *et al.* demonstrated that EMT induced by inflammatory stimuli activated immunomodulatory mechanisms, including IDO1 expression, in various cancer cell lines (202).

In BTC, however, direct evidence linking EMT to immune evasion mechanisms remains limited. While EMT plays an important role in GBC, with the expression of EMT markers and EMT-TFs closely linked to development, progression, and treatment outcomes, its impact on tumor immunology is incompletely understood (203). Similarly, although EMT marker expression in advanced BTC patients has been associated with poor survival and increased T_{reg} infiltration, a comprehensive characterization of a potential crosstalk between EMT and immune evasion mechanisms is still lacking (204).

1.9. Influence of innate immunity on ICs

With the rise of immunomodulatory cancer therapies such as ICIs, attention has increasingly shifted from focusing solely on the adaptive immune system to recognizing the significant involvement of the innate immune system as well (205,206).

Innate immunity is a fundamental part of the immune system, serving two main functions: first, it is essential for mounting an effective adaptive immune response upon detecting molecular abnormalities, such as damage-associated alterations or changes caused by viral and bacterial infections; second, it performs key effector functions like phagocytosis or natural cytotoxicity (206,207). Since innate immune pathways are ubiquitously present in various cell types, including immune cells such as dendritic cells, macrophages, NK cells, as well as non-immune cells, it is likely that innate immunity plays a pivotal role in the TME, where damage-associated molecular patterns (DAMPs) are abundant due to environmental stressors such as hypoxia, cytotoxic immune cells, or genotoxic treatments (205,206,208,209).

DAMPs such as aberrant nucleic acids, including fragmented DNA and atypical double-stranded RNA (dsRNA), are detected by pattern recognition receptors (PRRs). Key PRPs include dsRNA-recognizing receptors such as Toll-like Receptor 3 (TLR3), Retinoic Acid-Inducible Gene 1 Protein (RIG-I), and Melanoma Differentiation-Associated Protein 5 (MDA5),

as well as the DNA-sensing machinery Cyclic GMP-AMP Synthase (cGAS) - Stimulator of Interferon Genes (STING) (205). Upon recognizing DAMPS, a wide range of innate immune pathways are triggered (205).

Typically, DAMP recognition initiates a signal transduction cascades that involve adapter molecules like Myeloid Differentiation Primary Response Protein 88 (MyD88), TIR Domain-containing Adaptor Protein inducing IFN-β (TRIF), Mitochondrial Antiviral-signaling Protein (MAVS), or STING. These cascades lead to the activation of transcription factors such as Interferon Regulatory Factor 3 (IRF3), Interferon Regulatory Factor 7 (IRF7), or NF-κB (205). Once activated, these transcription factors drive the expression of various genes favoring an active immune response, including a plethora of pro-inflammatory cytokines, chemokines, and type I interferons (205). In turn, antiviral effectors such as oligoadenylate synthetase 1 (OAS1), MX Dynamin like GTPase 1 (MX1), and Protein Kinase R (PKR) are also frequently induced to limit pathogen spread by blocking viral transcription, degrading viral RNA, and modify protein function (210).

Targeting PRRs such as TLRs, STING, or RIG-I with synthetic agonists has provided promising results in preclinical models, leading to tumor size reduction both at the injection site and more distant locations (206). These treatments have demonstrated a range of antitumor effects, including the direct induction of tumor cell death, increased production of type I IFNs and proinflammatory cytokines, and enhanced secretion of T cell-tropic chemokines (206). Moreover, these therapies have shown to promote activation and expansion of tumor-specific $CD8^+$ T cells, contributing to sustained antitumor immunity (206).

However, innate immune responses have also been implicated in establishing immunosuppressive conditions in the TME, primarily through the upregulation of ICs (205,206). For example, Liu *et al.* demonstrated that cGAS-STING activation was associated with an increased expression of PD-L1, a process dependent on Ariadne RBR E3 Ubiquitin-protein Ligase 1 (ARIH1)-mediated degradation of DNA-dependent protein kinase catalytic subunit (DNA-PKcs) (211). Similarly, cytosolic DNA sensing via STING and subsequent type I interferon signaling was reported to activate IDO1 in Lewis lung carcinoma (LLC) mouse models (212). Moreover, tumor-intrinsic RIG-I signaling was found to influence the efficacy of anti-CTLA-4 immunotherapy in melanoma cells, an effect that could be augmented through the addition of synthetic RIG-I agonists (213).

Therefore, with innate immunity playing dual roles – on the one hand, driving antitumor immunity through the secretion of pro-inflammatory cytokines and chemokines that promote

an active immune response, and on the other hand, upregulating immunosuppressive ICs – a combination of PRR agonists and ICIs may offer an effective treatment strategy for solid cancers, including BTC. In fact, early clinical trials are already exploring the potential synergy of such treatment combinations. In patients with metastatic melanoma, stimulation of TLR9 with SD-101 in combination with anti-PD-1 therapy led to immune activation at the tumor site, increasing the infiltration of immune cells such as $CD8^+$ T cells, NK cells, dendritic cells, and B cells (214). Similarly, the synthetic TLR3/RIG-I ligand Riboxxim enhanced type I interferon secretion, dendritic cell maturation, and improved priming and activation of $CD8^+$ T cells (215). This effect could be further amplified by anti-CTLA-4 treatment to facilitate effective tumor cell killing (215).

1.10. Study Rationale and Objectives

Despite continuous advances in molecular characterization and therapeutic management, BTC remains an aggressive malignancy with limited treatment options. Investigating the cellular networks and molecular processes that shape this disease is essential, not only to deepen our understanding of BTC development and progression but also to identify novel molecular mechanisms that could lead to innovative therapeutic strategies.

Emerging evidence has highlighted a connection between EMT and immune evasion mechanisms, such as IC expression, across various cancer types. While first molecular interactions between EMT and ICs have been characterized, a comprehensive analysis of this crosstalk in BTC, particularly involving the miR-200 family as potential regulatory interface, is lacking. Therefore, the initial aim of this project was to investigate the role of the EMT-regulating miR-200 family in modulating IC expression in BTC.

Based on preliminary findings that revealed promising relationships between miR-200 family members, EMT markers, and ICs, we sought to explore the underlying molecular interactions. Specifically, we aimed to understand if and how manipulating miR-200 family levels in BTC cells influenced their EMT state, and how these changes, in turn, affected IC expression. However, unexpected non-specific effects of miRNA mimics - molecular tools used to transiently upregulate miRNA levels - shifted the focus of our research. This led us to investigate the role of dsRNA-mediated innate immunity in the regulation of IC expression instead.

Our new objective became to understand the non-specific molecular mechanisms behind the IC upregulation upon miRNA mimic transfection. By extending these findings to other dsRNA

species to confirm broader applicability and translating these insights into pathophysiological scenarios with potential clinical relevance, we aimed to enhance our understanding of the interplay between innate immunity and immunosuppression in BTC. Furthermore, given cisplatin's known immunomodulatory effects, we sought to explore the influence of dsRNA-mediated innate immunity on the cisplatin-induced IC upregulation.

Ultimately, we hoped that insights into the relationship between dsRNA-mediated innate immune activation and IC expression in BTC would contribute the development of therapeutic strategies that effectively unleash antitumor immunity, thereby facilitating more effective tumor cell eradication.

2. Materials and Methods

2.1. Cell lines and culturing conditions

Throughout the project, a number of human BTC cell lines originating from various tissues was used. The ICC cell lines HuCC-T1 (JCRB0425 (216)), HuH-28 (JCRB0426 (217)), OZ (JCRB1032 (218)), KKU-055 (JCRB1551), KKU-213 (JCRB1557), the GBC cell lines OCUG-1 (JCRB0191 (219)), NOZ (JCRB1033 [33]), the hilar cholangiocarcinoma cell line KKU-100 (JCRB1568 (220)), and the SV40T- and hTERT-immortalized human cholangiocyte cell line MMNK-1 (JCRB1554 (221)) were obtained from the Japanese Collection of Research Bioresources Cell Bank (JCRB). The cholangiocarcinoma cell lines EGI-1 (ACC385) and TFK-1 (ACC344 (222)) were purchased from the German Collection of Microorganisms and Cell Cultures GmbH (DSMZ).

All cell lines were cultured in either Dulbecco's Modified Eagle Medium (DMEM) containing L-Glutamine, 4.5 g/l glucose, and 25 mM HEPES (Catalog #: 42430025, Gibco, Thermo Fisher Scientific, Vienna, Austria), or DMEM containing 4.5 g/l glucose (Catalog #: 11960044, Gibco, Thermo Fisher Scientific). The medium was supplemented with 10% fetal bovine serum (FBS; Catalog #: S-FBS-SA-015, Serana Europe GmbH, Pessin, Germany) and 1% penicillin-streptomycin solution containing 10,000 units penicillin and 10 mg/ml streptomycin (Catalog #: P4333-100ML, Sigma-Aldrich Handels GmbH, Vienna, Austria).

Cells were incubated in a humidified incubator under standard conditions maintaining a temperature of 37°C, oxygen and carbon dioxide levels of 21% and 5%, respectively, and 90-98% humidity to prevent excessive evaporation from the media. Cells were split on a regular basis with cell densities between 40-80% to promote balanced and uninhibited growth behavior.

2.2. Transient overexpression and knockdown

To study the relevance of miRNAs, transient transfection experiments were performed. Unless otherwise specified, cells were transfected for 48 hours following the fast-forward protocol of the HiPerFect transfection reagent (Catalog #: 301704, QIAGEN, Hilden, Germany). In brief, the transfection mix, containing transfection reagent and the desired concentration of nucleic acids, was incubated for 10 minutes on room temperature (RT) to facilitate complex formation. Cell suspensions were then added to 6-well culture plates, followed by the transfection mix.

To transfect cells for WST-1 and Caspase-3/7 Glo® assays, the HiPerFect reverse transfection protocol was used. In this method, the transfection mix was added to the wells before the cell suspension, resulting in higher transfection efficiencies compared to the fast-forward approach in 96-well plates.

2.2.1. Transient miRNA overexpression and knockdown

For miRNA overexpression experiments, cells were seeded in 6-well plates at a density of 40-60% and transfected with either 10 nM Syn-hsa-miR-141-3p miScript miRNA mimic (Catalog #: MSY0000432, QIAGEN), 10 nM Syn-hsa-miR-200c-3p miScript miRNA mimic (Catalog #.: MSY0000617, QIAGEN, Hilden, Germany), or 5 nM of each mimic. Cells transfected with 10 nM AllStars Negative Control siRNA (Catalog #: 1027281; QIAGEN) served as negative control. Alternatively, cells were transfected with 10 nM mirVana™ miR-200c-3p mimic (Catalog #: 4464066, Thermo Fisher Scientific) or 10 nM mirVana™ miRNA mimic Negative Control #1 (Catalog #: 4464058, Thermo Fisher Scientific) as corresponding negative control.

For miRNA knockdown experiments, cells were seeded in 6-well plates at a density of 40-60% and transfected with 50 nM hsa-miR-141-3p miRCURY LNA miRNA inhibitor (Catalog #: 339121, QIAGEN), 50 nM hsa-miR-200c-3p miRCURY LNA miRNA inhibitor (Catalog #: 339121, QIAGEN), or 25 nM of each. Cells transfected with 50 nM miRCURY LNA miRNA Inhibitor Control (Catalog #: 339126, QIAGEN) served as corresponding negative control.

2.2.2. Transient ZEB1 knockdown

Transient knockdown of ZEB1 was achieved by siRNA transfection. Cells were seeded in 6-well plates at a density of 40-60% and transfected with 50 nM siRNA directed against ZEB1 (Hs_ZEB1_2 FlexiTube siRNA, Catalog #: SI04272492, QIAGEN) or 50 nM AllStars Negative Control siRNA as corresponding negative control.

2.2.3. Transfection with polyinosinic:polycytidylic acid (poly(I:C))

Polyinosinic:polycytidylic acid (poly(I:C)) is a synthetic dsRNA analog, which consists of an inosine homopolymer annealed to cytidine homopolymer, with an average size ranging from 1.5 kb to 8 kb (according to the manufacturer InvivoGen). To ensure efficient cellular uptake of poly(I:C), cells were seeded in 6-well plates at a density of 40-60% and transfected with 2000 ng/ml high molecular weight poly(I:C) (Catalog #: tlr-pic, InvivoGen, San Diego, CA, USA). As negative control, cells were transfected with transfection mix lacking nucleic acids, termed mock control.

2.2.4. Unassisted uptake (= gymnosis) of poly(I:C)

To confirm that cells are able to take up dsRNA species like poly(I:C) in an unassisted manner, gymnosis experiments were conducted. To this end, cells were seeded in 6-well plates at a density of 40-60% and 2000 ng/µl poly(I:C) was added to the medium without transfection reagent briefly after. As negative control, an equal volume of standard growth medium was added.

2.3. Treatments

2.3.1. Cisplatin

Cells were treated with cisplatin to analyze subsequent transcriptional and phenotypic changes. To this end, cells were seeded in 6-well plates 24 hours prior to cisplatin treatment, aiming for a density of 40-60% on the day of treatment. Cells were treated with 20 µM cisplatin (EBEWE Pharma Ges.m.b.H. Nfg. KG, Unterach, Austria) or equal volumes of physiological 0.9% sodium chloride (NaCl) solution as negative control for 48 hours.

2.3.2. Cisplatin-conditioned medium

For experiments with cisplatin-conditioned medium, cells were seeded 24 hours before cisplatin treatment, aiming for a density of 40-60% on the day of treatment. HuCC-T1 and OCUG-1 cells were treated with 50 µM and 100 µM cisplatin or corresponding volumes of NaCl as negative control, respectively. Two hours after cisplatin addition, the medium was removed and cells were washed twice with phosphate-buffered saline (PBS; Catalog #: P04-36500, PAN-Biotech GmbH, Aidenbach, Germany) to ensure complete removal of cisplatin. Fresh standard growth medium was then added, followed by another medium replacement two hours later to ensure cisplatin-free culturing conditions. After 24 hours, medium from treated cells was transferred to cells cultured in parallel without cisplatin. These cells were incubated with cisplatin-conditioned medium for 48 hours.

2.4. Co-treatment experiments

Co-treatment experiments were conducted to investigate the function of integral pathway components.

2.4.1. JAK/STAT pathway inhibition

For co-treatment experiments using the JAK1, JAK2, and Tyrosine Kinase 2 (TYK2) inhibitor ruxolitinib (Catalog #: HY-50856, MedChemExpress), cells were seeded and transfected with poly(I:C) as previously described. In addition to the normal transfection process, 20 µM ruxolitinib or equivalent volumes of dimethyl sulfoxide (DMSO) as negative control were added to the medium for the full duration of the standard 48-hour incubation.

2.4.2. Nucleases

For experiments involving nucleases, cells were treated with cisplatin as previously described. Additionally, 10 U/ml RNase III, or 40 U/ml Benzonase were added for the full duration of the standard 48-hour treatment. Respective concentrations of nucleases were selected based on concentrations found in published studies. Preliminary test experiments confirmed the effectiveness of nucleases.

2.5. Generation of stable miRNA overexpression cell lines

In an effort to confirm results of our transient miR-200c-3p overexpression experiments, we generated cell lines with stable miR-200c-3p overexpression using a lentiviral approach. OCUG-1 and MMNK-1 cells were seeded into 12-well plates at a density of 40-60% and incubated for 24 hours under standard conditions. Subsequently, the medium was replaced with standard growth medium containing 10 µg/ml polybrene (Catalog #: sc-134220, Santa Cruz Biotechnology Inc., Dallas, Texas, USA) and 0.5% ViralEntry™ Transduction Enhancer (Catalog #: G515, Applied Biological Materials, Vancouver, Canada). Additionally, 25µl of either LentimiRa-GFP-hsa-miR-200c-3p virus (Catalog #: mh15263, Applied Biological Materials; detailed vector map shown in Figure 1a) or Lenti-III-mir-GFP Control virus (Catalog #: m002, Applied Biological Materials; detailed vector map shown in Figure 1b) as control counterpart were added to facilitate viral transduction. Both lentiviral vectors included a gene encoding for green fluorescent protein (GFP) and a puromycin resistance gene ($Puro^R$).

To ensure enrichment of successfully transduced cells, we performed continuous selection with a sublethal concentration of puromycin (Catalog #: A1113803, Gibco Thermo Fisher Scientific) for up to eight weeks. To further isolate cells with above-average miRNA overexpression levels, transduced cells were sorted based on their GFP intensity via Fluorescence-Activated Cell Sorting (FACS) using the FACSARia IIIu (BD Biosciences, Franklin Lakes, New Jersey, USA). Cells displaying the top 20% GFP intensity were cultured

and used for subsequent experiments. Cell sorting was performed by the Flow Cytometry Core Facility at the Center for Medical Research (ZMF), Medical University of Graz, Graz, Austria.

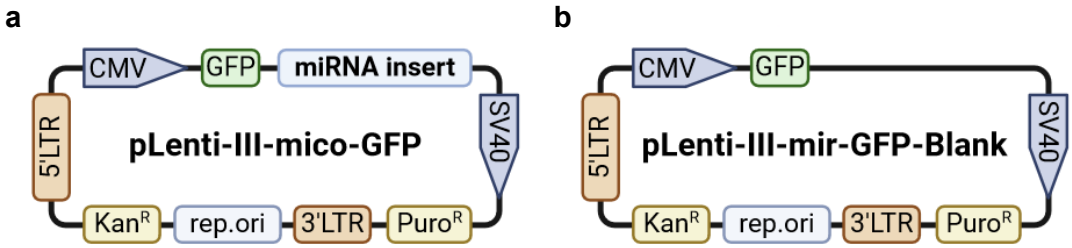

Figure 1: Schematic representations of used lentiviral vectors. Cells were transduced with either **(a)** pLenti-III-mico-GFP or **(b)** pLenti-III-mir-GFP-Blank. Both vectors are under the control of a CMV promoter and SV40 promoter, and contain genes coding for GFP, a puromycin resistance gene ($Puro^R$), a kanamycin resistance gene (Kan^R), an origin of replication (rep.ori), and 3' long terminal repeat (3'LTR) and 5'LTR. Additionally, pLenti-III-mico-GFP contains the gene coding for miR-200c-3p (miRNA insert), which is missing in the pLenti-III-mir-GFP-Blank vector. Reproduced with modifications from vector maps provided by the manufacturer Applied Biological Materials. Image created with Biorender.com.

2.6. Reverse transcription quantitative PCR (RT-qPCR)

Reverse transcription quantitative PCR (RT-qPCR) was used to assess transcriptional changes at the RNA level. Therefore, RNA was isolated, reversely transcribed to complementary DNA (cDNA), and relative mRNA levels of genes of interest were measured.

2.6.1. RNA isolation

RNA was isolated from 70-90% confluent cells using TRIzol™ Reagent (Catalog #: 15596026, Thermo Fisher Scientific) according to the manufacturer's instructions. In brief, growth medium was removed and cells were washed once with PBS. Subsequently, 1 ml of TRIzol was added to the wells, cells were detached, and TRIzol lysates were transferred to Eppendorf tubes. TRIzol lysates were either stored at -20°C or immediately processed.

For RNA isolation, TRIzol lysates were passed through Sterican® 22G needles (Catalog #: 4650018, B.Braun Melsungen AG, Melsungen, Germany) to ensure complete cell lysis. After a 15-minute incubation at RT to facilitate the dissociation of nucleoprotein complexes, 100 µl of 1-bromo-3-chloropropane (BCP) was added to each tube. Tubes were shaken vigorously, incubated for 3 minutes on RT, and centrifuged at 13,000 rounds per minute (rpm) and 4°C for 20 minutes, leading to a phase separation. The upper aqueous phase containing RNA was transferred to a fresh tube containing isopropyl alcohol (Catalog #: 1096341011, Merck KGaA, Darmstadt, Germany), mixed properly and centrifuged at 13,000 rpm and 4°C for 30 minutes. Precipitated RNA formed a pellet at the bottom of the tubes. The supernatant was discarded,

75% ethanol (Catalog #: 1009831000, Merck KGaA) was added, followed by a centrifugation at 13,000 rpm and 4°C for 5 minutes. This washing step was repeated a total of three times. After the last washing step, the supernatant was completely removed and the RNA pellet was dried at RT to ensure complete removal of ethanol. Subsequently, the RNA pellet was resuspended in 20 µl RNase-free water.

RNA concentration and purity was assessed on NanoDrop™ 2000/2000c spectrophotometer (Catalog #: ND-2000, Thermo Fisher Scientific). Purity was evaluated by the ratio of absorbance at 260 nm (A260) and 280 nm (A280), which indicates protein contamination, and the ratio of A260 to A230, which mainly detects phenol contamination. RNA samples with an A260/A280 ratio above 1.8 and an A260/A230 ratio above 2.0 were considered to be sufficiently pure for further analysis.

2.6.2. Reverse transcription

Reverse transcription of RNA into cDNA was performed using the miScript II RT Kit (Catalog #: 218161, QIAGEN) according to the manufacturer's instructions. In a 20 µl reaction, 1 µg of total RNA was combined with 10x miScript Nucleics Mix, 5x miScript Reverse Transcriptase Mix and 5x miScript HiFlex Buffer to enable quantification of both miRNAs and mRNAs. For each reverse transcription run, we included a no-template control (NTC) lacking RNA to detect nucleic acid contamination in the kit components, as well as a control lacking reverse transcriptase (RT- control) to detect potential genomic DNA contamination in our RNA sample. After a 60-minute incubation on 37°C and a 5-minute incubation at 95°C to inactivate the reverse transcriptase, cDNA was either stored at -20°C or -80°C, or immediately used for qPCR.

2.6.3. Quantitative PCR (qPCR)

Quantitative PCR was performed using the QuantiTect SYBR® Green PCR Kit (Catalog #: 204145, QIAGEN) following a slightly adapted version of the manufacturer's two-step RT-qPCR protocol, optimized for the simultaneous detection of miRNA and mRNA.

For the detection of miRNAs, 1 ng template cDNA was mixed with 2x QuantiTect SYBR Green PCR Master Mix, 10x miScript Universal Primer, 10x miScript Primer assay targeted at the specific miRNA of interest, and RNase-free H_2O to reach a total volume of 10 µl per reaction. Hs_miR-141_1 miScript Primer Assay (Catalog #: MS00003507, QIAGEN), Hs_miR-200a_1 miScript Primer Assay (Catalog #: MS00003738, QIAGEN), Hs_miR-200b_3 miScript Primer Assay (Catalog #: MS00009016, QIAGEN), Hs_miR-200c_1 miScript Primer Assay (Catalog

#: MS00003752, QIAGEN), Hs_miR-429_1 miScript Primer Assay (Catalog #: MS00004193, QIAGEN), and Hs_RNU6-2_11 miScript Primer Assay (Catalog #: MS00033740, QIAGEN) were used, with RNU6-2 (=RNU6B) serving as reference gene.

For mRNA detection, 10 ng of template cDNA was combined with 2x QuantiTect SYBR Green PCR Master Mix, 0.4 µM of forward and reverse primer specific to the gene of interest, and RNase-free H_2O to a final volume of 10 µl. Primers were designed using the NIH Primer Blast Tool (https://www.ncbi. nlm.nih.gov/tools/ primer-blast/; last accessed on 20.09.24), opting for a PCR product size of 70-200 bp, a primer GC content of 40-60%, and an optional GC clamp of 1-2. When applicable, primers were designed to span exon junctions or be located on different exons to exclude amplification of genomic DNA. Primers were obtained from Eurofins Scientific SE (Luxembourg City, Luxembourg). Sequences for the forward and reverse primer pairs are listed in Table 1. The average expression of GAPDH and U6 was used as reference.

After initial denaturation at 95°C for 15 minutes, samples underwent 40 cycles of denaturation at 94°C for 15 seconds, annealing at 55°C for 30 seconds, and extension at 70°C for 30 seconds. After each cycle, resulting SYBR® Green fluorescence was acquired for quantification. A melting curve analysis was performed to confirm specific amplification. Each sample was measured in technical duplicates.

The quantification of miRNAs and mRNAs was normalized to the respective reference genes, reported as ΔCt values. For relative expression analysis, ΔΔCt values were calculated by subtracting the mean ΔCt of corresponding negative controls from ΔCt of treated samples. Unless otherwise indicated, expression differences throughout the project were reported as ΔΔCt values. Quantitative PCR was performed on the LightCycler® 480 (Roche, Mannheim, Germany). RT-qPCR results were considered reliable only if the NTC and RT- control were negative for all tested genes.

Table 1. Primer sequences used for RT-qPCR. Reproduced with modifications from (1) with permission via the CC BY 4.0 license.

Target	forward primer (5' to 3')	reverse primer (5' to 3')
KRT8	ATGTTGTCCATGTTGCTTCG	CCAGGAGAAGGAGCAGATCA
CDH1	TGAAGGTGACAGAGCCTCTGGAT	GGGTGAATTCGGGCTTGTT
N-cadherin	GACGGTTCGCCATCCAGAC	TCGATTGGTTTGACCACGG
COL3A1	ATATTTGGCATGGTTCTGGC	TGGCTACTTCTCGCTCTGCT
Vimentin	CCTTGAACGCAAAGTGGAATC	GACATGCTGTTCCTGAATCTGAG
ZEB1	GATGATGAATGCGAGTCAGATGC	ACAGCAGTGTCTTGTTGTTGT
ZEB2	CAAGAGGCGCAAACAAGCC	GGTTGGCAATACCGTCATCC
B7H2	GCAGCCTTCGAGCTGATACTC	GTTTTCGACTCACTGGTTTGC

Table 1. (continued)

Target	forward primer (5' to 3')	reverse primer (5' to 3')
B7H3	CACTGTGGTTCTGCCTCACA	AGATGAGGTTGAGCTGTGCC
B7H4	TCTGGGCATCCCAAGTTGAC	TCCGCCTTTTGATCTCCGATT
B7H5	ACGCCGTATTCCCTGTATGTC	TTGTAGAAGGTCACATCGTGC
CD47	TCCGGTGGTATGGATGAGAAA	ACCAAGGCCAGTAGCATTCTT
CD80	AAACTCGCATCTACTGGCAAA	GGTTCTTGTACTCGGGCCATA
CD86	CTGCTCATCTATACACGGTTACC	GGAAACGTCGTACAGTTCTGTG
CEACAM1	CCACTTCACAGAGTGCGTGT	CCAAAAAGTTGCTGGGGCAG
CLEC4G	AGTCCTTTGGGCTGTGATTCT	AGGCGTTTGTCCTCAGCAG
HLA-A	CATCTCTGACCATGAGGCCA	GGCAGGTGTATCTCTGCTCC
HLA-DPA1	ATGCGCCCTGAAGACAGAATG	ACACATGGTCCGCCTTGATG
HMGB1	TTTGTGCAAACTTGTCGGGAG	TTCCACCTCTCTGAGCACTT
IDO1	GCCAGCTTCGAGAAAGAGTTG	ATCCCAGAACTAGACGTGCAA
LGALS3	ATGGCAGACAATTTTTCGCTCC	GCCTGTCCAGGATAAGCCC
LGALS9	GGACGGACTTCAGATCACTGT	CCATCTTCAAACCGAGGGTTG
PD-L1	TGGCATTTGCTGAACGCATTT	TGCAGCCAGGTCTAATTGTTTT
PD-L2	ATTGCAGCTTCACCAGATAGC	AAAGTTGCATTCCAGGGTCAC
TNFRSF5	ACTGAAACGGAATGCCTTCCT	CCTCACTCGTACAGTGCCA
TNFRSF14	GTGCAGTCCAGGTTATCGTGT	CACTTGCTTAGGCCATTGAGG
TNFSF4	CCAGGCCAAGATTCGAGAGG	CCGATGTGATACCTGAAGAGCA
TNFSF9	GGCGTCCATCTTCACACTGA	CACCCAGGCTGGACGTTATT
TLR3	AAAACCTTTGCCTTCTGCACG	TTCCAGCTGAACCTGAGTTCC
RIG-I	GACCCTACCTACATCCTGAGC	CTTCATAAAGTCCAGAATAACCTGC
MDA5	TTGGCAGAAGGAAGTGTCAGC	TTCTTCCCTTCCAAGGCTGG
IFNB1	CAACCTTTCGAAGCCTTTGC	TCCCATTCAATTGCCACAGG
IFNL1	TCTGAGAACGTCAACCCACC	TATGTCTCAGTCAGGGCTGC
IFNL2	GAATTGTGTTGCCAGTGGGG	CATTTTCCTGGAGGTGAGTTGG
IFNL3	TGAAACTAGACATGACCGGGG	GAGACAGGGACTTGAACTGGG
MX1	GGACATCGCAAAAGCTGATCC	GTTGTTCTCAGCCACCGAGC
PKR	CTTCCATCTGACTCAGGTTTGC	TCTTCTTCCCGTATCCTGGTTGG
OAS1	AAGCTCAAGAGCCTCATCCG	TCCAAGACCGTCCGAAATCC
IFNAR1	GCACACACCATGGATGAAAAGC	GCCAAATTTTAGAGGTATTTCCTGG
IFNAR2	ATAGCAAAGATGCTTTTGAGCC	TGCAAGATTCATCTGTGTAATCAGG
IFNLR1	TGGCCTATCAGAGCTCTCCC	TCAGGATCTCCTCCGTCTGG
IL10RB	ACAACCCATGACGAAACGG	GAATTCCTAGGGGAGAAGGCG
GAPDH	AAGGTCGGAGTCAACGGATTT	ACCAGAGTTAAAAGCAGCCCTG
U6	CTCGCTTCGGCAGCACA	AACGCTTCACGAATTTGCGT

2.7. Western blot

2.7.1. Sample preparation

For protein isolation, cells at a density of 70-90% were washed once with cold PBS. Radioimmunoprecipitation assay (RIPA) buffer containing 150 mM NaCl, 50 mM Tris-HCl, 1% Triton X-100, 0.1% SDS, 0.1% sodium deoxycholate, 1% Nonidet P-40, at pH 7.5, supplemented with 1% Protease Inhibitor Cocktail (Catalog #: P8340, Sigma-Aldrich Handels GmbH, Vienna, Austria) and 0.5% Phosphatase Inhibitor Cocktail 3 (Catalog #: P044-1ML, Sigma-Aldrich Handels GmbH), was added. Cells were mechanically detached from the culture dish on ice using a cell scraper, and lysates were transferred to fresh tubes. After a 20-minute incubation on ice, the lysates were centrifuged at 13,000 rpm and 4°C for 15 minutes to obtain a cell debris-free protein solution. Protein concentration was determined using the Pierce™ BCA Protein Assay (Catalog #: 23225, Thermo Fisher Scientific) according to the manufacturer's instructions. 30 µg of total protein per sample was mixed with 4x Laemmli Sample Buffer (Catalog #: 1610747, Bio-Rad Laboratories, Inc., Hercules, CA, USA) containing 10% β-mercaptoethanol and denatured at 95°C for 10 minutes.

2.7.2. Procedure

Proteins were separated on 4-15% Mini-PROTEAN® TGX Stain-free™ Gels (Catalog #: 4568084, Bio-Rad Laboratories, Inc.) by gel electrophoresis at 120 V. The separated proteins were transferred to a 0.45 µm nitrocellulose membrane (Catalog #: 1620115, Bio-Rad Laboratories, Inc.) in Tris/glycine buffer (Catalog #: 1610734, Bio-Rad Laboratories, Inc.) with 20% methanol at 400 mA and 4°C for up to two hours. Membranes were blocked with 5% milk powder in Tris-buffered saline with 0.1% Tween® 20 (TBS-T) for one to five hours, then incubated with primary antibodies at 4°C for 16 hours. After three washing steps with TBS-T, membranes were incubated with the corresponding secondary horseradish peroxidase (HRP)-conjugated antibodies at RT for one hour. Following three additional washing steps with TBS-T, membranes were incubated with SuperSignal™ West Pico PLUS Chemiluminescent Substrate (Catalog #: 34579, Thermo Fisher Scientific) or SuperSignal™ West Femto Maximum Sensitivity Substrate (Catalog #: 34094, Thermo Fisher Scientific) at RT for 5 minutes. Chemiluminescent signals were captured using a ChemiDoc™ Touch (Bio-Rad Laboratories, Inc.).

To ensure equal protein loading, membranes were stripped using a buffer containing 15 g/l glycine, 1 g/l sodium dodecyl sulfate (SDS), 1% Tween® 20, and pH 2.2 (according to the

Abcam Mild stripping protocol). Membranes were then re-probed with primary antibody directed against Cofilin at 4°C for 16 hours, followed by three washing steps and a 1-hour incubation with the corresponding secondary HRP-conjugated antibody at RT. Chemiluminescent signals were detected and imaged as described above. Antibodies used are listed in Table 2.

Table 2. Primary and secondary antibodies used for western blot. Reproduced with modifications from (1) with permission via the CC BY 4.0 license.

Primary antibodies			
Antibody	Dilution	Catalog #	Manufacturer
E-cadherin (G-10)	1:1000	sc-8426	Santa Cruz Biotechnology
TCF8/**ZEB1** (D80D3) Rabbit mAb	1:1000	#3396	Cell Signaling Technology®
IDO Recombinant Rabbit Monoclonal Antibody (7H8L17)	1:2000	#702743	Thermo Fisher Scientific
PD-L1/CD274 Monoclonal antibody	1:5000	66248-1-Ig	Proteintech Group, Inc.
IRF-3 (D6I4C) XP® Rabbit mAb	1:2000	11904	Cell Signaling Technology®
P-IRF-3 (S386) (E7J8G) XP® Rabbit mAb	1:1000	37829	Cell Signaling Technology®
Anti-**Cofilin** antibody	1:5000	ab42824	Abcam
Secondary antibodies			
Antibody	Dilution	Catalog #	Manufacturer
Rabbit **Anti-Mouse** IgG (Light Chain Specific) (D3V2A) mAb (HRP Conjugate)	1:2000	#58802	Santa Cruz Biotechnology
Peroxidase AffiniPure Goat **Anti-Rabbit** IgG antibody	1:10000	111-035-144	Jackson ImmunoResearch

2.8. Immunofluorescence

To evaluate intracellular localization of NF-κB following poly(I:C) transfection, immunofluorescence was used. HuCC-T1 cells were seeded in 6-well plates containing cover slips at the bottom of the wells, at a density of 70-80%. After a 3-hour transfection with poly(I:C), cover slips were removed and washed with ice-cold PBS. Subsequently, cells were fixed with cold 100% methanol at -20°C for 15 minutes and permeabilized with 0.5% Triton™ X-100 (Catalog #: T8787, Sigma-Aldrich Handels GmbH) in PBS at -20°C for 15 minutes. After additional washing steps with PBS, 6% bovine serum albumin (BSA; Catalog #: 9998S, Cell Signaling Technology) in PBS was added to the cover slips to prevent unspecific antibody binding.

The cover slips were incubated with primary antibody against NF-κB (NF-κB p65 (D14E12) XP® Rabbit mAb, Catalog #: 8242, Cell Signaling Technology; diluted 1:100 in Dako Antibody Diluent) or with Dako Antibody Diluent (Catalog #: S0809, Agilent, Santa Clara, CA, USA) as

negative control at 4°C for 16 hours in a humidified atmosphere. After additional washing steps with PBS, fluorescent dye-conjugated secondary antibody (Goat Anti-Rabbit IgG (H+L), Highly Cross-Adsorbed Secondary Antibody, Alexa Fluor Plus 594, Catalog #: A32740, Invitrogen; diluted 1:1,000 in 3% BSA in PBS) was added at 4°C for 60 minutes in darkness. Following a 20-minute nuclear staining with 4',6-Diamidino-2-Phenylindole (DAPI, Catalog #: D1306, Thermo Fisher Scientific) at RT, cover slips were mounted onto the object slides with Dako Fluorescence Mounting Medium (Catalog #: S3023, Agilent) and placed to 4°C over night. Cells were examined and imaged using a Nikon A1 Confocal Laser Scanning Microscope (Nikon, Tokyo, Japan).

2.9. Enzyme-linked Immunosorbent Assay (ELISA)

To measure extracellular Interferon Beta (IFN-β) concentrations after poly(I:C) transfection or cisplatin treatment, an Enzyme-linked Immunosorbent Assay (ELISA) was performed using the Human IFN-β Quantikine ELISA Kit (Catalog #: DIFNB0, Bio-Techne, Minneapolis, Minnesota, USA). Poly(I:C) transfection and cisplatin treatment were performed as previously described. After 48 hours, the culture supernatants were collected, centrifuged at 1,500 rpm for 10 minutes to remove cell debris, and either stored at -20°C or immediately processed.

For the ELISA procedure, manufacturer's instructions were followed. In short, Assay Diluent RD1-19 was added to the wells of a 96-well plate pre-coated with antibodies directed against IFN-β. Technical duplicates of provided standards, corresponding controls, and samples were added to the wells. The plate was incubated at RT for two hours on a horizontal orbital microplate shaker Titramax 1000 (Heidolph Instruments GmbH & Co. KG, Schwabach, Germany). After four washing steps with prepared Wash Buffer, Human IFN-β conjugate was added to the wells, followed by a two-hour incubation at RT on the horizontal orbital microplate shaker. After four additional washing steps with Wash Buffer, Substrate Solution was added, and the plate was incubated at RT for 30 minutes. Stop Solution was added and optical density was measured at 450 nm, with 540 nm for wavelength correction, using the CLARIOstar Plus Microplate Reader (BMG LABTECH GmbH, Ortenberg, Germany).

2.10. WST-1 assay

In order to determine the different effects that miRNA mimics have on the number of viable cells, WST-1 assay (Catalog #: CELLPRO-RO, Roche, Basel, Switzerland) was performed. To this end, HuCC-T1 and OCUG-1 cells were seeded in 96-well plates at a density of 40-60%. As previously mentioned, cells were transfected according to the reverse transfection protocol

of the HiPerFect transfection reagent. 24, 48, 72, and 96 hours after transfection, WST-1 reagent was added to each well and resulting optical density was measured at 450 nm, with 620 nm as reference wavelength, after a 1-hour incubation using the SPECTROstar Omega Microplate Reader (BMG LABTECH GmbH).

2.11. Caspase 3/7 Glo® assay

The apoptotic behavior of cells upon transfection of miRNA mimics was evaluated using Caspase 3/7 Glo® assay (Cat. #: G8090, Promega, Madison, Wisconsin, USA) according to the manufacturer's recommendations. Similar to the transfection procedure for WST-1 assay, cells were seeded in 96-well plates at a density of 40-60% and transfected following the HiPerFect reverse-transfection protocol. After 72 hours, Caspase 3/7 Glo® Reagent was added to each well and resulting luminescent signal was measured on the LUMIstar Omega Microplate Reader (BMG LABTECH GmbH).

2.12. Statistical analysis

All experiments were conducted at least three independent times, unless stated otherwise. Data are presented as mean ± standard deviation (SD). Statistical analyses were performed using GraphPad Prism version 10.0.2 for macOS (GraphPad Software, Boston, Massachusetts, USA). Non-parametric tests were used for sample sizes of $n \geq 5$, while parametric tests were applied for $n \leq 3$, to address the limited power of non-parametric tests with small sample sizes. Although non-parametric tests are generally preferred for biological data as they avoid assumptions about the data distribution, parametric tests were deemed acceptable in that case, provided that careful consideration was given to statistical significances for small biological differences. In a methodological paper by de Winter, the t test was demonstrated to perform reliably with extremely small sample sizes, especially when effect sizes are large, making it preferable to rank-based tests like the Mann-Whitney test in such scenarios (223). Generally, P values smaller than $\alpha = 0.05$ were considered statistically significant. * $P \leq 0.05$, ** $P \leq 0.01$, *** $P \leq 0.001$.

The heatmap was generated in R version 4.4.1 using the "ComplexHeatmap" package (224,225). Within the heatmap, RT-qPCR data were normalized within the respective genes across different cell lines using z-scores.

3. Results

3.1. Endogenous relationship between miR-200 family, EMT markers, and ICs

In order to validate the robustness of our cell models in mimicking pathophysiology and capturing various of EMT states, we first examined the well-described connection between miR-200 family members and EMT marker expression. To this end, we measured the endogenous expression levels of miR-141-3p, miR-200a-3p, miR-200b-3p, miR-200c-3p, and miR-429, epithelial markers CDH1 and KRT8, and mesenchymal markers ZEB1, ZEB2, Vimentin, COL3A1, and N-cadherin across ten BTC cell lines and the immortalized cholangiocyte cell line MMNK-1 by RT-qPCR (Figure 2a, left panel).

Unsupervised hierarchical clustering revealed two distinct groups of cells. The cell lines OZ, KKU-213, EGI-1, HuCC-T1, and TFK-1 displayed epithelial characteristics, with high endogenous miR-200 family and epithelial marker expression and low mesenchymal marker expression. Conversely, HuH-28, KKU-100, NOZ, OCUG-1, KKU-055, and MMNK-1 cells exhibited a mesenchymal state, characterized by low miR-200 family and epithelial marker expression, and increased mRNA levels of mesenchymal markers.

This presence of clear epithelial and mesenchymal clusters, together with the strong positive correlation between miR-200 family member expression and epithelial markers (Figure 2b) and the negative correlation with mesenchymal markers (Figure 2c), confirm the capacity of our cell models to accurately reflect the EMT process.

To investigate a potential relationship between the EMT status and IC expression, we measured the endogenous expression levels of 21 ICs across our cell lines (Figure 2a, right panel). ICs like B7 Homolog 3 (B7H3) and High Mobility Group Box 1 Protein (HMGB1), displayed consistently high expression across multiple cell lines, whereas others, such as Major Histocompatibility Complex, Class II, DP Alpha 1 (HLA-DPA1), Tumor Necrosis Factor Ligand Superfamily Member 4 (TNFSF4), and IDO1 were only expressed in individual cell lines, with no clear association with the EMT status.

However, ICs such as PD-L1, Cluster of Differentiation 47 (CD47), and LGALS9 showed high expression levels in epithelial cell lines, with negligible expression in mesenchymal cell lines. Conversely, Tumor Necrosis Factor Ligand Superfamily Member 9 (TNFSF9) was

predominantly expressed in mesenchymal cell lines. While miR-200 family expression did not correlate with overall IC expression (Figure 2d), specific ICs such as LGALS9 were positively correlated with miR-200 family levels (Figure 2e).

Furthermore, we observed a weak positive correlation between miR-200 family and PD-L1 expression (Figure 2f) and a marginal negative correlation with TNFSF9 expression (Figure 2g). Despite these insignificant correlations, it is worth noting that the highest PD-L1 expression levels are found within epithelial cell lines HuCC-T1, EGI-1, and KKU-213, while highest TNFSF9 expression were detected in mesenchymal cells, suggesting a more cell line-specific but still EMT-related regulation of these ICs.

3.2. Transient miR-141-3p and miR-200c-3p overexpression influences EMT

Initial *in vitro* gain-of-function studies offer a quick and efficient method to investigate a potential relationship between specific targets and their immediate effects on phenotypes or gene expression patterns. By transfecting cells with miRNA mimics – synthetic dsRNA molecules consisting of the mature miRNA of interest and a passenger strand – desired miRNAs can be transiently overexpressed and their downstream targets and associated phenotypic changes can be studied.

We transfected epithelial HuCC-T1 cells and mesenchymal OCUG-1, HuH-28, and MMNK-1 cells with either miR-141-3p mimic or miR-200c-3p mimic and evaluated intracellular levels of respective miRNAs and resulting transcriptional changes of epithelial markers CDH1 and KRT8, and mesenchymal markers ZEB1 and ZEB2 compared to cells transfected with negative control. Additionally, we tested whether a co-transfection of both miRNA mimics was required to trigger phenotypic changes.

After 48 hours, miR-141-3p levels were significantly increased in cells transfected with miR-141-3p mimic, while miR-200c-3p levels remained unchanged. Similarly, intracellular levels of mature miR-200c-3p were markedly increased upon transfection of miR-200c-3p mimic in all cell lines (Figure 3a-d), confirming the selective and efficient action of miRNA mimics. Co-transfection of both miRNA mimics led to a robust overexpression of both miRNAs, reaching similar levels as transfections with the individual miRNA mimics.

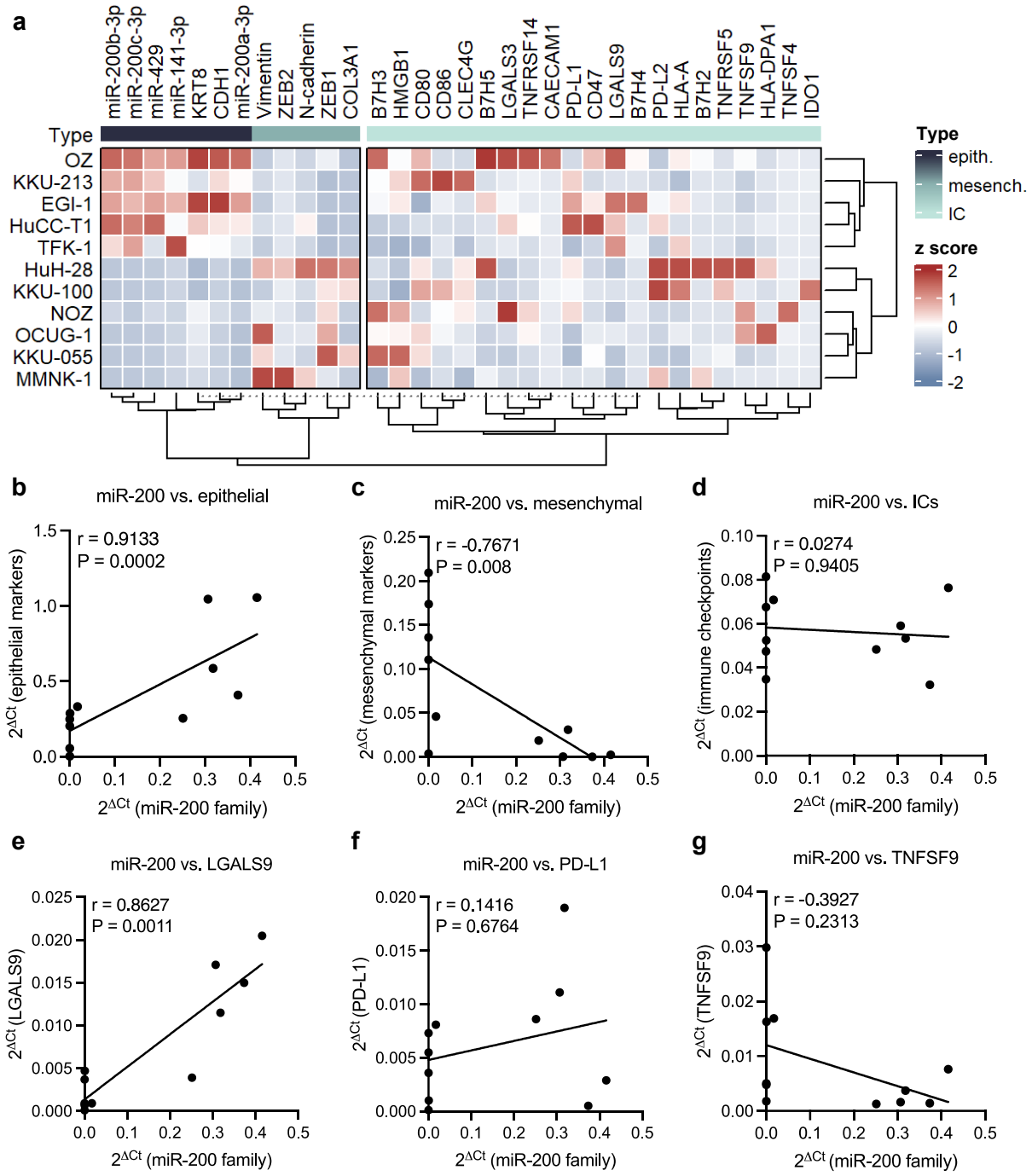

Figure 2: Endogenous expression of miR-200 family members distinguishes epithelial and mesenchymal BTC cell lines and correlates with IC expression. (a) Unsupervised hierarchical clustering of normalized endogenous expression levels (z score) of miR-200 family members (miR-141-3p, miR-200a-3p, miR-200b-3p, miR-200c-3p, miR-429), epithelial markers (CDH1, KRT8), mesenchymal markers (ZEB1, ZEB2, Vimentin, COL3A1, N-Cadherin), and ICs (right panel) across ten BTC cell lines and the immortalized cholangiocyte cell line MMNK-1. **(b-g)** Spearman's rank correlation between the average miR-200 family expression and the average expression of epithelial markers, mesenchymal markers, ICs, or the individual expression of LGALS9, PD-L1, and TNFSF9. Spearman's rank correlation coefficient (r) and significance level (P) are indicated within the graphs. Reproduced with modifications from (1,2) with permission via the CC BY 4.0 license.

The effects of miRNA mimic transfection on EMT marker expression varied. In HuH-28 and MMNK-1 cells, transient overexpression of miR-200c-3p, but not miR-141-3p, resulted in a significant increase in epithelial marker expression and a partial decrease of mesenchymal markers, indicating an expected miR-200 family-mediated shift from a mesenchymal to a more epithelial phenotype (Figure 3g, h). Co-transfection of both mimics delivered similar results as individual miR-200c-3p overexpression.

No significant changes of EMT marker expression upon transient miRNA overexpression were observed in HuCC-T1 cells (Figure 3e), suggesting that an additional supply of miR-200 family members does not further influence a pre-existing epithelial phenotype. Of note, although baseline CDH1 transcript levels were below the RT-qPCR detection limit in OCUG-1 cells and therefore not quantified (Figure 3f), transient miR-141-3p and miR-200c-3p overexpression resulted in detectable CDH1 levels, indicating a partial shift toward an epithelial state. However, expression levels of KRT8 or ZEB1 were not influenced.

Consistent with results on RNA level, ZEB1 and CDH1 protein levels were only marginally influenced by transient miR-141-3p or miR-200c-3p overexpression in the epithelial HuCC-T1 cells (Figure 4a). In contrast, mesenchymal HuH-28 and MMNK-1 cells displayed a notable decrease in ZEB1 protein levels upon miR-141-3p mimic and miR-200c-3p mimic transfection compared to cells transfected with negative control (Figure 4b, c). Of note, although RT-qPCR detected minimal levels of CDH1 mRNA in these mesenchymal cells, protein levels could not be determined due to the lower sensitivity of western blotting.

In conclusion, both RNA and protein data suggest that transient overexpression of miR-141-3p and miR-200c-3p via miRNA mimic transfection is effective and generally capable of inducing epithelial characteristics in originally mesenchymal cell lines.

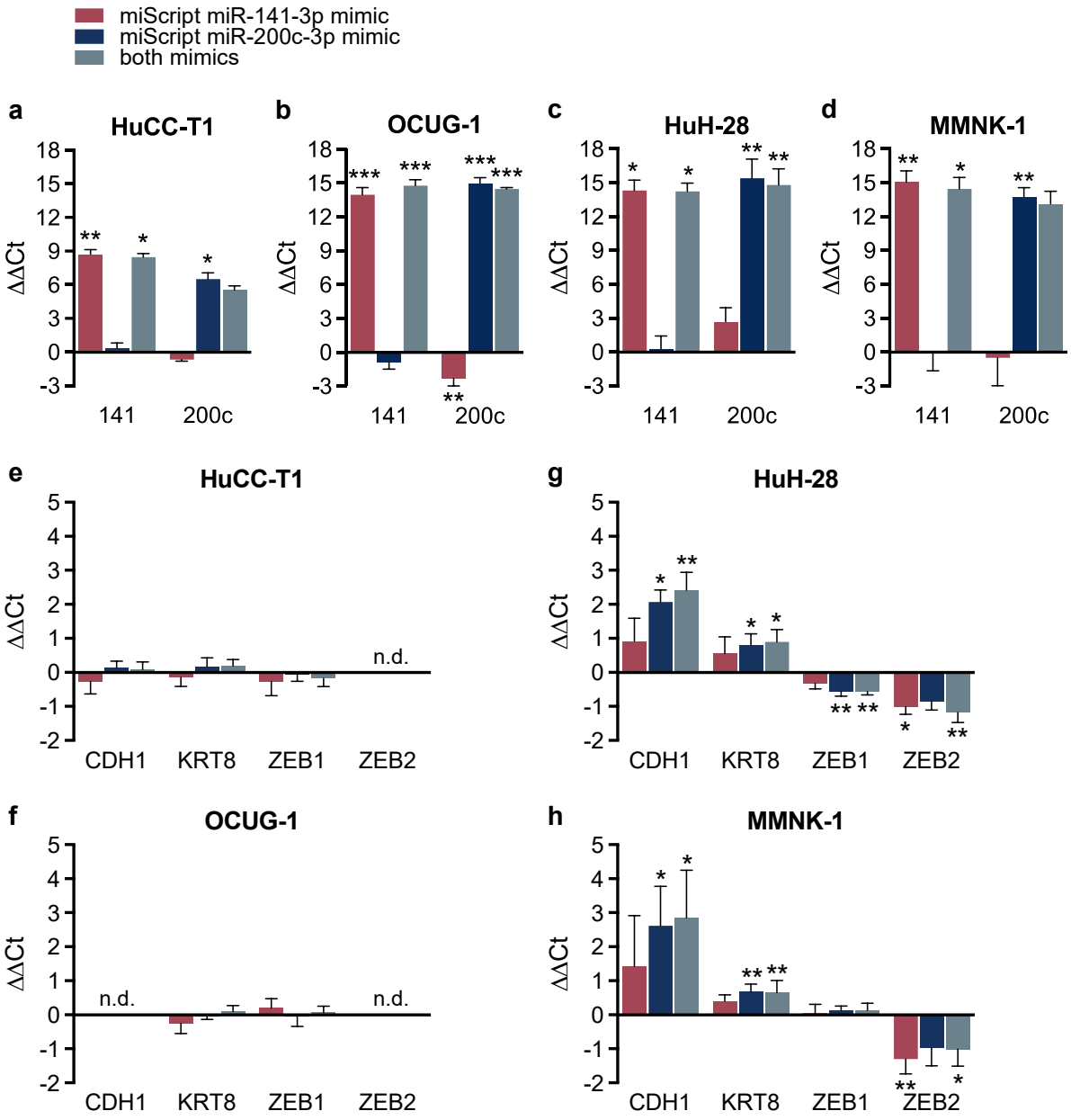

Figure 3: Transfection of miR-141-3p mimic and miR-200c-3p mimic increases levels of intracellular mature miRNAs and influences epithelial and mesenchymal marker expression. HuCC-T1 (n=5), OCUG-1 (n=3), HuH-28 (n=5), and MMNK-1 (n=5) cells were transfected with miScript mir-141-3p mimic, miScript miR-200c-3p mimic, both mimics, or Allstars Negative Control for 48 hours. Resulting intracellular RNA levels of **(a-d)** mature miRNAs, **(e-h)** epithelial markers CDH1, KRT8 or mesenchymal markers ZEB1, ZEB2 were measured by RT-qPCR. Data is presented as mean ± SD. Statistical significance was determined using one-way ANOVA corrected for multiple comparisons with the Bonferroni method for n=3 data and Kruskal-Wallis test corrected for multiple comparisons with the Dunn method for n = 5 data. * P≤0.05, ** P≤0.01, *** P≤0.001. 141 = miScript miR-141-3p, 200c = miScript miR-200c-3p. n.d. = not detectable. Reproduced with modifications from (1) with permission via the CC BY 4.0 license.

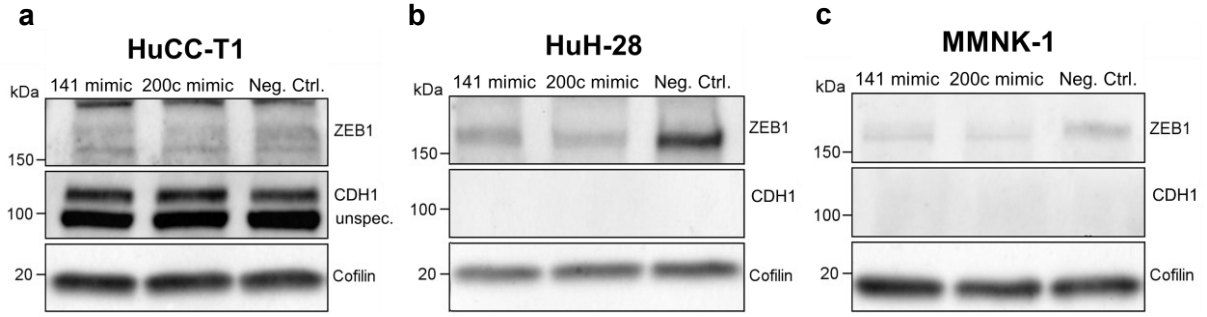

Figure 4: Transient miR-141-3p and miR-200c-3p overexpression decreases ZEB1 protein levels. **(a)** HuCC-T1, **(b)** HuH-28, and **(c)** MMNK-1 cells were transfected with miScript mir-141-3p mimic, miScript miR-200c-3p mimic, or Allstars Negative Control for 72 hours. Resulting intracellular protein levels of CDH1, ZEB1, and Cofilin (used as loading control) were analyzed by western blot. 141 mimic = miScript miR-141-3p mimic, 200c mimic = miScript miR-200c-3p mimic, Neg. Ctrl. = Allstars Negative Control. Reproduced with modifications from (1) with permission via the CC BY 4.0 license.

3.3. Transient miR-141-3p and miR-200c-3p overexpression impact IC expression

After confirming the successful and functional overexpression of miR-141-3p and miR-200c-3p, we sought to determine the influence on IC expression. To this end, cells were transfected with either miR-141-3p mimic, miR-200c-3p mimic, or both mimics, and resulting changes in the expression levels of multiple ICs were analyzed via RT-qPCR.

While the transient overexpression of miR-141-3p had a negligible influence on the transcript levels of ICs, transfection of the miR-200c-3p mimic consistently elevated mRNA levels of LGALS9, PD-L1, and IDO1 across all tested cell lines (Figure 5a-d). Additionally, ICs such as Galectin-3 (LGALS3), Carcinoembryonic Antigen-Related Cell Adhesion Molecule 1 (CEACAM1), Programmed Cell Death 1 Ligand 2 (PD-L2), and B7 Homolog 2 (B7H2) showed increased expression upon miR-200c-3p mimic transfection in individual cell lines, though these ICs were not further studied due to cell-line specific effects.

Co-transfection of miR-141-3p and miR-200c-3p mimics altered the expression levels of ICs (Figure 5a-d). However, since the overexpression patterns closely mirrored the miR-200c-3p mimic-driven changes, we concluded that this effect was primarily driven by the miR-200c-3p mimic alone rather than any synergistic action of the miRNA mimic combination.

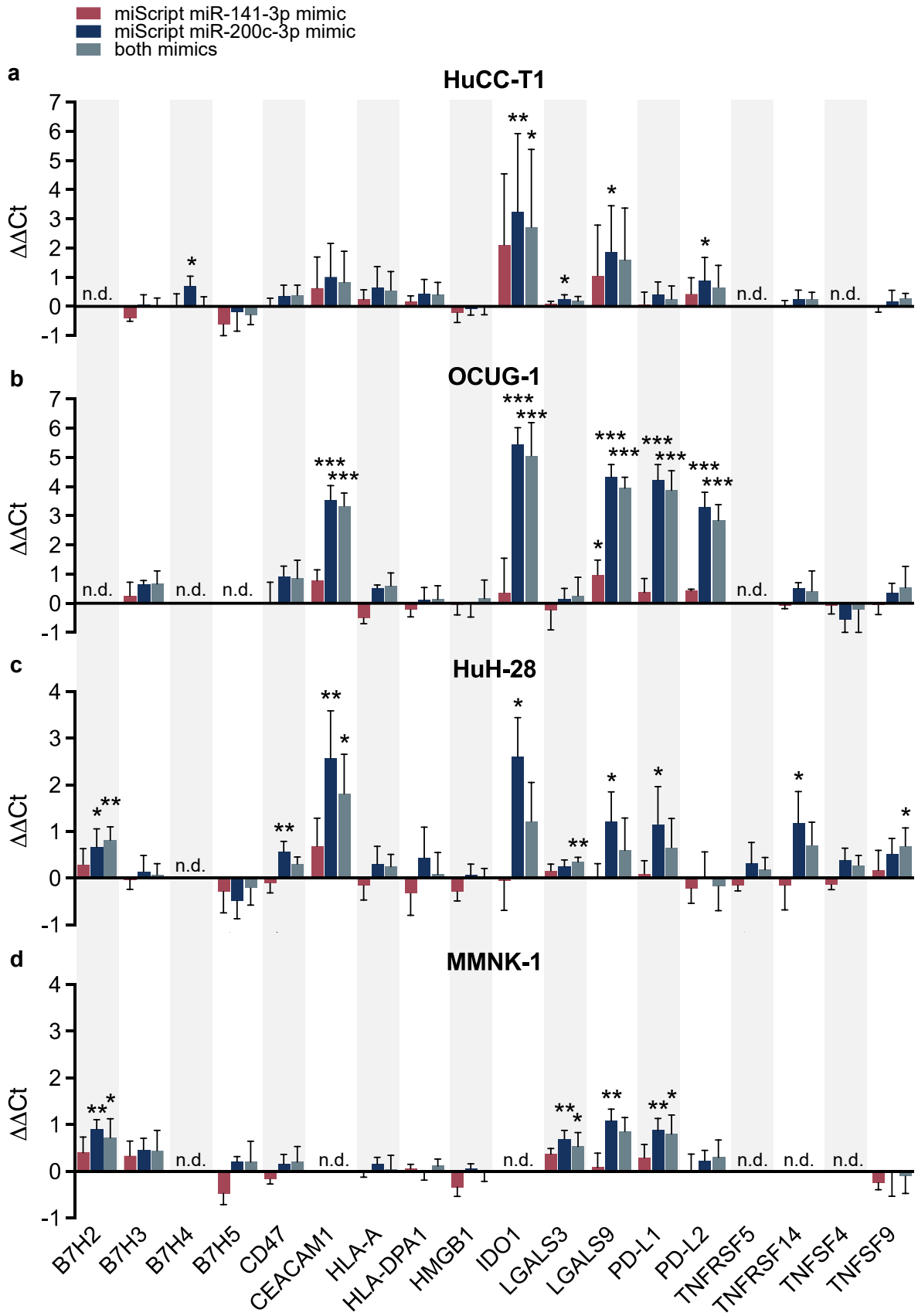

Figure 5: Transfection of miR-200c-3p mimic, but not miR-141-3p mimic, leads to an increased IC expression. (a) HuCC-T1 (n=5), **(b)** OCUG-1 (n=3), **(c)** HuH-28 (n=5), and **(d)** MMNK-1 (n=5) cells

were transfected with miScript mir-141-3p mimic, miScript miR-200c-3p mimic, both mimics, or Allstars Negative Control for 48 hours. Resulting intracellular RNA levels of ICs were analyzed by RT-qPCR. Data is presented as mean ± SD. Statistical significance was determined using one-way ANOVA corrected for multiple comparisons with the Bonferroni method for n=3 data and Kruskal-Wallis test corrected for multiple comparisons with the Dunn method for n=5 data. * P≤0.05, ** P≤0.01, *** P≤0.001. n.d. = not detectable. Reproduced with modifications from (1) with permission via the CC BY 4.0 license.

Observed expression changes at the RNA level were partly validated at the protein level. In HuCC-T1 cells, transient overexpression of miR-200c-3p resulted in a minimal increase in PD-L1 protein, whereas IDO1 protein levels were significantly elevated compared to negative-control-transfected cells. Transfection with miR-141-3p mimic also increased IDO1 level, although to a lesser extent (Figure 6a). In HuH-28 cells, transient overexpression of miR-200c-3p, but not miR-141-3p, caused a notable increase in both PD-L1 and IDO1 protein (Figure 6b). In MMNK-1 cells, while IDO1 remained undetectable consistent with its mRNA level, PD-L1 protein was notably increased upon transfection with miR-200c-3p mimic, but unaffected by miR-141-3p mimic.

Collectively, RNA and protein data demonstrate that especially miR-200c-3p mimic transfection results in a consistent upregulation of LGALS9, PD-L1, and IDO1 across all tested cell lines, implying a promising regulatory connection between miR-200c-3p and these ICs.

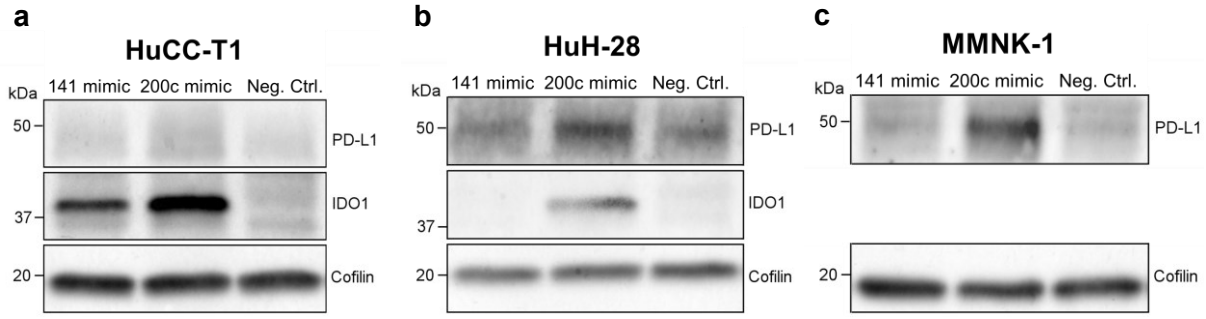

Figure 6: Transfection of miR-141-3p mimic and miR-200c-3p mimic increases PD-L1 and IDO1 protein. (a) HuCC-T1, **(b)** HuH-28, and **(c)** MMNK-1 cells were transfected with miScript mir-141-3p mimic, miScript miR-200c-3p mimic, or Allstars Negative Control for 72 hours. Resulting intracellular protein levels of PD-L1, IDO1, and Cofilin (used as loading control) were analyzed by western blot. 141 mimic = miScript miR-141-3p mimic, 200c mimic = miScript miR-200c-3p mimic, Neg. Ctrl. = Allstars Negative Control. Reproduced with modifications from (1) with permission via the CC BY 4.0 license.

3.4. Influence of miR-200c-3p on ICs is independent of miR-200/ZEB1 axis

The miR-200 family is known to influence EMT primarily through its negative regulation of ZEB1 (182). Therefore, to explore the extent to which the observed miR-200c-3p-mediated

effects on ICs are dependent on this interaction, we transiently knocked down ZEB1 expression in mesenchymal OCUG-1, HuH-28, and MMNK-1 cells using siRNA transfection, and analyzed the resulting expression levels of ICs on RNA level.

SiRNA-mediated knockdown of ZEB1 significantly reduced intracellular ZEB1 transcript levels in HuH-28 and MMNK-1 cells and resulted in tendentially increased expression levels of CDH1 (Figure 7b, c). In OCUG-1 cells, although ZEB1 knockdown was less efficient, we could notice a non-quantifiable upregulation of CDH1 similar to what we observed in the transient miRNA overexpression experiments, indicating a functional manipulation of ZEB1 (Figure 7a). However, despite these changes, the expression levels of ICs remained mostly unchanged across all cell lines (Figure 7d-f).

These results suggest that the observed miR-200c-3p-mediated upregulation of ICs is likely independent of its interaction with ZEB1, indicating that alternative mechanisms beyond the miR-200c-3p/ZEB1 axis are involved in regulating IC expression.

3.5. Reduction of miR-200c-3p levels does not influence IC expression

Given the ZEB1-independent influence of miR-200c-3p on ICs, we hypothesized that miR-200c-3p might regulate ICs through mechanisms involving different negative regulators of ICs, whether related to EMT or not. Specifically, reducing miR-200c-3p could increase expression levels of these regulators, which might then result in a decreased expression of ICs such as LGALS9, PD-L1, and IDO1.

To follow up on this hypothesis, we reduced the levels of functional miR-141-3p and miR-200c-3p in epithelial HuCC-T1 cells using miRNA inhibitors – synthetic nucleotides designed to bind and effectively sequester target miRNAs, thereby reducing their functional pool in the cell. We then examined transcriptional changes in EMT markers and ICs via RT-qPCR.

Transfection with the miR-141-3p inhibitor led to a minimal reduction in miR-141-3p levels, making it challenging to draw clear conclusions regarding its downstream effects. In contrast, miR-200c-3p inhibitor significantly reduced miR-200c-3p levels (Figure 8a). Despite this effective reduction, the mRNA levels of EMT markers (Figure 8b), or ICs (Figure 8c) remained mostly unchanged. Comparable results were observed for HuCC-T1 cells simultaneously transfected with both miRNA inhibitors (Figure 8a-c).

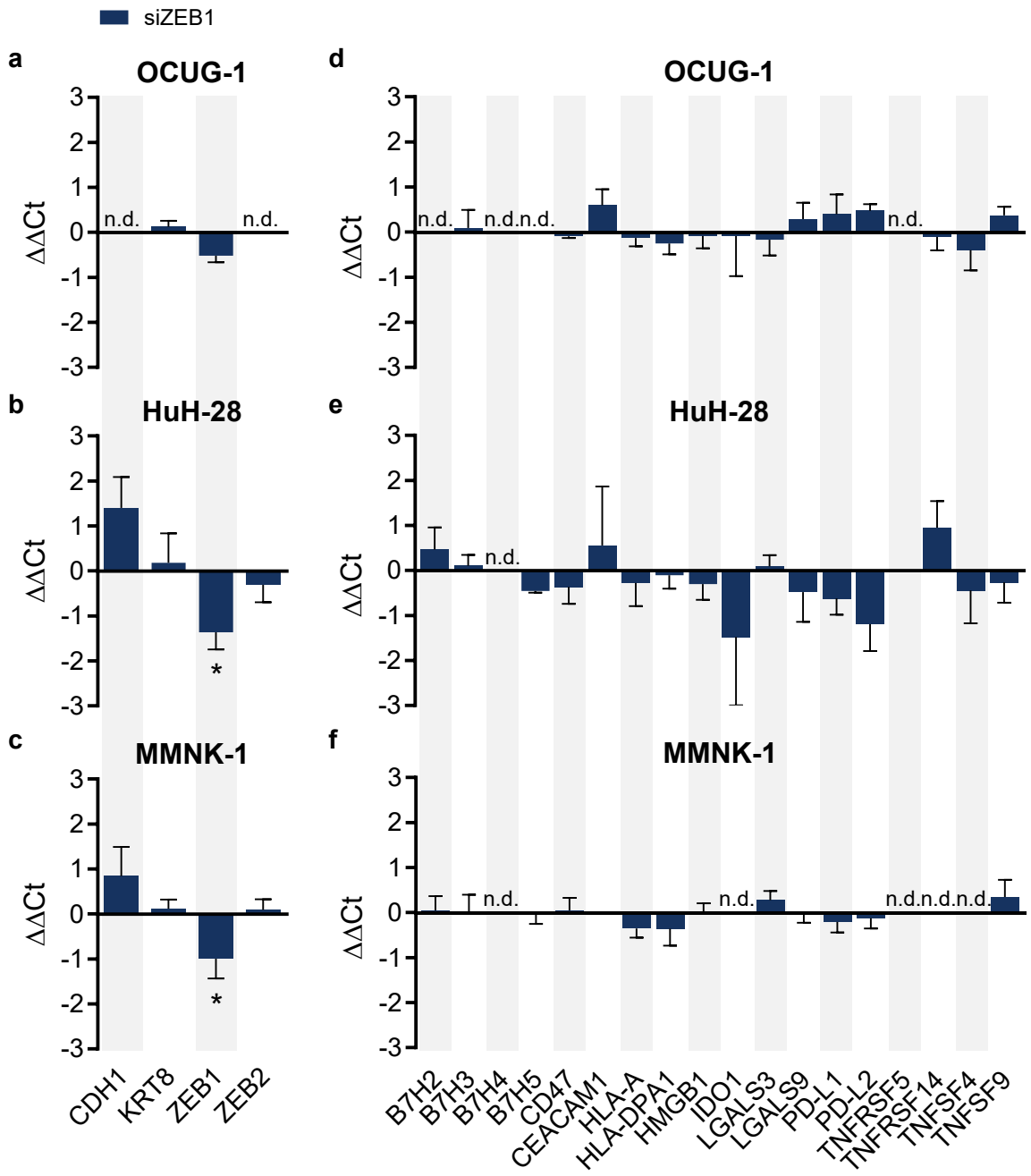

Figure 7: ZEB1 knockdown does not affect IC expression. OCUG-1 (n=3), HuH-28 (n=5), and MMNK-1 (n=5) cells were transfected with a siRNA targeting ZEB1 (siZEB1) or Allstars Negative Control for 48 hours. Resulting intracellular RNA levels of **(a-c)** epithelial markers CDH1, KRT8, mesenchymal markers ZEB1, ZEB2, and **(d-f)** ICs were analyzed by RT-qPCR. Data is presented as mean ± SD. Statistical significance was determined using Mann-Whitney test for n=5 data and unpaired t test for n=3 data. Analysis was corrected for multiple comparisons using the Bonferroni-Dunn method. * P≤0.05. n.d. = not detectable. Reproduced with modifications from (1,2) with permission via the CC BY 4.0 license.

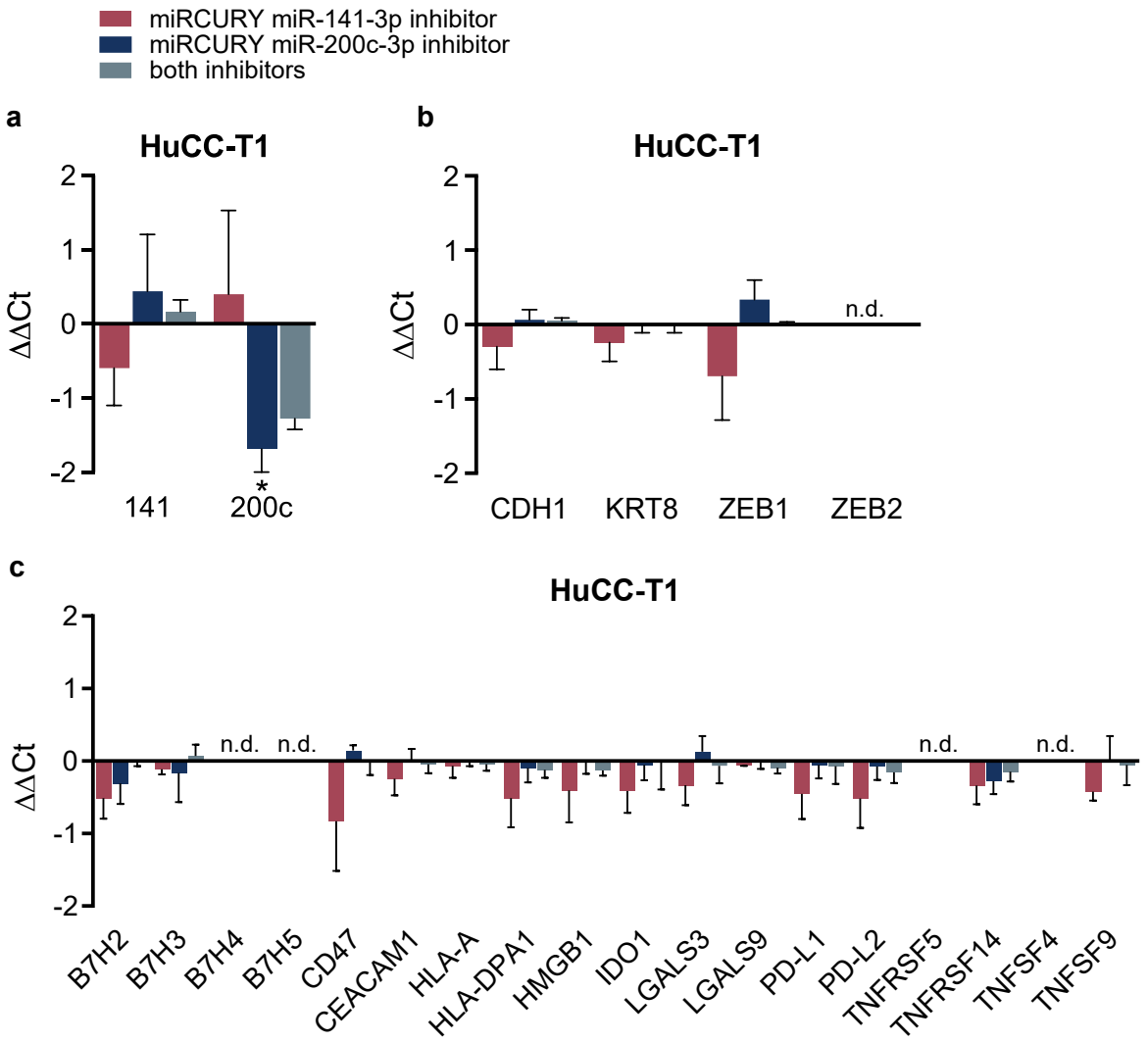

Figure 8: Reduction of miR-200c-3p levels fails to induce transcriptional changes in EMT markers and ICs. HuCC-T1 (n=3) cells were transfected with miRCURY mir-141-3p inhibitor, miRCURY miR-200c-3p inhibitor, both inhibitors, or miRCURY miRNA Inhibitor Control for 48 hours. Resulting intracellular RNA levels of **(a)** miR-141-3p and miR-200c-3p, **(b)** epithelial markers CDH1, KRT8, mesenchymal markers ZEB1, ZEB2, and **(c)** ICs were analyzed by RT-qPCR. Data is presented as mean ± SD. Statistical significance was determined using one-way ANOVA corrected for multiple comparisons with the Bonferroni method. * P≤0.05. n.d. = not detectable.

3.6. miR-200c-3p does not target Bridging Integrator-1 (BIN1)

In an effort to understand the miR-200c-3p effect on LGALS9, PD-L1, and IDO1, we extended our investigation to its potential impact on known negative regulators of respective ICs. While identifying direct negative regulators of ICs proved challenging due to their complex and context-dependent regulatory networks, Bridging Integrator-1 (BIN1) emerged as promising candidate for further exploration. BIN1 expression has been reported to be inversely correlated with IDO1 expression in acute myeloid leukemia and has been confirmed to be a direct

negative regulator of IDO1 expression (226,227). Thus, we hypothesized that miR-200c-3p might directly target BIN1, explaining its positive impact on IDO1 expression.

We performed computational analysis using TargetScan v8.0 (228), miRDB (229), and mirWalk v3.0 (230), which identify complementary sequences between the seed region of miRNAs and potential target transcripts. However, none of these algorithms predicted any miR-200c-3p binding sites within the BIN1 gene, including its 3' and 5' UTRs.

Given the limitations of computational predictions, we conducted additional experimental validation, which confirmed that BIN1 expression levels remained unaffected by transient miR-200-3p overexpression (Figure 9a-d). This ruled out the possibility that miR-200c-3p-dependent BIN1 downregulation is responsible for the observed increase in IDO1 expression levels upon miR-200c-3p overexpression.

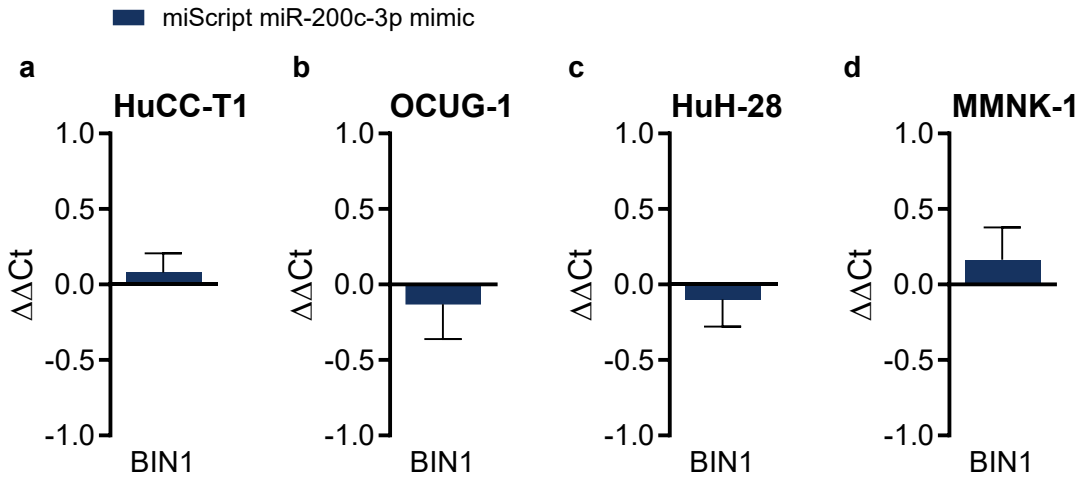

Figure 9: miR-200c-3p does not regulate BIN1 expression. (a) HuCC-T1 (n=5), **(b)** OCUG-1 (n=3), **(c)** HuH-28 (n=5), and **(d)** MMNK-1 (n=5) cells were transfected with miScript miR-200c-3p mimic or Allstars Negative Control for 48 hours. Resulting intracellular RNA levels of BIN1 were analyzed by RT-qPCR. Data is presented as mean ± SD. Statistical significance was determined using Mann-Whitney test for n=5 data, and unpaired t test for n=3 data.

3.7. Stable miR-200c-3p overexpression fails to replicate transient effects

In light of our ongoing challenges in clarifying the relationship between miR-200c-3p and the regulation of LGALS9, PD-L1, and IDO1, we sought further insight by utilizing additional experimental models. To this end, we generated stable miR-200c-3p overexpression cell lines using lentiviral transduction. In contrast to transient overexpression with miRNA mimics, stable

overexpression requires endogenous miRNA biogenesis and maturation, providing a more physiological setting to study miRNA functions.

After selecting and enriching for cells with high levels of integrated miR-200c-3p, we compared the mRNA levels of EMT markers and ICs to matched control cells transduced with empty lentiviral vectors. Although we successfully generated OCUG-1 and MMNK-1 cells that displayed significantly elevated expression levels of miR-200c-3p and an epithelial-like state compared to their control counterparts, this stable overexpression model failed to replicate the robust upregulation of LGALS9, PD-L1, and IDO1 observed in the miR-200c-3p mimic transfection experiments (Figure 10a, b).

This implies that mechanisms beyond the physiological function of miR-200c-3p may drive the regulation of IC expression, prompting us to consider non-specific effects.

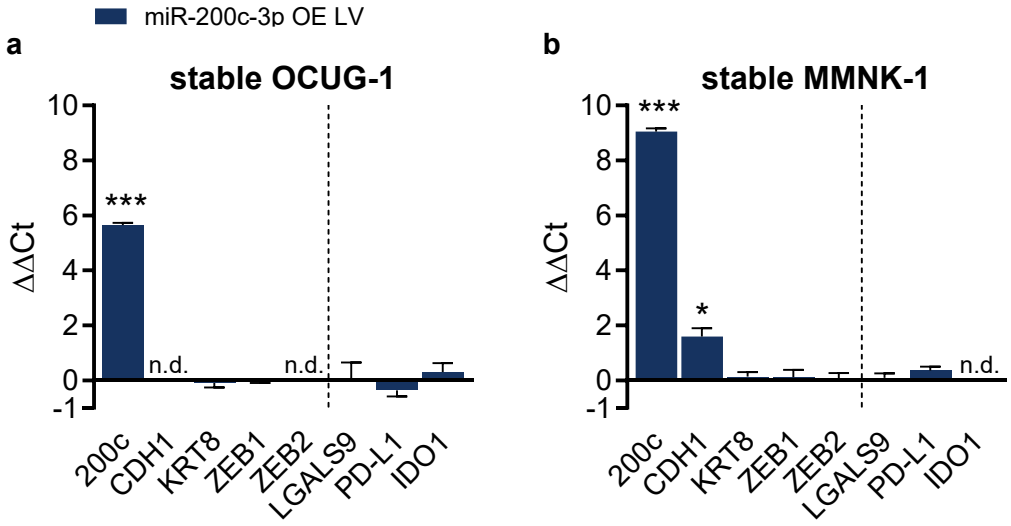

Figure 10: Stable miR-200c-3p overexpression cells do not have altered IC expression levels. (a) OCUG-1 (n=3) and **(b)** MMNK-1 (n=3) cells were transduced with lentiviruses harboring miR-200c-3p gene-containing vectors and selected and enriched for successful miR-200c-3p gene integration. Resulting intracellular RNA levels of miR-200c-3p, epithelial markers CDH1, KRT8, mesenchymal markers ZEB1, ZEB2, and ICs LGALS9, PD-L1, IDO1 were analyzed by RT-qPCR. Data is presented as mean ± SD. Statistical significance was determined using unpaired t test corrected for multiple comparisons using the Bonferroni-Dunn method. * P≤0.05, *** P≤0.001. n.d. = not detectable. Reproduced with modifications from (1,2) with permission via the CC BY 4.0 license.

3.8. The miScript miR-200c-3p mimic leads to the IC upregulation

Given the concerning discrepancy between transient and stable miR-200c-3p overexpression models, coupled with the inconclusive outcomes of previous experiments, we started to question the origin of the IC upregulation following miR-200c-3p mimic transfection. Having considered many conventional explanations for a miR-200c-3p-mediated IC upregulation, we hypothesized that the observed effects may not be driven by the introduced miR-200c-3p itself, but rather by the miR-200c-3p mimic used in the transient overexpression experiments.

To investigate this possibility, we utilized a miR-200c-3p mimic from a different manufacturer. Unlike the initially used miScript miR-200c-3p mimic, which contained the mature miRNA sequence and its complementary passenger strand, the new mirVana miR-200c-3p mimic was additionally chemically modified to minimize any potential off-target effects. By comparing the effects of the original miScript mimic with the mirVana version, we hoped to clarify the underlying mechanisms driving the IC upregulation.

As anticipated, while reached intracellular miR-200c-3p levels and the effects on CDH1 were highly comparable between the two miR-200c-3p mimics, the upregulation of LGALS9, PD-L1, and IDO1 was completely absent when transfecting cells with the mirVana mimic (Figure 11a-d). This confirmed that the IC upregulation following a transfection with miScript miR-200c-3p mimic was likely caused by non-specific effects, rather than the action of the mature miR-200c-3p itself.

3.9. The miScript miR-200c-3p mimic triggers innate immunity

Realizing that the IC upregulation was driven by non-specific effects, we aimed to better understand the mechanisms behind the drastic differences regarding IC regulation between the miScript miR-200c-3p mimic and the mirVana miR-200c-3p mimic. We hypothesized that the miScript miR-200c-3p mimic might be recognized as foreign dsRNA, thereby triggering an innate immune response in transfected cells.

To investigate this, we transfected cells with either miScript miR-200c-3p mimic, mirVana miR-200c-3p mimic, or miScript miR-141-3p mimic and analyzed transcriptional changes in key components indicative of an innate immune response. We focused on the expression of dsRNA sensors such as TLR3, RIG-I, and MDA5, interferons including type I IFN-β, type III Interferon Lambda 1 (IFN-λ1), and Interferon Lambda 2 (IFN-λ2), as well as antiviral effectors such as OAS1, MX1, and PKR.

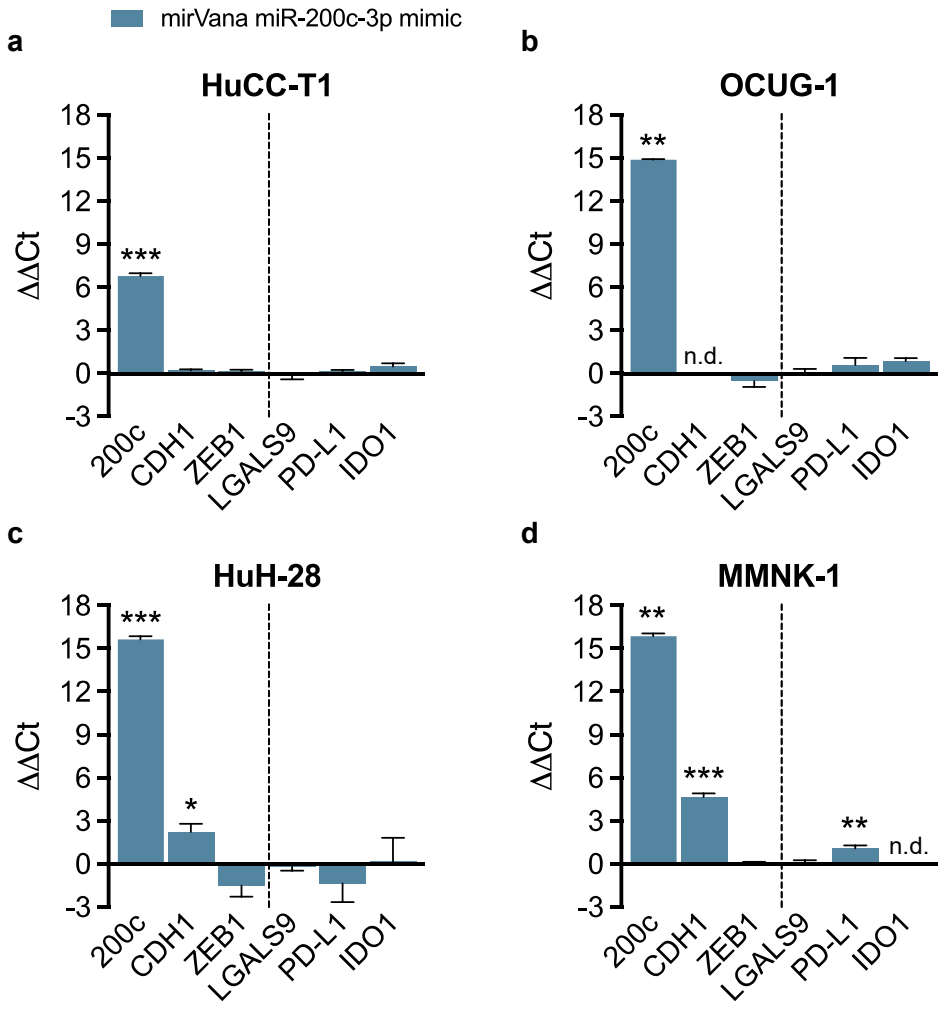

Figure 11: mirVana miR-200c-3p mimic does not influence IC expression. (a) HuCC-T1 (n=3), **(b)** OCUG-1 (n=3), **(c)** HuH-28 (n=3), and **(d)** MMNK-1 (n=3) cells were transfected with mirVana miR-200c-3p mimic or mirVana mimic Negative Control for 48 hours. Resulting intracellular RNA levels of miR-200c-3p, epithelial marker CDH1, mesenchymal marker ZEB1, and ICs LGALS9, PD-L1, IDO1 were analyzed by RT-qPCR. Data is presented as mean ± SD. Statistical significance was determined using unpaired t test corrected for multiple comparisons using the Bonferroni-Dunn method. * P ≤0.05, ** P≤0.01, *** P≤0.001. n.d. = not detectable. Reproduced with modifications from (1,2) with permission via the CC BY 4.0 license.

Upon transfection of HuCC-T1 and OCUG-1 cells with miScript miR-200c-3p mimic, but not mirVana miR-200c-3p mimic, expression levels of RIG-I and MDA5, IFN-β IFN-λ1, and IFN-λ2, and MX1 and OAS1 were markedly increased (Figure 12a, c). A similar miScript miR-200c-3p mimic-driven upregulation of interferons was detected in HuH-28 cells (Figure 12e). In contrast, we did not observe a consistent increase in interferon levels of cells transfected with miScript miR-141-3p mimic (Figure 12b, d, f), nor in stable miR-200c-3p overexpression cell lines (Figure 12g).

These findings suggest that the miScript miR-200c-3p mimic triggers a dsRNA-mediated innate immune response, indicated by an induction of interferon expression and the upregulation of antiviral effector genes. Since this response was absent in cells transfected with mirVana miR-200c-3p mimic transfection and in stable miR-200c-3p overexpression models, it appears evident that these effects are independent of physiological function of miR-200c-3p.

3.10. The miScript miR-200c-3p mimic impacts cell viability

An activation of innate immunity frequently triggers programmed cell death (231). Therefore, to investigate whether the transcriptional changes induced by miScript miR-200c-3p mimic correspond to phenotypic alterations indicative of an active innate immune response, we compared cell numbers and apoptotic rates in HuCC-T1 and OCUG-1 cells transfected with miScript miR-200c-3p mimic, mirVana miR-200c-3p mimic, or miScript miR-141-3p mimic.

In HuCC-T1 cells, miScript miR-200c-3p mimic significantly reduced the number of metabolically active cells 96 hours post-transfection, compared to cells transfected with the corresponding negative control. In contrast, both the mirVana miR-200c-3p mimic and miScript miR-141-3p mimic only led to a tendential decrease (Figure 13a). Similarly, in OCUG-1 cells, transfection with miScript miR-200c-3p mimic led to the strongest reduction in cell numbers, whereas the mirVana miR-200c-3p mimic and miR-141-3p mimic resulted in mild decreases (Figure 13c).

To evaluate the role of apoptosis, we measured the activity of effector caspases-3 and -7 using a Caspase 3/7 Glo® assay. In OCUG-1 cells, transfection with the miScript miR-200c-3p mimic resulted in an increased caspase-3 and -7 activity indicative of apoptosis induction, while the other mimics had a negligible effect (Figure 13d). Interestingly, in HuCC-T1 cells, no notable differences in caspase activity were observed between the miRNA mimic transfections, suggesting that apoptosis likely did not account for the reduced cell numbers in the WST-1 assay (Figure 13b).

In summary, these results indicate that while apoptosis may be induced in OCUG-1 cells, it does not seem to be the predominant form of cell death in miScript miR-200c-3p mimic-transfected HuCC-T1 cells. Instead, other forms of cell death or additional effects on cell cycle progression might contribute to the observed cell number reductions.

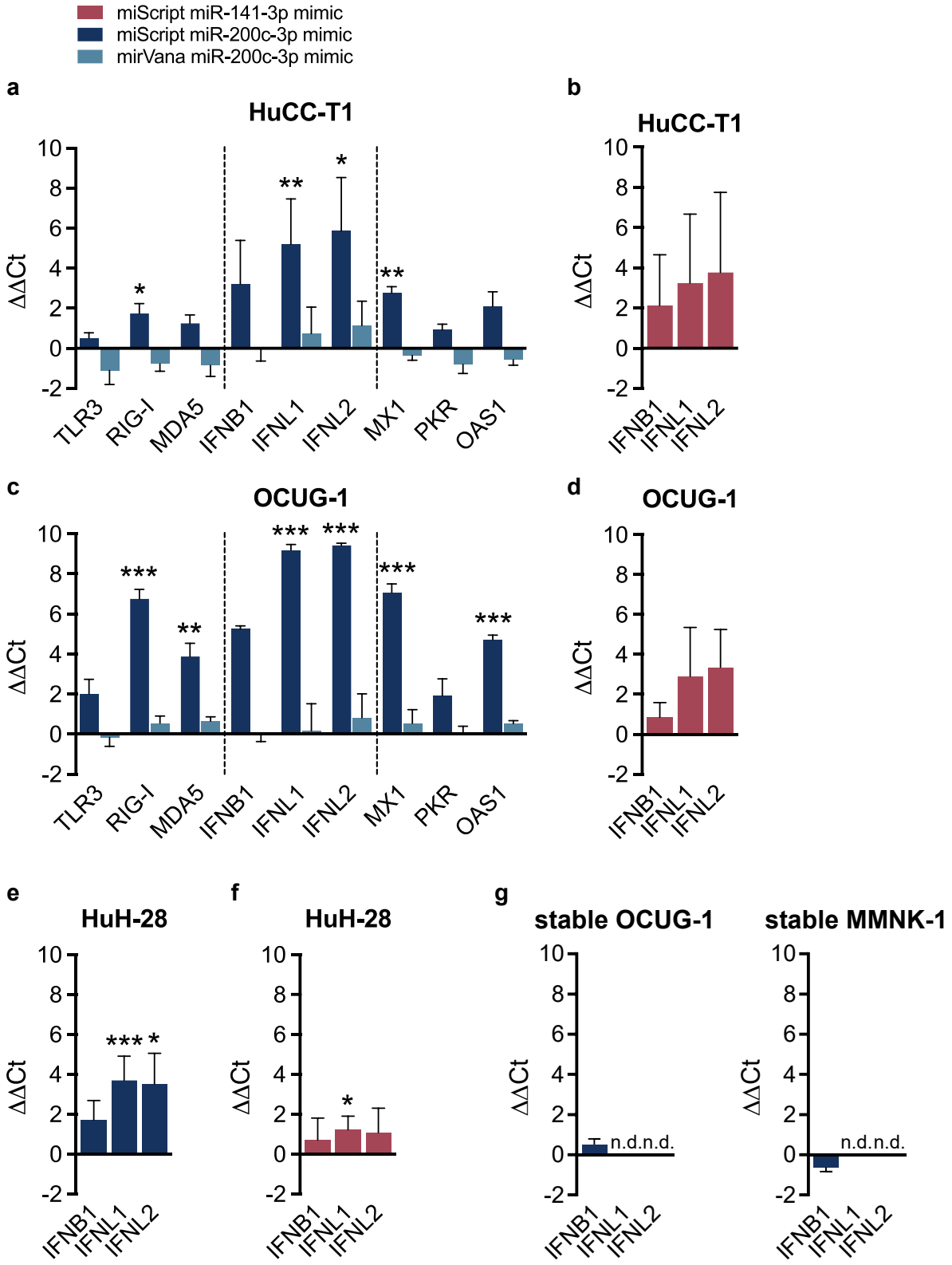

Figure 12: The miScript miR-200c-3p mimic triggers innate immune responses. HuCC-T1 (n=5), OCUG-1 (n=3), HuH-28 (n=5) were transfected with miScript miR-141-3p mimic, miScript miR-200c-3p mimic, mirVana miR-200c-3p mimic, or corresponding negative controls for 48 hours. **(a-f)** Resulting intracellular RNA levels of dsRNA sensors TLR3, RIG-I MDA5, interferons IFN-β (IFNB1), IFN-λ1 (IFNL1), IFN-λ2 (IFNL2), and antiviral effectors OAS1, MX1, PKR were analyzed by RT-qPCR. **(g)** The

intracellular RNA levels of IFN-β (IFNB1), IFN-λ1 (IFNL1), and IFN-λ2 (IFNL2) of stable miR-200c-3p overexpression OCUG-1 and MMNK-1 cells were analyzed by RT-qPCR. Data is presented as mean ± SD. For (a, c), statistical significance was determined using one-way ANOVA corrected for multiple comparisons with the Bonferroni method for n=3 data, and Kruskal-Wallis test corrected for multiple comparisons with the Dunn method for n=5 data. For (b, d, e-g), unpaired t test was used for n=3 data and Mann-Whitney test for n=5 data, corrected for multiple comparisons with the Bonferroni-Dunn method. * P≤0.05, ** P≤0.01, *** P≤0.001. n.d. = not detectable. Reproduced with modifications from (1) with permission via the CC BY 4.0 license.

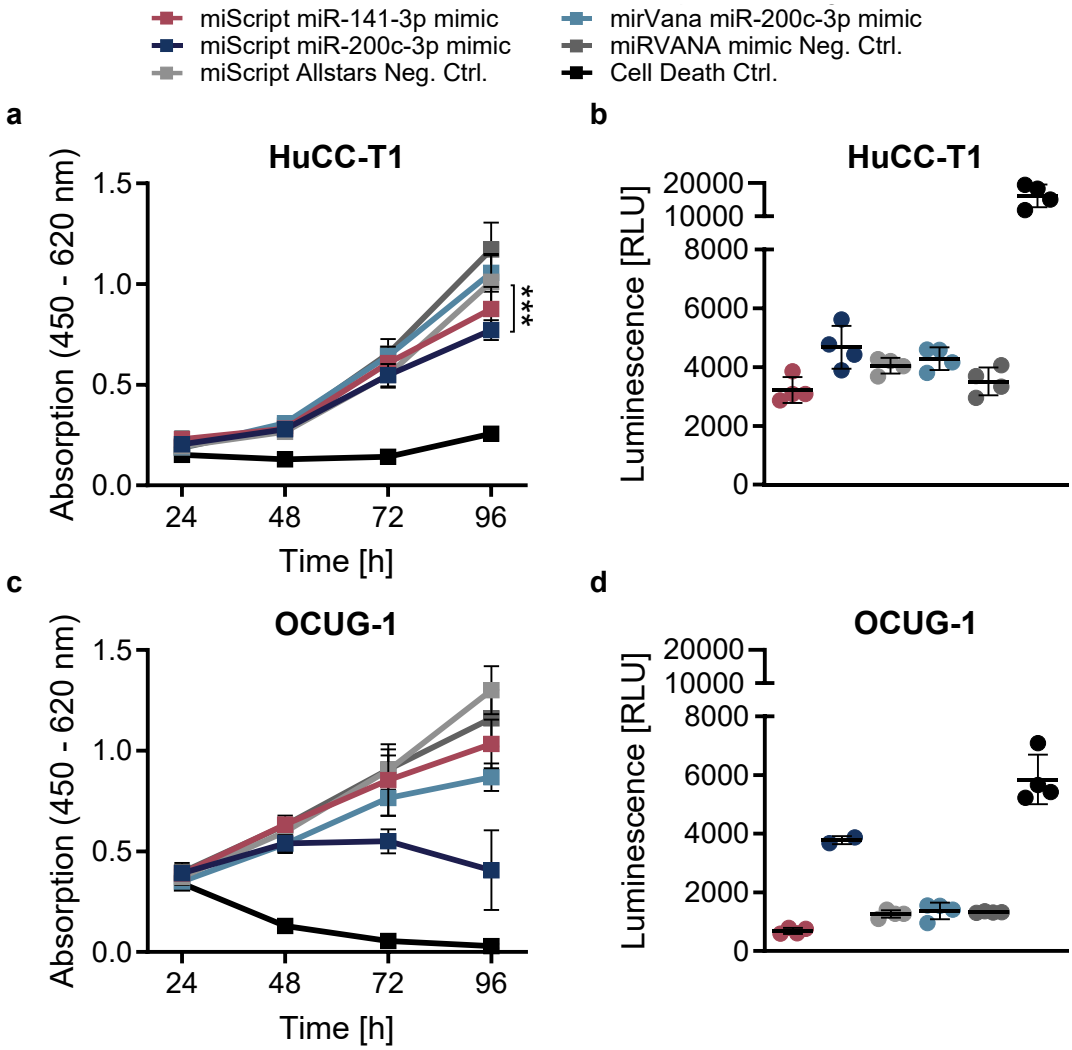

Figure 13: The miScript miR-200c-3p mimic influences cell viability. (a) HuCC-T1 (n=6) and **(c)** OCUG-1 (n=6) cells were transfected with miScript miR-141-3p mimic, miScript miR-200c-3p mimic, mirVana miR-200c-3p mimic, corresponding negative controls, or cell death control for up to 96 hours. Metabolically active cells were determined using a WST-1 assay. **(b)** HuCC-T1 (n=4; miScript miR-200c-3p n=2) and **(d)** OCUG-1 (n=4) were transfected with miScript miR-141-3p mimic, miScript miR-200c-3p mimic, mirVana miR-200c-3p mimic, corresponding negative controls, or cell death control for 72 hours. Activity of effector caspases-3 and -7 was measured using a Caspase3/7 Glo® assay. Data are shown as mean ± SD. Statistical significance was determined using Kruskal-Wallis test corrected for multiple comparisons with the Dunn method. *** P≤0.001. RLU = Relative Light Unit. Reproduced with modifications from (1) with permission via the CC BY 4.0 license.

3.11. The effect of miScript miR-200c-3p mimic extends to further dsRNA species

Considering our evidence that the miScript miR-200c-3p mimic triggers a dsRNA-mediated innate immune response, resulting in the upregulation of interferons and antiviral effectors, we aimed to determine whether this effect was specific to this miRNA mimic or could extend to further dsRNA species.

To investigate this further, we made use of poly(I:C), a synthetic dsRNA analog known for its potent activation of innate immunity. Since poly(I:C) is structurally distinct from the miScript miR-200c-3p mimic and lacks sequence similarities, it served as valuable surrogate to evaluate whether the miRNA mimic-induced effects were generalizable. Replicating our findings with poly(I:C) would not only reinforce the hypothesis that the miScript miR-200c-3p mimic induces canonical dsRNA-mediated innate immune responses, but also allow us to shift focus from the non-specific effects of the miRNA mimic to a broader mechanism of innate immunity activation.

When OCUG-1 and HuCC-T1 cells were transfected with poly(I:C), we observed strikingly similar effects to those induced by the miScript miR-200c-3p mimic. In both cell lines, poly(I:C) triggered a robust upregulation of dsRNA sensors TLR3, RIG-I and MD5, the induction of interferons IFN-β, IFN-λ1, and IFN-λ2 expression, and transcriptional alterations in antiviral effectors OAS1, MX1, and PKR (Figure 14a, b). Of note, although IFN-λ1 and IFN-λ2 expression levels were below the RT-qPCR detection limit in OCUG-1 control cells, these interferons were clearly detectable in poly(I:C)-transfected cells, indicating a considerable, albeit non-quantifiable, upregulation (Figure 14b).

Importantly, the similar upregulation patterns between poly(I:C) and miScript miR-200c-3p mimic extended to ICs as well. Poly(I:C) transfection led to a significant increase in the expression of ICs LGALS9, PD-L1, and IDO1 (Figure 14a, b).

These findings confirmed that the miR-200c-3p mimic caused a typical dsRNA-mediated innate immune system, which is not unique to the specific mimic but is reproducible with further dsRNA species like poly(I:C).

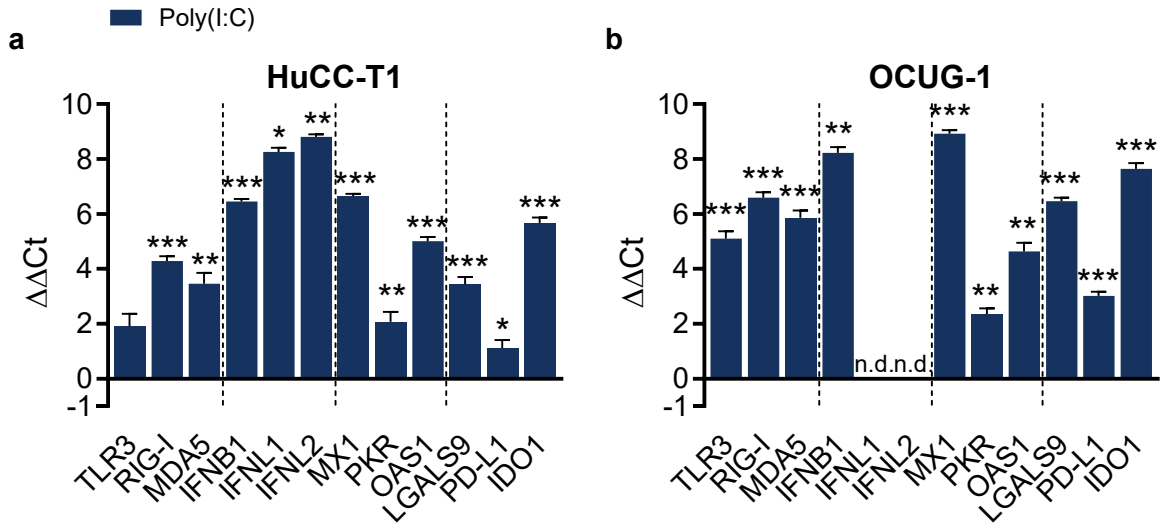

Figure 14: Poly(I:C) transfection mirrors miScript miR-200c-3p mimic effects. (a) HuCC-T1 (n=3) and **(b)** OCUG-1 (n=3) cells were transfected with poly(I:C) or Mock Control for 48 hours. Resulting intracellular RNA levels of dsRNA sensors TLR3, RIG-I, MDA5, interferons IFN-β (IFNB1), IFN-λ1 (IFNL1), IFN-λ2 (IFNL2), antiviral effectors MX1, PKR, OAS1, and ICs LGALS9, PD-L1, IDO1 were analyzed with RT-qPCR. Data are shown as mean ± SD. Statistical significance was determined using unpaired t test corrected for multiple comparisons with the Bonferroni-Dunn method. * P≤0.05, ** P≤0.01, *** P≤0.001. n.d. = not detectable.

Additionally, while the activation of key transcription factors involved in dsRNA-mediated innate immunity was not detected in cells transfected with miScript miR-200c-3p mimic - possibly due to its weaker overall effects - we were able to confirm the involvement of NF-κB and IRF3 following poly(I:C) transfection. Specifically, poly(I:C)-transfected HuCC-T1 cells showed higher levels of NF-κB nuclear translocation compared to control cells, as evidenced by the increased overlap between the red NF-κB signal and the blue nuclear DAPI staining (Figure 15a, b). Furthermore, increased levels of phosphorylated IRF3 were detected in poly(I:C)-transfected HuCC-T1 cells compared to control cells (Figure 15c). Together, these findings indicate the activation of NF-κB and IRF3 following poly(I:C) transfection.

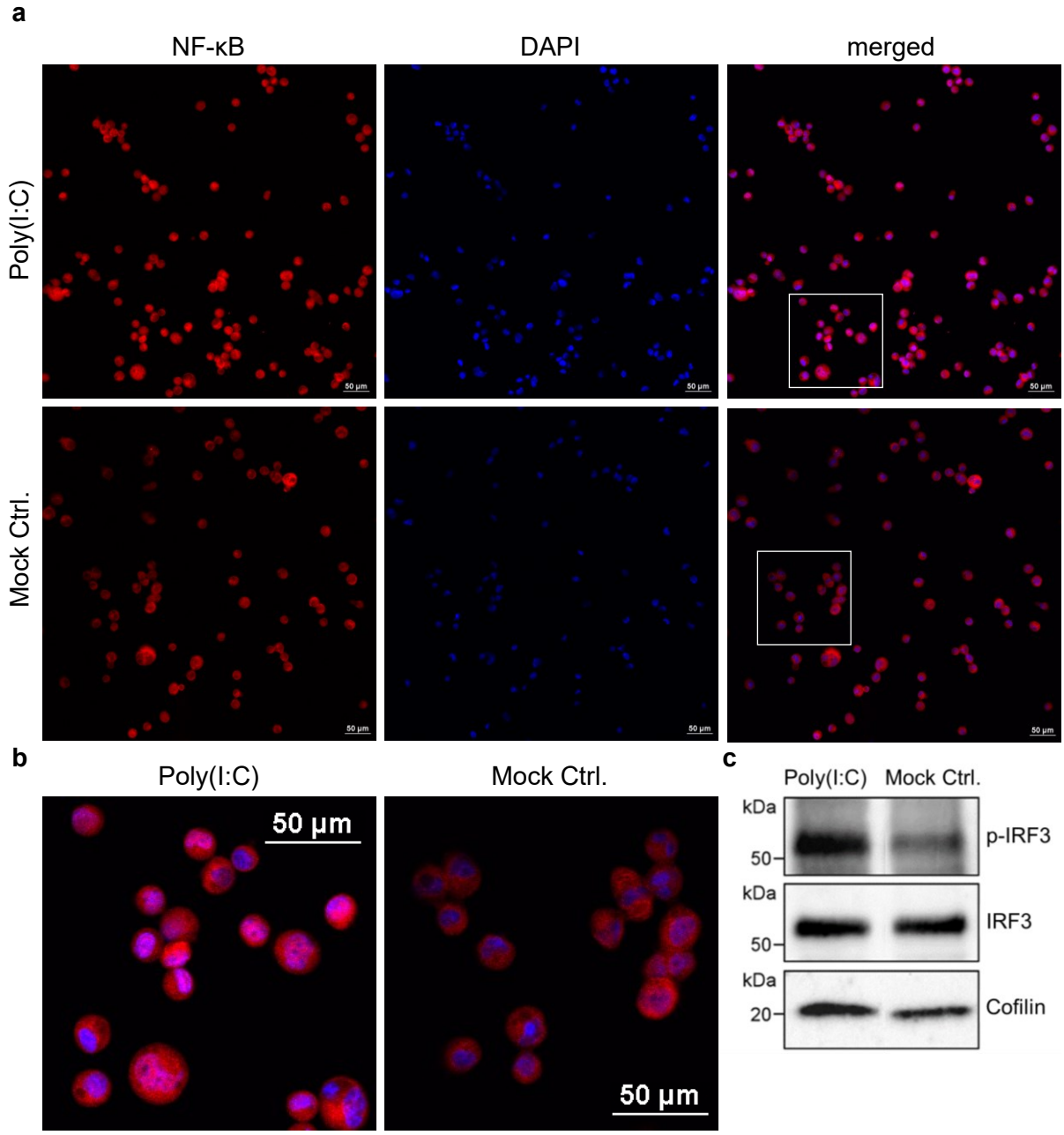

Figure 15: Poly(I:C) promotes nuclear translocation of NF-κB and leads to elevated levels of phosphorylated IRF3. (a) HuCC-T1 cells were transfected with poly(I:C) or Mock Control for 3 hours. Intracellular NF-κB (red) and DAPI-stained nuclei (blue) were visualized by immunofluorescence. Representative images of the nuclear plane were captured using 20x objective magnification. **(b)** Zoomed-in images of selected sections marked in white. **(c)** HuCC-T1 cells were transfected with poly(I:C) or Mock Control for 3 hours. Resulting intracellular protein levels of phosphorylated IRF3, total IRF3, and Cofilin (used as loading control) were analyzed by western blot. The first lane (Poly(I:C)) and the last lane (Mock Ctrl.) of a full membrane were cropped and pasted next to each other, as the middle lanes were not relevant for this particular analysis.

3.12. Upregulation of ICs is dependent on JAK/STAT signaling

After establishing that both miScript miR-200c-3p mimic and poly(I:C) triggered innate immune responses, while also leading to the upregulation of ICs, we aimed to investigate the potential connection between these two processes. Based on previous findings linking IFN-β to the expression of PD-L1 in NSCLC, we hypothesized that IFN-β might play a pivotal role in bridging innate immune responses and IC expression (232).

To follow up on this hypothesis, we first aimed to confirm that poly(I:C) transfection not only increased IFN-β mRNA levels, but also resulted in an elevated secretion of IFN-β protein. Using an ELISA assay to analyze the extracellular IFN-β concentration in the cell culture supernatants, we found that both HuCC-T1 and OCUG-1 cells transfected with poly(I:C) exhibited significantly higher extracellular IFN-β concentrations compared to the non-detectable levels of control cells. (Figure 16a, b). Furthermore, we demonstrated that both HuCC-T1 and OCUG-1 cells show baseline expression of the receptor subunits IFNAR1 and IFNAR2, which form the heterodimeric receptor for type I interferons. The expression levels of these subunits were comparable to those of the housekeeper GAPDH, indicating that the cells are generally equipped to react to extracellular IFN-β (Figure 16c, d).

We hypothesized that extracellular IFN-β may engage with interferon receptors on the same or neighboring cells in an autocrine or paracrine manner, thereby regulating the IC expression via the activation of the JAK/STAT signaling pathway. To test this, we inhibited JAK/STAT signaling using ruxolitinib, a well-established inhibitor of JAK1, JAK2, and TYK2. In HuCC-T1 and OCUG-1 cells, co-treatment with ruxolitinib significantly reduced the poly(I:C)-induced upregulation of LGALS9, PD-L1, and IDO1, returning their expression levels back to baseline. Similarly, the poly(I:C)-mediated overexpression of dsRNA sensors TLR3, RIG-I, and MDA5, and antiviral effectors MX1, PKR, and OAS1 was potently diminished by ruxolitinib co-treatment. Interestingly, poly(I:C)-mediated interferon expression, although reduced, remained elevated despite ruxolitinib treatment, suggesting that the regulation of interferon expression occurs primarily upstream of the JAK/STAT signaling pathway (Figure 16e, f).

Of note, while we primarily focused on IFN-β, we cannot exclude an effect of type III interferons such as IFN-λ1 and IFN-λ2 on the IC upregulation, as we also noticed baseline expression of subunits for their respective receptors IFNLR1 and IL10RB (Figure 16c, d).

Conclusively, these findings highlight the essential role of the JAK/STAT signaling pathway in linking the dsRNA-mediated activation of innate immune responses to the upregulation of ICs.

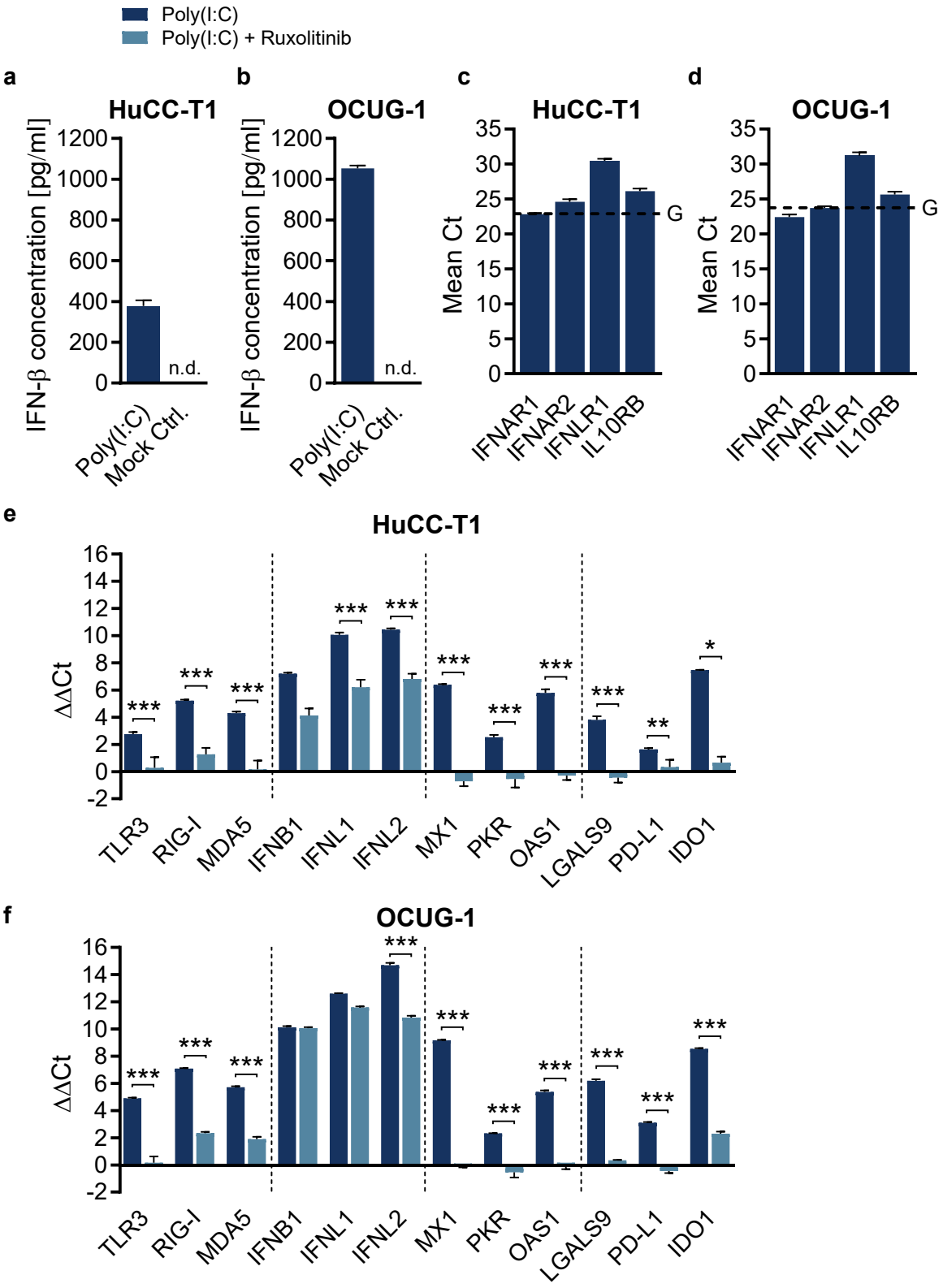

Figure 16: Poly(I:C)-induced downstream effects depend on JAK/STAT signaling. (a, b) HuCC-T1 (n=3) and OCUG-1 (n=3) cells were transfected with poly(I:C) or Mock Control for 48 hours. The extracellular IFN-β concentration was determined by an ELISA of the cell culture supernatant. Data are shown as mean ± SD. **(c, d)** Endogenous levels of interferon receptor subunits IFNAR1, IFNAR2, IFNLR1, IL10RB of HuCC-T1 (n=6) and OCUG-1 (n=6) were analyzed with RT-qPCR. Mean Ct values

are shown. For comparison, mean Ct values of GAPDH (G) are depicted as dotted line. **(e, f)** HuCC-T1 (n=3) and OCUG-1 (n=3) cells were transfected with poly(I:C), poly(I:C) + ruxolitinib, or corresponding negative controls for 48 hours. Resulting intracellular RNA levels of dsRNA sensors TLR3, RIG-I, MDA5, interferons IFN-β (IFNB1), IFN-λ1 (IFNL1), IFN-λ2 (IFNL2), antiviral effectors MX1, PKR, OAS1, and ICs LGALS9, PD-L1, IDO1 were analyzed with RT-qPCR. Data are shown as mean ± SD. Statistical significance was determined using one-way ANOVA corrected for multiple comparisons with the Bonferroni method. * P≤0.05, ** P≤0.01, *** P≤0.001. n.d. = not detectable.

3.13. Cells take up dsRNA in a more physiological setting

While our experimental findings using the miScript miR-200c-3p mimic and poly(I:C) provide first insights into the dsRNA-mediated activation of innate immunity leading to an upregulation of ICs, we questioned whether these findings might hold translational value.

We speculated about a pathophysiological scenario wherein BTC cells undergoing immunogenic cell death release dsRNA species into the TME. These extracellular dsRNAs could then be sensed by neighboring tumor cells as DAMPs, triggering an innate immune response, similar to what we observed in our experimental setup. As interferons accumulate in the TME, neighboring cells could adopt an immunosuppressive state by upregulating ICs in a JAK/STAT-dependent manner.

For this speculative scenario to be feasible, however, a key question is whether tumor cells are naturally capable of taking up extracellular dsRNA without relying on artificial lipid-based transfection reagents, which are only relevant in an experimental setting.

To test this, poly(I:C) was directly added to HuCC-T1 and OCUG-1 cells without transfection reagent, and the expression levels of ICs, dsRNA sensors, interferons, and antiviral effectors were analyzed via RT-qPCR. In HuCC-T1 cells, the expression levels of most genes were significantly increased compared to control cells, following patterns similar to those observed with poly(I:C) transfection (Figure 17a). Interestingly, in OCUG-1 cells, no significant poly(I:C)-induced upregulation of any of the tested genes was observed under these conditions (Figure 17b).

Nevertheless, the fact that transcriptional changes were induced by unassisted poly(I:C) delivery in HuCC-T1 cells generally supports the notion that tumor cells can naturally take up dsRNAs like poly(I:C), even though additional factors are likely to influence this ability.

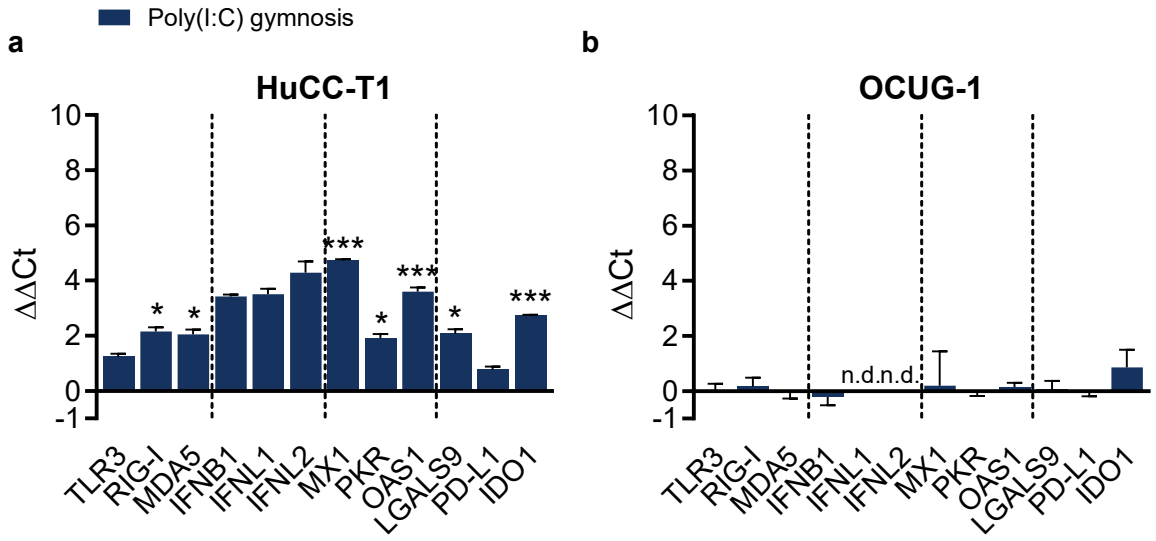

Figure 17: Unassisted delivery (=gymnosis) of poly(I:C) leads to transfection-like effects in HuCC-T1 cells. Poly(I:C) without transfection reagent was added to the culture medium of **(a)** HuCC-T1 (n=3) and **(b)** OCUG-1 (n=3) cells for 48 hours. Resulting intracellular RNA levels of dsRNA sensors TLR3, RIG-I, MDA5, interferons IFN-β (IFNB1), IFN-λ1 (IFNL1), IFN-λ2 (IFNL2), antiviral effectors MX1, PKR, OAS1, and ICs LGALS9, PD-L1, IDO1 were analyzed with RT-qPCR. Data are shown as mean ± SD. Statistical significance was determined using unpaired t test corrected for multiple comparisons with the Bonferroni-Dunn method. * P≤0.05, *** P≤0.001. n.d. = not detectable.

3.14. Cisplatin treatment influences IC expression

Given previous reports that genotoxic stress can lead to the accumulation of atypical dsRNA species within tumor cells, we were intrigued by the possibility that GemCis treatment of BTC cells could induce similar effects (233). We hypothesized that GemCis-mediated accumulation of endogenous dsRNA could activate innate immune responses and lead to the upregulation of ICs through a mechanism analogous to that observed with poly(I:C).

To explore this hypothesis, we treated HuCC-T1 and OCUG-1 cells with cisplatin and evaluated the expression levels of various ICs. Remarkably, cisplatin treatment resulted in an upregulation of several ICs, including LGALS9, PD-L1, and IDO1 (Figure 18c, d).

Next, we sought to determine whether this upregulation could be mediated through dsRNA-induced innate immune responses. To this end, we analyzed the expression levels of dsRNA sensors, interferons, and antiviral effectors following cisplatin treatment. Interestingly, cisplatin treatment of HuCC-T1 resulted in increased levels of dsRNA sensors TLR3, RIG-I, and MDA5, interferon IFN-β, and antiviral effectors MX1, PKR, and OAS1 (Figure 18a). Similar, though less pronounced, effects were observed in cisplatin-treated OCUG-1 cells (Figure 18b).

Interestingly, despite the robust upregulation of interferon-related genes, cisplatin treatment did not lead to a detectable extracellular accumulation of IFN-β, unlike what was seen with poly(I:C) transfection (Figure 18e, f).

In summary, these findings support the possibility that cisplatin treatment can induce the upregulation of ICs such as LGALS9, PD-L1, and IDO1 potentially through dsRNA-mediated innate immune activation. While this process might be partially driven by dsRNA sensing, as observed with miScript miR-200c-3p mimic or poly(I:C), the generally broader IC upregulation and absence of detectable extracellular IFN-β indicate that other additional mechanisms may also contribute to this effect.

3.15. Cisplatin effect is independent of extracellular dsRNA

We hypothesized that cisplatin treatment of BTC cells might induce genotoxic stress, leading to the accumulation of dsRNA species, activation of innate immunity, and immunogenic cell death. Thereby released intracellular components including dsRNA, could then be taken up by neighboring cells, triggering innate immune responses and upregulating ICs, similar to the effects observed with poly(I:C) transfection. In this model, release of endogenous dsRNA into the extracellular space would play a central role.

Therefore, to investigate the potential role of extracellular dsRNA in the cisplatin-mediated IC upregulation, we treated HuCC-T1 and OCUG-1 cells with cisplatin and added either Benzonase, a general nuclease, or RNase III, which specifically degrades dsRNA. If released dsRNA were responsible for the effect, nuclease-mediated degradation should mitigate it.

However, despite cisplatin treatment increasing the RNA levels of tested genes as expected, addition of neither Benzonase nor RNase III reversed these effects, suggesting that extracellular nucleic acids do not contribute to the cisplatin-mediated upregulation of ICs (Figure 19a, b). Of note, the increased expression of certain genes upon RNase III addition is likely due to the sensitivity of HuCC-T1 cells to the nuclease-solvent glycerol, rather than any biological impact of RNase III itself (Figure 19a).

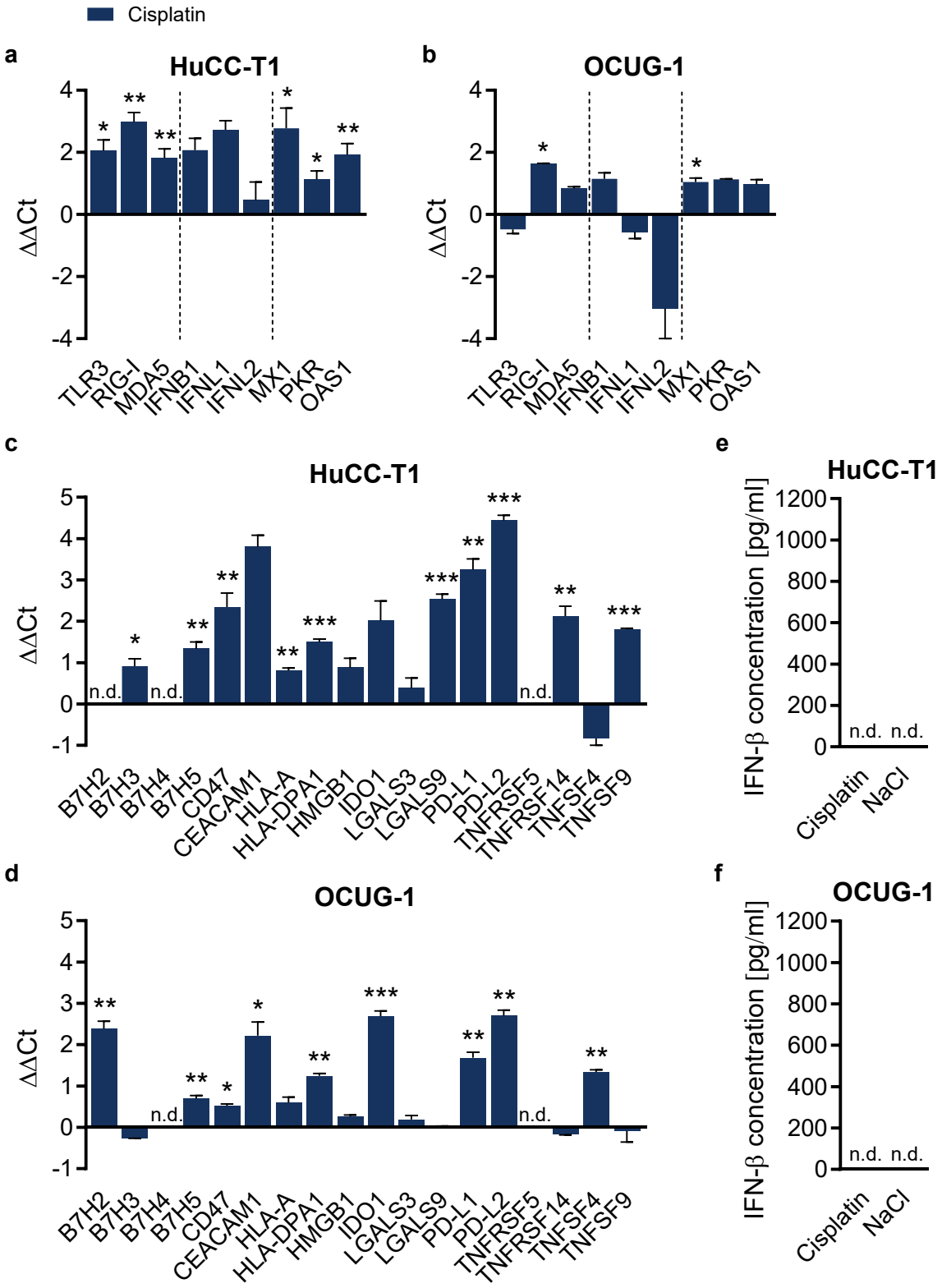

Figure 18: Cisplatin induces innate immune responses and leads to increased IC expression. HuCC-T1 (n=3) and OCUG-1 (n=3) cells were treated with cisplatin or NaCl for 48 hours. Resulting RNA levels of **(a, b)** dsRNA sensors TLR3, RIG-I, MDA5, interferons IFN-β (IFNB1), IFN-λ1 (IFNL1), IFN-λ2 (IFNL2), antiviral effectors MX1, PKR, OAS1, and **(c, d)** various ICs were analyzed with RT-qPCR. **(e, f)** The extracellular IFN-β concentration was determined by an ELISA of the culture supernatants. Data

are shown as mean ± SD. Statistical significance was determined using unpaired t test corrected for multiple comparisons with the Bonferroni-Dunn method. * P≤0.05, ** P≤0.01, *** P≤0.001. n.d. = not detectable.

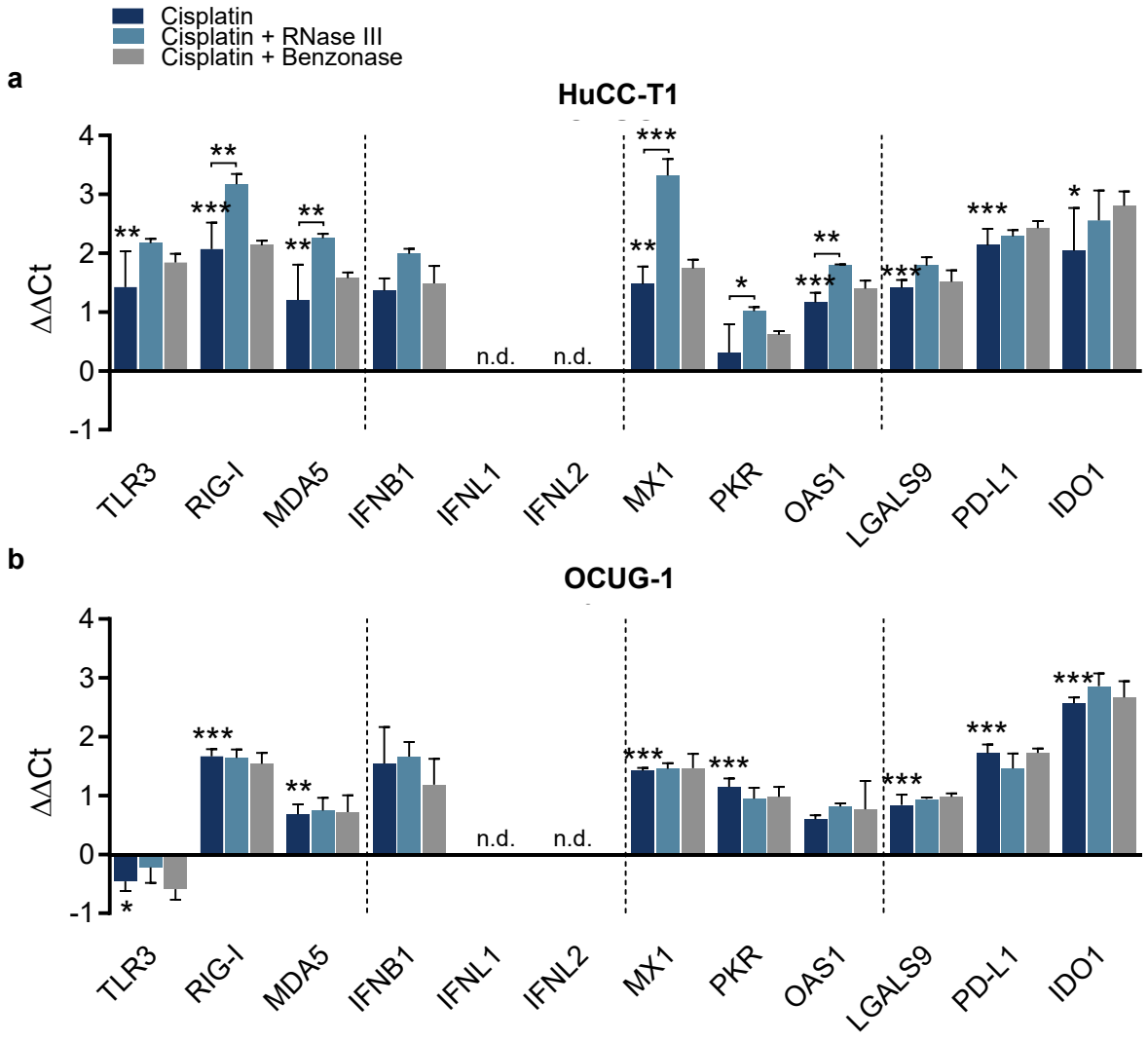

Figure 19: Cisplatin effect is not mediated by free extracellular nucleic acids. (a) HuCC-T1 (n=3) and **(b)** OCUG-1 (n=3) cells were treated with cisplatin alone, cisplatin with added RNase III (dsRNA-specific nuclease) or Benzonase (general nuclease), or corresponding negative controls for 48 hours. Resulting intracellular RNA levels of dsRNA sensors TLR3, RIG-I, MDA5, interferons IFN-β (IFNB1), IFN-λ1 (IFNL1), IFN-λ2 (IFNL2), antiviral effectors MX1, PKR, OAS1, and ICs LGALS9, PD-L1, IDO1 were analyzed with RT-qPCR. Data are shown as mean ± SD. Statistical significance was determined using one-way ANOVA corrected for multiple comparisons with the Bonferroni-Dunn method. * P≤0.05, ** P≤0.05, *** P≤0.001. n.d. = not detectable.

Frequently, DAMPs including various RNA species are released within extracellular vesicles (EVs) (234,235). Therefore, we speculated that upon cisplatin treatment, endogenous dsRNA might be secreted within EVs, protecting it from nuclease degradation in our earlier experiment, thus explaining the lack of effects.

To test this hypothesis, we treated HuCC-T1 and OCUG-1 cells with cisplatin for 48 hours, harvested the medium potentially enriched for extracellular vesicles with contents influencing the IC expression in the tumor cells, and incubated culture-matched cells with this cisplatin-conditioned medium. However, even with this experimental setup we could not detect any transcriptional changes (Figure 20a, b).

Together, these findings rule out extracellular nucleic acids, including those potentially carried by EVs, as contributors to the cisplatin-induced upregulation of ICs. Although not further pursued within this dissertation, this suggests that cisplatin triggers innate immunity and subsequent IC expression in a cell-intrinsic mechanism, independent of autocrine or paracrine signaling involving nucleic acids or IFN-β. Ongoing research is focused on investigating these potential cell-autonomous processes.

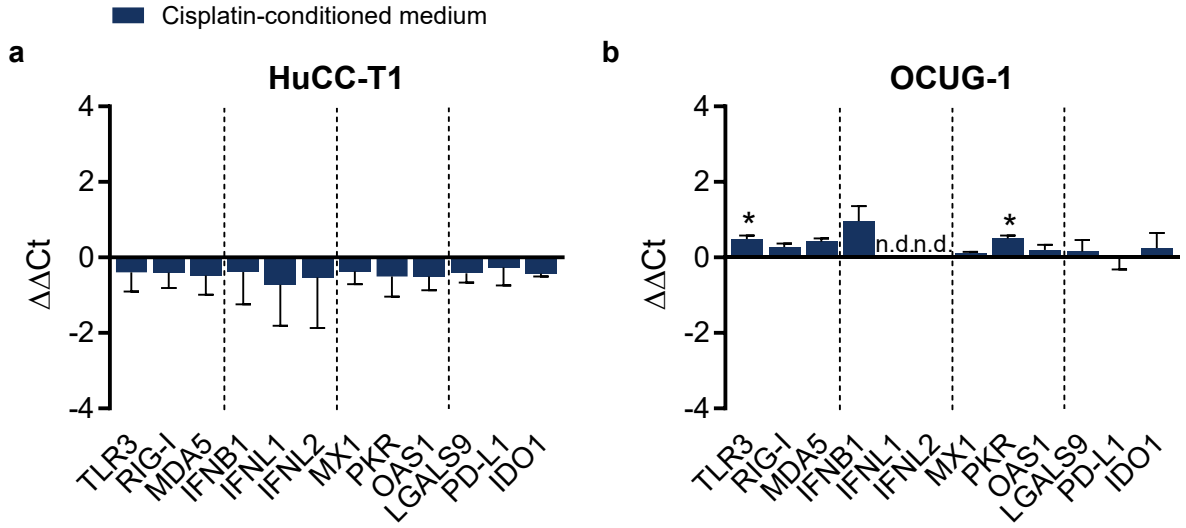

Figure 20: Cisplatin effect is not dependent on extracellular mediators. (a) HuCC-T1 (n=3) and **(b)** OCUG-1 (n=3) cells were treated with cisplatin-conditioned medium or standard growth medium for 48 hours. Resulting intracellular RNA levels of dsRNA sensors TLR3, RIG-I, MDA5, interferons IFN-β (IFNB1), IFN-λ1 (IFNL1), IFN-λ2 (IFNL2), antiviral effectors MX1, PKR, OAS1, and ICs LGALS9, PD-L1, IDO1 were analyzed with RT-qPCR. Data are shown as mean ± SD. Statistical significance was determined using unpaired t test corrected for multiple comparisons with the Bonferroni-Dunn method. * P≤0.05. n.d. = not detectable.

4. Discussion

4.1. miR-200 family, EMT, and ICs

The initial goal of this PhD project was to investigate the miR-200 family as a potential regulatory link between EMT and immune evasion mechanisms in BTC. This hypothesis was based on several key factors: [1] members of the miR-200 family have been extensively characterized and shown to play crucial roles in regulating EMT across various cancer types (182,236,237); [2] EMT has been associated with immune evasion mechanisms such as the expression of ICs and has been shown to predict immunotherapy responses (194,238–242); [3] certain miR-200 family members have been found to directly repress immunosuppressive factors, including ICs such as PD-L1 (199,243–248); [4] miR-200 family members have been proposed as biomarkers in several cancer types, including cholangiocarcinoma, highlighting their clinical relevance (249–253).

Initial correlation analyses of endogenously expressed miR-200 family members, EMT markers, and ICs across eleven BTC cell lines revealed a potential link between the EMT status and the expression of ICs. Unsupervised hierarchical clustering based on these expression profiles identified two distinct epithelial and mesenchymal clusters among our cell lines. This aligns with the established role of the miR-200 family/ZEB feedback loop in regulating EMT and confirms that our *in vitro* cell line models effectively capture different EMT states (186,254,255).

When analyzing the expression of ICs within the two clusters, certain ICs such as PD-L1, or LGALS9 were predominantly expressed in cell lines with epithelial traits, whereas others like TNFSF9 were exclusively expressed in cell lines with mesenchymal transcription patterns. Of note, while ICs like PD-L1 and TNFSF9 only showed tendential correlation, PD-L1 expression was highest in epithelial cell lines, whereas TNFSF9 expression was highest in mesenchymal cells. This suggests that although the expression of certain ICs may preferentially align with specific EMT states, the regulation of ICs like PD-L1 may be influenced by additional mechanisms that are potentially origin- and context-specific. This speculation is supported by contrasting findings showing that miR-200 family members can suppress PD-L1 expression in different cancer entities and contexts (199,256). Nevertheless, the observed endogenous expression patterns in BTC cell lines point to EMT-driven differences in IC expression, with the miR-200 family acting as potential regulatory interface.

We selected two miRNAs – miR-141-3p and miR-200c-3p – as representative surrogates to further investigate the relationship between the miR-200 family, EMT, and IC regulation. This selection was driven by two key factors. First, miR-141-3p and miR-200c-3p belong to the same genomic cluster, indicating they share transcriptional regulation (257). Second, despite this shared origin, they belong to different functional clusters due to a single-base difference within their seed sequences. This variation allows them to potentially target different transcripts or the same transcripts at different sites. Since this combination of traits suggests a coordinated expression of these miRNAs, with potential interdependent functions to influence a cells' phenotype, we hoped to capture the cooperative, yet flexible regulatory roles of the miR-200 family through this selection (258).

For our cell line selection, we chose HuCC-T1 as a representative epithelial BTC cell line, and HuH-28 and OCUG-1 as model BTC cell lines with predominantly mesenchymal phenotypes. Additionally, we included the telomerase-immortalized cholangiocyte cell line MMNK-1 with mesenchymal characteristics, to allow for comparisons between cancer cells and non-cancerous cells (221). Tissue origin also influenced our choice. HuCC-T1 and HuH-28 cells originate from ICC, while OCUG-1 cells are derived from GBC (216,217,219). This selection enabled us to compare cancer cells with different EMT states from a similar tissue origin, as well as cells from distinct origins but with similar EMT characteristics, providing a broader perspective on EMT and IC regulation across BTC biology.

4.2. Transient miR-200 family overexpression

To mechanistically explore the connection between the miR-200 family members, EMT, and the regulation of ICs, we conducted gain-of-function experiments using miRNA mimics. In this transient overexpression setting, we successfully upregulated the levels of miR-141-3p or miR-200c-3p in our cell lines, and observed mostly expected downstream effects on the expression of EMT markers. In HuH-28, MMNK-1, and to a lesser extent in OCUG-1 cells, transient miR-200c-3p overexpression, but not miR-141-3p overexpression, resulted in an increased levels of epithelial markers CDH1 and KRT8 and a concomitant decrease of mesenchymal markers ZEB1 and ZEB2. The lacking effects in HuCC-T1 cells can be explained by the fact that this epithelial cell line displays inherently high levels of miR-200 family members and minimal levels of ZEB1 and ZEB2, thereby diminishing the suppressive impact of additional miR-200 family supply within the miR-200/ZEB axis and consequently its influence on the epithelial markers.

In line with the RNA data, HuCC-T1 cells displayed inherently low protein levels of ZEB1 and high CDH1, both of which were only marginally affected by miR-141-3p or miR-200c-3p mimic

transfection. However, in HuH-28 and MMNK-1 cells, high endogenous ZEB1 protein levels were reduced by miR-200c-3p and to a lesser extent by miR-141-3p mimic transfection. CDH1 levels were too low to be detected, underscoring the profound inherent mesenchymal phenotype of these cells. The slightly stronger downregulation of ZEB1 by miR-200c-3p is likely due to its greater number in putative binding sites in the 3'UTR of ZEB1 compared to miR-141-3p (259). Interestingly, in MMNK-1 cells, ZEB1 downregulation was observed at the protein level but not at RNA level. However, this discrepancy is not surprising for direct miRNA targets, as translational repression often precedes mRNA decay, indicating that while RNA levels remain unchanged at early time points, translation is already inhibited, leading to detectable reductions in protein levels (260,261). Overall, transient miR-141-3p and miR-200c-3p overexpression through miRNA mimic transfection was effective and sufficient to initiate a MET program in mesenchymal cell lines, corroborating the well-established regulatory role of miR-200 family members in EMT within our *in vitro* BTC models.

We observed that miR-200c-3p mimic transfection, but not miR-141-3p mimic transfection, resulted in a robust upregulation of PD-L1, LGALS9, and IDO1 across all four tested cell lines. This aligned with the positive correlation between endogenous expression levels of miR-200 family members and LGALS9 and PD-L1. Furthermore, these results could be replicated on protein level for IDO1 and PD-L1. LGALS9 protein, however, was undetectable in any of the cell lines. While we expected to observe transient changes of the LGALS9 protein based on prior studies in different contexts, it is possible that the predominantly secreted nature of LGALS9 and faster secretion dynamics in our cell lines caused intracellular protein levels to fall below detection limits by the 72-hour mark (56,59,262). To this end, LGALS9 ELISA should have been performed to additionally capture secreted LGALS9 in the cell culture supernatant.

Several studies highlighted the cooperative role of miRNAs, showing that when multiple miRNAs bind to various components of the same signaling pathway, their combined effect often surpasses that of targeting a single component (263,264). For instance, Zhou *et al.* demonstrated that in the context of EMT in gastric cancer, overexpression of both miR-141-3p and miR-200c-3p produced a significantly stronger effect than overexpressing either miRNA alone (259). While we observed a similar, though less pronounced, effect on EMT marker expression in BTC cells - with co-transfection of both miRNA mimics showing slightly enhanced effects compared to individual miR-200c-3p mimic transfections – the same was not true in the context of IC regulation. In fact, the effects of the combined miRNA mimics were generally weaker than those of miR-200c-3p mimic transfection alone. This discrepancy is likely due to the reduced miR-200c-3p mimic concentration in the dual transfection setting, rather than any

meaningful biological contribution from the miR-141-3p mimic. Therefore, IC upregulation appears to be primarily driven by miR-200c-3p mimic, with miR-141-3p mimic having a negligible impact in the analyzed BTC cell lines.

4.3. Connection between miR-200c-3p and IC expression

MiRNAs are well-known for downregulating the expression levels of their direct targets (265). Consequently, we considered the possibility that miR-200c-3p does not directly target the ICs, but rather leads to the downregulation of individual negative regulators or a potential common negative regulator of LGALS9, PD-L1, and IDO1. In doing so, transcriptional constraints on the respective ICs would be released, leading to their upregulation. This hypothesis seemed worth investigating for several reasons. First, if miR-200c-3p regulates multiple ICs, it could enhance our understanding of the crosstalk between EMT and immune evasion mechanisms. Second, identifying miR-200c-3p-targeted negative regulators of ICs could illuminate the regulatory networks that contribute to immune evasion in BTC. Lastly, these insights could have clinical implications, as miR-200c-3p or potential target regulators might either serve as useful biomarkers with their presence indicating certain immunotherapy strategies, or act as potential therapeutic targets.

If miR-200c-3p targeted negative regulators of ICs and led to their downregulation upon transient overexpression, a reduction in miR-200c-3p levels should in theory result in an inverse effect – higher levels of negative regulators would dampen the baseline expression of ICs. However, transfecting cells with miR-200c-3p inhibitor did not influence the expression of either EMT markers or ICs. In the context of EMT regulation, the removal of one or two miRNAs may not overcome the cooperative action of the remaining miR-200 family members, which keep maintaining ZEB1 repression and the overall epithelial state in HuCC-T1 cells. The lacking effect on ICs, however, questions the hypothesis of a miR-200c-3p-dependent regulation of either a common or individual negative regulators of LGALS9, PD-L1, or IDO1 expression. This notion was further supported when neither computational analysis of potential miR-200c-3p binding sites, nor experimental validation revealed evidence of miR-200c-3p influencing BIN1, a well-described direct negative transcriptional regulator of IDO1 (227).

The miR-200 family primarily affects the EMT process through its interaction with the pro-mesenchymal transcription factor ZEB1 (254). Therefore, to clarify whether the observed upregulation of ICs upon miR-200c-3p mimic transfection is dependent on a reduction of ZEB1 levels, we examined the effect of siRNA-mediated ZEB1 knockdown on IC expression. Efficient knockdown of ZEB1 in the mesenchymal cell lines OCUG-1, HuH-28, and MMNK-1, did not

result in significant changes in the expression levels of any ICs, suggesting a negligible role of ZEB1 in their transcriptional regulation.

4.4. Unspecific effects of miRNA mimics

Despite ongoing improvements over the last 40 years, transient overexpression systems remain problematic due to the highly artificial conditions, which can disrupt various cellular processes (266,267). To address this, generating stable overexpression cell lines can provide insights into molecular alterations in a more physiological setting, helping to confirm findings from transient overexpression studies (267). However, after successfully establishing stable miR-200c-3p overexpression in OCUG-1 and MMNK-1 cells, we realized that the effects on LGALS9, PD-L1, and IDO1 could not be replicated.

The levels of miR-200c-3p achieved in stable overexpression cells were significantly lower than those observed with transient overexpression. This difference can be explained by the requirement for physiological processing and maturation in stable miRNA overexpression systems, whereas transient miRNA mimic transfection allows for an immediate increase of already mature miRNAs, bypassing the cellular biogenesis limitations. However, we believe that these comparably lower miR-200c-3p do not fully account for the absence of effects on ICs. This belief is mainly supported by our observation that stable miR-200c-3p overexpression in MMNK-1 cells resulted in the upregulation of CDH1, demonstrating that even at lower levels, miR-200c-3p can effectively induce biological downstream changes.

The contrasting results between transient and stable miR-200c-3p overexpression on ICs, coupled with the lack of IC regulation in miR-200c-3p inhibitor and ZEB1 knockdown experiments, and the absence of confirmed direct targets of miR-200c-3p, raised questions about the source of IC upregulation following miR-200c-3p mimic transfection. These uncertainties were further exacerbated by previous studies reporting contrasting results, with miR-200c-3p negatively impacting PD-L1 and IDO1 expression. For instance, Anastasiadou *et al.* demonstrated that miR-200c-3p overexpression reduced PD-L1 expression in ovarian cancer and both PD-L1 and IDO1 in adipose-derived stem cells (256,268). Additionally, Pyzer *et al.* reported miR-200c-dependent downregulation of PD-L1 in acute myeloid leukemia (269). These conflicting findings, along with our inconclusive results, prompted us to look beyond physiological miR-200c-3p functions and explore the possibility of unintended, non-specific effects caused by the miR-200c-3p mimic.

MiRNA mimics are synthetic dsRNA molecules consisting of the mature miRNA sequence and a complimentary passenger strand (270). Upon transfection, these strands separate, with the passenger strand being degraded, while the mature miRNA is loaded into the RISC. Once incorporated, the miRNA guides the RISC to mRNA targets in a sequence-dependent manner, leading to translational repression or mRNA decay. Therefore, this method allows for the investigation of the effects of transiently increased miRNA levels within cells. However, despite their widespread use as useful tools for studying miRNA functions *in vitro*, concerns regarding their specificity and potential unintended effects exist.

Different manufacturers design miRNA mimics in various ways. For instance, the originally used miScript miRNA mimics are unmodified dsRNA molecules, whereas mirVana miRNA mimics additionally include chemical modifications intended to limit non-specific effects. By comparing the effects of cells transfected with either miScript or mirVana miR-200c-3p mimic, we aimed to evaluate the extent to which the miScript miR-200c-3p mimic itself contributes to the upregulation of LGALS9, PD-L1, and IDO1. Our observations revealed that while transfection with the mirVana miR-200c-3p mimic resulted in similarly increased levels of mature miR-200c-3p and CDH1 in HuH-28 and MMNK-1 cells - indicating physiological effects of miR-200c-3p – the ICs were not affected. This clearly demonstrated that the miScript miR-200c-3p mimic impacted the IC expression of BTC cells beyond its intended function.

Owing to this realization, we explored potential underlying cellular responses, particularly focusing on the involvement of dsRNA-mediated innate immunity. We demonstrated that transfecting HuCC-T1 and OCUG-1 cells with miScript miR-200c-3p mimic resulted in a strong upregulation of cytosolic dsRNA sensors, including RIG-I and MDA5, as well as the induction of IFN-β, type III interferons, and antiviral effectors MX1 and OAS1. Interestingly, previous studies have suggested that miRNAs can act as physiological ligands for human Toll-like receptor 8, thereby triggering innate immune responses (271,272). However, since no notable effects were observed in cells transfected with the mirVana miR-200c-3p mimic or in the stable miR-200c-3p overexpression setting, we concluded that miR-200c-3p does not physiologically induce innate immunity. Interestingly, miScript miR-141-3p mimic transfection did not lead to a comparable induction of innate immune responses.

Goldgraben *et al.* reported similar findings when analyzing the effects of miScript miRNA mimics in breast cancer cell lines (273). In an attempt to explain discrepant results of earlier studies, they found that several miScript miRNA mimics were capable of triggering the cells' interferon response and lead to cell growth reduction in a non-specific manner (273). In a series

of experiments using modified and mutated mimic versions, two key factors contributing to these unintended effects were identified: the length of the miRNA mimic and the complementary passenger stand (273). While 23-mer miRNA mimics potently induced interferon signaling, shorter miRNA mimics caused no significant changes (273). This could explain the disparate results we observed for miScript miR-200c-3p and miR-141-3p mimics. The 23-mer miScript miR-200c-3p mimic markedly induces innate immune responses, whereas the 22-mer miScript miR-141-3p mimic does not.

Furthermore, Goldgraben *et al.* demonstrated that mutating the seed sequences of the 23-mer mimic passenger strands mitigated the activation of innate immunity, suggesting that passenger strand-directed mRNA targeting might also contribute to non-specific effects (273). The importance of the passenger strand in the context of unintended effects upon miRNA mimic transfection was further emphasized by Søkilde *et al.* (274). Their *in silico* analysis of existing miRNA microarray data and sequencing of small RNAs associated with AGO revealed that unintentional loading of miRNA mimic passenger strands into the RISC may be connected to considerable side-effects (274).

Nevertheless, while we did not directly investigate a potential passenger strand activity, we argue that the non-separated, full miRNA mimic molecule plays a predominant role in the observed activation of innate immune responses, particularly given the strong upregulation of dsRNA sensors. Supporting this hypothesis, Thomson *et al.* noticed that upon miRNA mimic transfection, only a small fraction of the introduced miRNAs are functional and biologically active, whereas the majority remain inaccessible for RISC loading, indicating faulty strand separation (275). While we see some physiological activity of miR-200c-3p in regulating EMT, indicating successful separation of the mimic strands and loading of mature miR-200c-3p into the RISC, we assume that the majority of transfected miScript miR-200c-3p mimics remains non-functional. These excess miRNA mimics may be recognized as artificial, non-self dsRNA molecules by the transfected cell, thereby initiating innate immune responses and resulting in the upregulation of ICs.

Additionally, Jin *et al.* observed that transient transfection of miRNA mimics can lead to unintended alterations in gene expression (276). They noticed that the transfection of high concentrations of miRNA mimics caused an intracellular accumulation of artificial, high molecular weight RNA species, which non-specifically influenced the expression of several genes (276). Interestingly, despite these effects, they did not observe an induction of interferon response, suggesting that miRNA mimics can unintendedly affect cellular processes without

necessarily triggering innate immunity (276). Of note, Jin *et al.* used miRIDIAN miRNA mimics in their study, which may explain the differences in cellular responses compared to our findings and those reported by Goldgraben *et al.* with miScript miRNA mimics (273,276). This also illustrates that non-specific effects are not exclusive to miScript miRNA mimics, but might extend to other manufacturers as well (273,276).

Given these findings, we can speculate on the observed discrepancies between the miScript and mirVana miR-200c-3p mimics. Both mimics are 23-mers, therefore ruling out aforementioned length-dependent effects as a contributing factor. However, unlike miScript mimics, which are unmodified dsRNA molecules, mirVana mimics contain additional chemical modifications. These modifications likely promote a more efficient separation and degradation of the passenger strand, thereby reducing the intracellular concentration of duplex miRNA mimics while also minimizing potential passenger strand activity. Consequently, this would limit the recognition of the artificially introduced, foreign dsRNA, and prevent the activation of innate immune responses, thereby explaining why transfection of the mirVana miR-200c-3p mimic did not impact IC expression.

Our observations, combined with those of others, have several important implications. First, given the frequent use of miRNA mimics in pre-clinical *in vitro* experiments, it is likely that previous projects aimed at uncovering miRNA functions may have misinterpreted physiological effects and reported distorted results. To limit this risk in future miRNA studies, we argue that validating miRNA effects using stable miRNA overexpression models is essential for demonstrating physiological miRNA effects. Additionally, monitoring for the potential activation of innate immune responses should be considered to ensure that similar unintended effects of miRNA mimics do not compromise biological findings.

Second, these results may have clinical relevance. Several miRNA-based therapeutical strategies are currently being evaluated for clinical applications (277). For instance, MRX34 – a synthetic miR-34 mimic encapsulated in a liposomal nanoparticle – was tested in in a first-in-human clinical trial across various cancer types, including NSCLC, liver cancer, and melanoma (277,278). This study was prematurely halted due to severe immune-related adverse effects, causing the death of four patients (279). While these adverse effects could potentially be attributed to the pleiotropic nature of miRNAs, we could also speculate that miRNA mimics *in vivo* might trigger similar non-specific activation of innate immunity, potentially leading to an overshooting immune response, which could severely affect systemic immune function in patients (280). Although continuous improvements have been made to

enhance tolerability, safety, and specificity of miRNA therapeutics, it remains crucial to thoroughly evaluate the potential of unintended effects, particularly in relation to innate immunity (277,281,282).

4.5. Role of immunogenic cell death

The induction of innate immunity frequently results in lytic, inflammatory forms of cell death, such as pyroptosis, necroptosis, or PANoptosis (283,284). Generally, these types of programmed cell death differ from apoptosis, which is a non-lytic process considered immunogenically silent. In contrast, pyroptosis, necroptosis, and PANoptosis actively promote inflammation by releasing pro-inflammatory cytokines, pathogen-associated molecular patterns (PAMPs), and DAMPs, including DNA fragments, single-stranded RNA (ssRNA), and dsRNA (283). The non-selective release of cytoplasmic components in these processes can further activate innate immune responses by stimulating PRRs of neighboring cells, potentially creating a feed-forward loop that amplifies inflammatory responses (285).

There are mechanistic differences in the execution of these cell death programs. Apoptosis is primarily driven by initiator caspases-8 and -9, which activate effector caspases-3 and -7, resulting in a controlled cellular disassembly (286,287). In contrast, pyroptosis involves inflammatory caspases-4 and -5, which, within the inflammasome complex, activate gasdermins (288,289). These gasdermins form membrane pores, causing water influx, membrane rupture, and cell death (288,289). Necroptosis is initiated by the activity of Receptor-interacting Protein Kinase 1 (RIPK1) and Receptor-interacting Protein Kinase 3 (RIPK3) in absence of caspase-8 (290,291). This pathway involves the phosphorylation and oligomerization of Mixed Lineage Kinase Domain-like Protein (MLKL), which disrupts membrane integrity, leading to ion influx, cell swelling, and uncontrolled release of intracellular material (290–292). PANoptosis is a distinct form of cell death that combines elements of pyroptosis, apoptosis, and necroptosis, utilizing components such as caspases, RIPKs, and pore-forming proteins like gasdermins and MLKL (293,294). However, it also involves distinct triggers, protein complexes, and execution mechanisms (293,294).

Considering the contextual and mechanistic differences in cell death pathways, we can interpret our observations regarding cell growth and apoptotic behavior upon miRNA mimic transfection. MiScript miR-200c-3p mimic transfection led to a reduction in cell numbers of HuCC-T1 and OCUG-1 cells, an effect that could not be entirely explained by the observed levels of activated caspases-3 and -7. While OCUG-1 cells showed moderately strong caspase-3 and -7 activity, this effect was absent in HuCC-T1 cells, suggesting that non-

caspase-dependent, lytic forms of cell death may be triggered in response to miScript miR-200c-3p mimic-mediated activation of innate immunity. Moreover, although caspase-3 and -7 are traditionally connected to apoptosis, recent studies have implicated their involvement in pyroptosis and PANoptosis, respectively (295–297). Thus, despite the observed activation of caspase-3 and -7, it is possible that immunogenic cell death, rather than classical apoptosis, may be predominant in OCUG-1 cells.

4.6. Poly(I:C)

By using poly(I:C), a well-known synthetic dsRNA analog to study innate immune responses, we demonstrated that the observed effect is not limited to the specific miScript miR-200c-3p mimic, but extends to further, dissimilar dsRNA species. This suggests that the immune activation we observed may be a broader response to the presence of artificial or foreign dsRNA, rather than being solely dependent on the specific characteristics of the miScript miR-200c-3p mimic.

Poly(I:C) was described to engage endosomal and cytosolic dsRNA sensors, such as TLR3, RIG-I, and MDA5, which signal through various adapter proteins and transcription factors including IRF3 or NF-κB to mount a potent interferon response (298–301). Interestingly, poly(I:C) was shown to induce distinct mechanisms in prostate cancer cells, resulting in different outcomes. Activation of a TLR3/Proto-oncogene Tyrosine-protein Kinase (Src)/Signal Transducer And Activator Of Transcription 1 (STAT1) axis predominantly led to apoptosis, whereas signaling through MDA5/RIG-I/IRF3 resulted in strong immunostimulatory IFN-β expression (301). While we did not specifically examine different modes of poly(I:C) action and speculate that both pathways may be triggered in our cell models, the outcomes are largely consistent with our observations. Following a lipid-based transfection of poly(I:C), we see strong upregulation of dsRNA sensors TLR3, RIG-I, and MDA5, an activation of transcription factors IRF3 and NF-κB, as well as an increased expression of interferons including IFN-β.

Of note, the method of poly(I:C) delivery into the cells seemed to matter. Dauletbaev *et al.* demonstrated that in well-differentiated airway epithelial cells, unassisted delivery of poly(I:C) only moderately stimulated IFN-β expression, whereas lipid-based transfection of poly(I:C) led to an induction of RIG-I and a concomitant strong upregulation of IFN-β (299). This is in line with our findings, as we observed generally lower effects of poly(I:C) gymnosis compared to transfection in HuCC-T1 cells. Nevertheless, despite these relatively lower induction of interferon response, it was still sufficient to elicit downstream effects, such as the upregulation of antiviral effectors and the expression of ICs. These findings suggest that lipid-based

transfection, while enhancing the magnitude of the response, is not strictly necessary to induce intracellular immune responses.

Interestingly, the effects of an unassisted uptake of poly(I:C) were entirely absent in OCUG-1 cells. Since nucleic acids, including poly(I:C), are negatively charged and therefore cannot passively traverse the cell membrane, they are dependent on active transport mechanisms such as endocytosis-mediated internalization. The binding of dsRNAs to cell surface receptors, such as Class A Scavenger Receptors (SR-A) or Raftlin, have been shown to facilitate clathrin-mediated endocytosis, enabling dsRNA recognition by endosomal TLR3 (302–306). Furthermore, by closely following the uptake of extracellular dsRNAs, Nguyen *et al.* demonstrated that once dsRNAs are internalized, they can be released from the endosomes into the cytoplasm via SID1 Transmembrane Family Member 2 (SIDT2), which allows cytosolic dsRNA activity and promotes antiviral immunity (307). We could speculate that while poly(I:C) is successfully internalized in HuCC-T1 cells through endocytosis, OCUG-1 cells might lack the expression of cell surface receptors like SR-A or Raftlin, impairing dsRNA uptake and consequent activation of innate immunity.

Several studies have highlighted the therapeutical potential of poly(I:C). For instance, Sultan *et al.* demonstrated in tumor mouse models that a specific formulation of poly(I:C) facilitated $CD8^+$ T cell infiltration and reduced tumor growth, dependent on active MDA5 and type I interferon signaling (308). Similarly, Anfray *et al.* found that an intratumoral combination of poly(I:C) with other TLR agonists increased infiltration of M1 macrophages and both $CD4^+$ and $CD8^+$ T cells, with a key involvement of the STAT1 pathway (309). However, while it is evident that immunomodulatory agents like poly(I:C) can promote immune cell infiltration and thereby support antitumor immunity, it is crucial to consider their potential role in the upregulating ICs and associated immunosuppressive consequences. In this context, a combination of poly(I:C) with ICIs may be promising (310).

4.7. Importance of JAK/STAT signaling

Based on our previous results with miScript miR-200c-3p mimic and poly(I:C), we concluded that a dsRNA-mediated innate immune response was triggered, accompanied by the upregulation of ICs such as LGALS9, PD-L1, and IDO1. However, the relationship between these processes remained largely unclear, prompting us to further explore the potential link between innate immunity and IC expression.

We identified JAK/STAT signaling as essential mediator connecting dsRNA-mediated IFN-β secretion with the upregulation of ICs such as LGALS9, PD-L1, and IDO1. Inhibition of JAK1/2 and TYK2 using ruxolitinib completely abrogated the poly(I:C)-induced effects on ICs, while leaving the interferon response mostly unaffected. This strongly suggest the presence of an autocrine and paracrine interferon loop and subsequent JAK/STAT activation as sources of dsRNA-mediated IC upregulation.

Several studies support our findings. For instance, the addition of exogenous recombinant IFN-β to glioma cells induced phosphorylation of STAT1 and increased expression levels of MX1 and PD-L1 (311). Conversely, knockdown of interferon receptor subunits Interferon-Alpha/Beta Receptor Alpha Chain (IFNAR1) and Interferon-Alpha/Beta Receptor Beta Chain (IFNAR2) produced opposite effects (311). Garcia-Diaz *et al.* identified a similar mechanism linking interferon receptor signaling to PD-L1 expression (312). They demonstrated that IFN-γ-mediated JAK/STAT signaling induced IRF1 expression, which in turn lead to increased PD-L1 expression in melanoma cells (312). Similarly, Benci *et al.* showed that sustained IFN-γ signaling can induce PD-L1 expression in tumor cells in a JAK/STAT-dependent manner (313). Accordingly, blocking JAK/STAT signaling with ruxolitinib abolished PD-L1 upregulation and restored sensitivity towards ICI monotherapy (313). Interestingly, computational models analyzing clinical anti-PD-1 responses revealed that high expression of MX1 was associated with a lower response probability in melanoma patients (313). This finding can be understood in the context of our results: since MX1 expression suggests an active innate immune response and interferon signaling, elevated levels may indicate an upregulation of additional ICs like LGALS9 or IDO1 in tumor cells, thereby diminishing the efficacy of anti-PD1 monotherapy by establishing further immunosuppressive mechanisms.

In a clinical context, Zak *et al.* demonstrated that combining ruxolitinib with anti-PD-1 therapy yielded favorable outcomes for patients with Hodgkin lymphoma, primarily by reprogramming myeloid cells from a suppressive to an immunostimulatory state (314). Similarly, Mathew *et al.* reported that combining itacitinib, a selective JAK1 inhibitor, with anti-PD-1 immunotherapy resulted in durable and high response rates in NSCLC patients (315). They found that inhibiting JAK/STAT signaling in preclinical mouse models allowed $CD8^+$ T cells to retain greater plasticity and reduce terminal differentiation, both features associated with improved immune functions (315). It can be speculated that JAK/STAT inhibition may have decreased the expression of additional ICs beyond PD-L1, such as LGALS9 and IDO1 on tumor cells. This reduction of ICs could further alleviate the immunosuppressive TME, thereby enhancing antitumor immunity and improving treatment responses (314,315). Given the broad repertoire

of immunosuppressive molecules present within the TME, strategies that target a wider range of ICs could potentially augment the efficacy ICI monotherapy.

4.8. Relevance of dsRNA

While our data and aforementioned reports support the relationship between interferon-mediated JAK/STAT signaling and the expression of ICs like PD-L1, there has been only limited attention to how dsRNA species contribute to these effects in a pathophysiological setting. Nevertheless, some important connections have been established.

For instance, Sistigu *et al.* demonstrated that anthracycline treatment of mouse fibrosarcoma cells led to an upregulation of type I interferons via TLR3 activation (316). Importantly, this effect was abolished by the addition of Benzonase, a non-specific nuclease, or RNase A, which specifically degrades ssRNA, indicating that self-RNA released from dying cells is crucial to this process (316).

Additionally, Choi *et al.* found that a depletion of DEAD-box RNA helicase 3X (DDX3X) resulted in an accumulation of aberrant cytoplasmic dsRNAs, which triggered type I interferon production in an MDA5-dependent manner (317). Similarly, Sheng *et al.* reported that inhibiting Lysine-specific Histone Demethylase 1A (LSD1) in cancer cells increased the expression of endogenous retroviral elements (ERVs), leading to elevated intracellular dsRNA levels (318). Subsequent recognition via dsRNA sensors such as TLR3, MDA5, and RIG-I activated type I interferons (318). Interestingly, while they observed enhanced antitumor immunity associated with increased T cell infiltration and immunogenicity in low or non-immunogenic tumors, LSD1 knockout cells also had elevated levels of PD-L1 (318).

In line with this, inhibition of N6-Adenosine-Methyltransferase 70 KDa Subunit (METTL3) was shown to result in endogenous dsRNA generation and provoke a cell-intrinsic interferon response (319). Sensing of dsRNA by RIG-I, PKR, or MDA5 resulted in the secretion of IFN-β, activation of JAK/STAT pathways, and an upregulation of interferon-stimulating genes (ISGs), including MHC-I and PD-L1 (319,320).

Collectively, these findings not only indicate the presence of endogenous dsRNA species in various pathophysiological settings, but also reinforce our observations regarding the connections between dsRNA generation, innate immunity, and IC regulation.

4.9. Cisplatin as a trigger of innate immunity

Intrigued by reports linking the generation of atypical endogenous dsRNA species with an induction of innate immunity and subsequent IC upregulation, we wondered about potential sources of immunogenic dsRNA in BTC cells. Multiple endogenous origins of dsRNA have been identified, including the epigenetic derepression of ERVs, deregulated RNA modification mechanisms, faulty RNA degradation machinery, and mitochondrial dysregulation (233). However, chemotherapy-induced genotoxic stress as origin of dsRNA species seemed particularly relevant in the context of BTC (233).

Upon treating OCUG-1 and HuCC-T1 cells with cisplatin, we observed an upregulation of several ICs, including LGALS9, PD-L1, and IDO1. Additionally, cisplatin treatment led to a robust increase in the expression of dsRNA sensor RIG-I, interferons, and the antiviral effectors MX1 and OAS1, suggesting that dsRNA-mediated activation of innate immunity might play a role in these effects.

Given that first-line chemotherapeutic treatment with GemCis yields only moderate responses in BTC patients, we speculated that an accumulation of atypical dsRNA, coupled with innate immune activation and a subsequent establishment of an immunosuppressive TME, could contribute to the limited therapeutic efficacy. This theory seemed particularly interesting in light of growing evidence indicating that host immune system activation is crucial for the efficacy of cytotoxic drugs (321). Notably, the phase III clinical trials TOPAZ-1 and KEYNOTE-966 demonstrated significant benefits from combining GemCis with anti-PD-L1 or anti-PD-1 immunotherapy in BTC patients (90,91).

Based on our findings, we hypothesize that the cisplatin-induced upregulation of ICs, including PD-L1, may limit immune system activation and diminish the antitumor effects. Blocking the PD-1/PD-L1 axis could counteract these immunosuppressive effects to some extent, thereby enhancing antitumor immunity and improving therapeutic outcomes. However, our data shows that cisplatin impacts not only PD-L1 expression but also increases the levels of several other ICs. As such, it remains to be determined to what extent targeting additional ICs could further optimize chemoimmunotherapy approaches.

Although genomic DNA has long been considered the primary pharmacological target of cisplatin, accumulating evidence indicates that additional molecular mechanisms and targets, including RNAs, contribute to its anticancer activity (322). For instance, Rose *et al.* demonstrated that cisplatin exposure led to RNA platination, which induced apoptosis and a

pro-inflammatory gene signature in cancer cells, partly mediated by TLR3 signaling (323). They proposed that cisplatin-mediated RNA cross-linking generates pseudo-dsRNA fragments, implicating a potential role of dsRNAs in that context (323). Additionally, Yang *et al.* discovered that cisplatin treatment strongly induced the formation of endogenous Z-RNA, an unusual form of dsRNA that typically does not occur in cells, triggering Z-DNA-binding Protein 1 (ZBP1)-mediated necroptosis in tumor cells (324). Moreover, cisplatin exposure has been shown to cause cytosolic leakage of mitochondrial dsRNA, leading to the subsequent activation of RIG-I (325).

Interestingly, gemcitabine-based chemotherapy has also been shown to induce immunogenic cell death in ICC cells, accompanied by increased PD-L1 expression (326). Furthermore, when Zeng *et al.* compared gene expression profiles of ICC patients responding and not responding to anti-PD-1 + GemCis combination therapy, they found that higher levels of ICs and immune-related pathways were related to better outcomes (326). Similarly, Chen *et al.* reported that GemCis treatment sensitized aggressive ICCs to anti-PD-1 therapy by promoting effector $CD8^+$ T cell infiltration through vascular normalization (327).

Considering reports of genotoxic agents causing dying cells to release immunogenic self-RNA into the extracellular space, we aimed to evaluate whether similar accumulation of extracellular nucleic acids upon cisplatin treatment can be observed (316). However, the addition of Benzonase (a non-specific nuclease) or RNase III (a dsRNA-specific nuclease) to the culture medium did not limit the effects of cisplatin, suggesting a negligible role of potentially secreted dsRNA species.

An alternative explanation could be that aberrant dsRNA species generated as a consequence of cisplatin treatment are not released as free RNA but instead packaged within extracellular vesicles (EVs). In this scenario, secreted RNAs would be protected from the activity of nucleases present in the medium. Various studies have reported a cisplatin-induced secretion of EVs containing biologically active molecules such as mRNAs, miRNAs, DNA fragments, lipids, proteins, and DAMPs, which can affect surrounding cells (328–333). Additionally, activation of RIG-I has been shown to promote the release of EVs (334). Therefore, we speculated that cisplatin treatment might lead to the release of dsRNA-containing EVs in the medium, potentially taken up by neighboring cells to activate innate immune pathways. However, our experiments did not reveal any gene expression changes indicative of innate immunity when cells were incubated with cisplatin-conditioned medium.

Based on these findings, we concluded that while cisplatin activated innate immunity with a potential contribution of dsRNAs, it likely does so through mechanisms distinct from those observed with poly(I:C). In line with this hypothesis, we could not detect an extracellular accumulation of IFN-β following cisplatin treatment, reinforcing the idea of a cell-intrinsic activation of innate immune responses, independent of autocrine or paracrine signaling mediated by dsRNAs or interferons.

Grabosch *et al.* provide further support for this speculation (87). While mainly focusing on the involvement of cGAS/STING signaling, they demonstrated that cisplatin upregulated PD-L1 in tumor cells without extracellular IFN-β accumulation (87). In an unrelated context, Brägelmann *et al.* reported that MAPK inhibition led to the upregulation of interferon-stimulated genes like IRF1 and OAS1, as well as dsRNA sensors TLR3, RIG-I, and MDA5 across several cancer cell lines (335). Importantly, this effect was independent of extracellular interferon accumulation or IFNAR1 engagement (335). Additionally, RIG-I activation has been shown to increase PD-L1 expression in a cell-intrinsic manner by limiting its proteasomal degradation in colon cancer cells (336).

Collectively, these studies suggest the existence of alternative, cell-autonomous pathways of innate immunity. While this was not further explored within the scope of this PhD project, it is plausible that similar non-classical innate immune mechanisms could contribute to the upregulation of ICs in cisplatin-treated BTC cell lines.

4.10. Conclusion and Outlook

In conclusion, this PhD project yielded several intriguing observations. Despite promising initial findings, we demonstrated that the EMT-regulating miR-200 family members, miR-141-3p or miR-200c-3p, do not have a physiological impact on IC regulation in BTC cells. Instead, we identified dsRNA-driven innate immunity, triggered by the specific miR-200c-3p mimic, as a crucial contributor to IC expression. Further exploration of these unintended effects using the synthetic dsRNA analog poly(I:C) led to the discovery that JAK/STAT signaling serves as important link between innate immune activation and IC expression.

Building on these results, we observed that cisplatin treatment of BTC cells leads to an induction of similar innate immune responses and an upregulation of ICs, potentially through mechanisms involving dsRNA. However, while initial connections have been established, the precise mechanisms linking cisplatin, innate immunity, and IC expression remain unclear.

Further research into these pathways may reveal additional insights into the interplay between innate immunity and IC regulation in BTC, particularly in response to chemotherapy.

Outstanding questions include identifying the specific immunogenic nucleic acids that trigger innate immunity upon cisplatin treatment and gaining deeper understanding of how dsRNA contributes to this process. Furthermore, clarifying the intracellular mechanisms that link innate immune activation with the upregulation of ICs is essential, as is determining whether JAK/STAT signaling or alternative non-canonical innate immune pathways are central to these effects. Investigating the potential involvement of additional interferons beyond IFN-β, could provide additional insights.

From a therapeutic standpoint, it is important to explore how these findings can be effectively translated into clinical practice. While our results provide a potential explanation for the improved outcomes observed when combining cisplatin with ICIs in BTC patients, additional strategies, such as incorporating dsRNA analogs or using inhibitors like ruxolitinib, may further enhance treatment-induced antitumor immunity. Given that cisplatin also leads to the upregulation of ICs beyond PD-L1, it is necessary to investigate whether targeting multiple ICs could further improve chemoimmunotherapy efficacy. Ideally, identifying upstream regulators of IC expression induced by chemotherapy could provide promising targets for therapeutic intervention, potentially abrogating immunosuppressive effects of cisplatin-mediated innate immune activation within the TME.

Despite many unresolved questions, our investigation into the non-specific effects of miRNA mimics has yielded valuable insights into the role of innate immunity in BTC, particularly regarding IC expression. We believe that our current findings, combined with ongoing research into dsRNA-mediated innate immune responses following chemotherapy, could contribute to the development of innovative treatment strategies, ultimately improving the clinical management of BTC.

Bibliography

1. Prinz F, Jonas K, Balihodzic A, Klec C, Reicher A, Barth DA, et al. MicroRNA mimics can distort physiological microRNA effects on immune checkpoints by triggering an antiviral interferon response. RNA Biol. 2022 Jan;19(1):1305–15.
2. Posch F, Prinz F, Balihodzic A, Mayr C, Kiesslich T, Klec C, et al. MiR-200c-3p Modulates Cisplatin Resistance in Biliary Tract Cancer by ZEB1-Independent Mechanisms. Cancers (Basel). 2021 Aug 8;13(16):3996.
3. Ferlay J, Ervik M, Lam F, Colombet M, Mery L, Piñeros M, et al. Global cancer observatory: cancer today. Lyon: International agency for research on cancer. 2020;20182020.
4. Bray F, Laversanne M, Sung H, Ferlay J, Siegel RL, Soerjomataram I, et al. Global cancer statistics 2022: GLOBOCAN estimates of incidence and mortality worldwide for 36 cancers in 185 countries. CA: A Cancer Journal for Clinicians. 2024;74(3):229–63.
5. Valle JW, Kelley RK, Nervi B, Oh DY, Zhu AX. Biliary tract cancer. The Lancet. 2021 Jan 30;397(10272):428–44.
6. Baria K, De Toni EN, Yu B, Jiang Z, Kabadi SM, Malvezzi M. Worldwide Incidence and Mortality of Biliary Tract Cancer. Gastro Hep Advances. 2022 Jan 1;1(4):618–26.
7. Vogel A, Bridgewater J, Edeline J, Kelley RK, Klümpen HJ, Malka D, et al. Biliary tract cancer: ESMO Clinical Practice Guideline for diagnosis, treatment and follow-up☆. Annals of Oncology. 2023 Feb 1;34(2):127–40.
8. Banales JM, Marin JJG, Lamarca A, Rodrigues PM, Khan SA, Roberts LR, et al. Cholangiocarcinoma 2020: the next horizon in mechanisms and management. Nat Rev Gastroenterol Hepatol. 2020 Sep;17(9):557–88.
9. Doleschal B, Taghizadeh H, Webersinke G, Piringer G, Schreil G, Decker J, et al. Real world evidence reveals improved survival outcomes in biliary tract cancer through molecular matched targeted treatment. Sci Rep. 2023 Sep 18;13(1):15421.
10. Sripa B, Kaewkes S, Sithithaworn P, Mairiang E, Laha T, Smout M, et al. Liver fluke induces cholangiocarcinoma. PLoS Med. 2007 Jul;4(7):e201.
11. Jusakul A, Kongpetch S, Teh BT. Genetics of Opisthorchis viverrini-related cholangiocarcinoma. Curr Opin Gastroenterol. 2015 May;31(3):258–63.
12. Sithithaworn P, Yongvanit P, Duenngai K, Kiatsopit N, Pairojkul C. Roles of liver fluke infection as risk factor for cholangiocarcinoma. Journal of Hepato-Biliary-Pancreatic Sciences. 2014;21(5):301–8.
13. Massarweh NN, El-Serag HB. Epidemiology of Hepatocellular Carcinoma and Intrahepatic Cholangiocarcinoma. Cancer Control. 2017 Sep 1;24(3):1073274817729245.
14. Clements O, Eliahoo J, Kim JU, Taylor-Robinson SD, Khan SA. Risk factors for intrahepatic and extrahepatic cholangiocarcinoma: A systematic review and meta-analysis. Journal of Hepatology. 2020 Jan 1;72(1):95–103.
15. Carpino G, Cardinale V, Folseraas T, Overi D, Grzyb K, Costantini D, et al. Neoplastic Transformation of the Peribiliary Stem Cell Niche in Cholangiocarcinoma Arisen in Primary Sclerosing Cholangitis. Hepatology. 2019 Feb;69(2):622–38.

16. Khan SA, Tavolari S, Brandi G. Cholangiocarcinoma: Epidemiology and risk factors. Liver International. 2019;39(S1):19–31.

17. Jusakul A, Cutcutache I, Yong CH, Lim JQ, Huang MN, Padmanabhan N, et al. Whole-Genome and Epigenomic Landscapes of Etiologically Distinct Subtypes of Cholangiocarcinoma. Cancer Discov. 2017 Oct;7(10):1116–35.

18. Andersen JB, Spee B, Blechacz BR, Avital I, Komuta M, Barbour A, et al. Genomic and genetic characterization of cholangiocarcinoma identifies therapeutic targets for tyrosine kinase inhibitors. Gastroenterology. 2012 Apr;142(4):1021-1031.e15.

19. Sia D, Hoshida Y, Villanueva A, Roayaie S, Ferrer J, Tabak B, et al. Integrative molecular analysis of intrahepatic cholangiocarcinoma reveals 2 classes that have different outcomes. Gastroenterology. 2013 Apr;144(4):829–40.

20. Boscoe AN, Rolland C, Kelley RK. Frequency and prognostic significance of isocitrate dehydrogenase 1 mutations in cholangiocarcinoma: a systematic literature review. J Gastrointest Oncol. 2019 Aug;10(4):751–65.

21. Javle M, Bekaii-Saab T, Jain A, Wang Y, Kelley RK, Wang K, et al. Biliary cancer: Utility of next-generation sequencing for clinical management. Cancer. 2016 Dec 15;122(24):3838–47.

22. Weinberg BA, Xiu J, Lindberg MR, Shields AF, Hwang JJ, Poorman K, et al. Molecular profiling of biliary cancers reveals distinct molecular alterations and potential therapeutic targets. J Gastrointest Oncol. 2019 Aug;10(4):652–62.

23. Izquierdo-Sanchez L, Lamarca A, La Casta A, Buettner S, Utpatel K, Klümpen HJ, et al. Cholangiocarcinoma landscape in Europe: Diagnostic, prognostic and therapeutic insights from the ENSCCA Registry. Journal of Hepatology. 2022 May 1;76(5):1109–21.

24. Sasaki T, Takeda T, Okamoto T, Ozaka M, Sasahira N. Chemotherapy for Biliary Tract Cancer in 2021. J Clin Med. 2021 Jul 14;10(14):3108.

25. Valle JW, Wasan H, Johnson P, Jones E, Dixon L, Swindell R, et al. Gemcitabine alone or in combination with cisplatin in patients with advanced or metastatic cholangiocarcinomas or other biliary tract tumours: a multicentre randomised phase II study - The UK ABC-01 Study. Br J Cancer. 2009 Aug 18;101(4):621–7.

26. Valle J, Wasan H, Palmer DH, Cunningham D, Anthoney A, Maraveyas A, et al. Cisplatin plus gemcitabine versus gemcitabine for biliary tract cancer. N Engl J Med. 2010 Apr 8;362(14):1273–81.

27. Okusaka T, Nakachi K, Fukutomi A, Mizuno N, Ohkawa S, Funakoshi A, et al. Gemcitabine alone or in combination with cisplatin in patients with biliary tract cancer: a comparative multicentre study in Japan. Br J Cancer. 2010 Aug 10;103(4):469–74.

28. de Sousa Cavalcante L, Monteiro G. Gemcitabine: Metabolism and molecular mechanisms of action, sensitivity and chemoresistance in pancreatic cancer. European Journal of Pharmacology. 2014 Oct 15;741:8–16.

29. Berdis AJ. Inhibiting DNA Polymerases as a Therapeutic Intervention against Cancer. Front Mol Biosci. 2017;4:78.

30. Cepeda V, Fuertes MA, Castilla J, Alonso C, Quevedo C, Pérez JM. Biochemical mechanisms of cisplatin cytotoxicity. Anticancer Agents Med Chem. 2007 Jan;7(1):3–18.

31. Tchounwou PB, Dasari S, Noubissi FK, Ray P, Kumar S. Advances in Our Understanding of the Molecular Mechanisms of Action of Cisplatin in Cancer Therapy. J Exp Pharmacol. 2021 Mar 18;13:303–28.

32. Brown A, Kumar S, Tchounwou PB. Cisplatin-Based Chemotherapy of Human Cancers. J Cancer Sci Ther. 2019;11(4):97.

33. Gonzalez VM, Fuertes MA, Alonso C, Perez JM. Is cisplatin-induced cell death always produced by apoptosis? Mol Pharmacol. 2001 Apr;59(4):657–63.

34. Galluzzi L, Senovilla L, Vitale I, Michels J, Martins I, Kepp O, et al. Molecular mechanisms of cisplatin resistance. Oncogene. 2012 Apr 12;31(15):1869–83.

35. Jia Y, Xie J. Promising molecular mechanisms responsible for gemcitabine resistance in cancer. Genes & Diseases. 2015 Dec 1;2(4):299–306.

36. Sakai D, Kanai M, Kobayashi S, Eguchi H, Baba H, Seo S, et al. Randomized phase III study of gemcitabine, cisplatin plus S-1 (GCS) versus gemcitabine, cisplatin (GC) for advanced biliary tract cancer (KHBO1401-MITSUBA). Annals of Oncology. 2018 Oct 1;29:viii205.

37. Shroff RT, Javle MM, Xiao L, Kaseb AO, Varadhachary GR, Wolff RA, et al. Gemcitabine, Cisplatin, and nab-Paclitaxel for the Treatment of Advanced Biliary Tract Cancers: A Phase 2 Clinical Trial. JAMA Oncol. 2019 Jun 1;5(6):824–30.

38. Sharma MR, Joshi SS, Karrison TG, Allen K, Suh G, Marsh R, et al. A UGT1A1 genotype-guided dosing study of modified FOLFIRINOX in previously untreated patients with advanced gastrointestinal malignancies. Cancer. 2019 May 15;125(10):1629–36.

39. Davis EJ, Griffith KA, Kim EJ, Ruch JM, McDonnell KJ, Zalupski MM. A Phase II Study of Biweekly Cisplatin, Fixed-Dose-Rate Gemcitabine and Infusional 5-Fluorouracil in Patients With Metastatic Pancreatic and Biliary Cancers. Am J Clin Oncol. 2018 Feb;41(2):128–32.

40. Shroff RT, Guthrie KA, Scott AJ, Borad MJ, Goff LW, Matin K, et al. SWOG 1815: A phase III randomized trial of gemcitabine, cisplatin, and nab-paclitaxel versus gemcitabine and cisplatin in newly diagnosed, advanced biliary tract cancers. JCO. 2023 Feb;41(4_suppl):LBA490–LBA490.

41. Phelip J marc, Desrame J, Edeline J, Barbier E, Terrebonne E, Michel P, et al. Modified FOLFIRINOX Versus CISGEM Chemotherapy for Patients With Advanced Biliary Tract Cancer (PRODIGE 38 AMEBICA): A Randomized Phase II Study. JCO. 2022 Jan 20;40(3):262–71.

42. Lowery MA, Burris HA, Janku F, Shroff RT, Cleary JM, Azad NS, et al. Safety and activity of ivosidenib in patients with IDH1-mutant advanced cholangiocarcinoma: a phase 1 study. Lancet Gastroenterol Hepatol. 2019 Sep;4(9):711–20.

43. Abou-Alfa GK, Macarulla T, Javle MM, Kelley RK, Lubner SJ, Adeva J, et al. Ivosidenib in IDH1-mutant, chemotherapy-refractory cholangiocarcinoma (ClarIDHy): a multicentre, randomised, double-blind, placebo-controlled, phase 3 study. Lancet Oncol. 2020 Jun;21(6):796–807.

44. Javle M, Lowery M, Shroff RT, Weiss KH, Springfeld C, Borad MJ, et al. Phase II Study of BGJ398 in Patients With FGFR-Altered Advanced Cholangiocarcinoma. J Clin Oncol. 2018 Jan 20;36(3):276–82.

45. Abou-Alfa GK, Sahai V, Hollebecque A, Vaccaro G, Melisi D, Al-Rajabi R, et al. Pemigatinib for previously treated, locally advanced or metastatic cholangiocarcinoma: a multicentre, open-label, phase 2 study. Lancet Oncol. 2020 May;21(5):671–84.

46. Lo JH, Agarwal R, Goff LW, Heumann TR. Immunotherapy in Biliary Tract Cancers: Current Standard-of-Care and Emerging Strategies. Cancers (Basel). 2023 Jun 23;15(13):3312.

47. Ishida Y, Agata Y, Shibahara K, Honjo T. Induced expression of PD-1, a novel member of the immunoglobulin gene superfamily, upon programmed cell death. EMBO J. 1992 Nov;11(11):3887–95.

48. Leach DR, Krummel MF, Allison JP. Enhancement of antitumor immunity by CTLA-4 blockade. Science. 1996 Mar 22;271(5256):1734–6.

49. Alegre ML, Frauwirth KA, Thompson CB. T-cell regulation by CD28 and CTLA-4. Nat Rev Immunol. 2001 Dec;1(3):220–8.

50. Hossen MM, Ma Y, Yin Z, Xia Y, Du J, Huang JY, et al. Current understanding of CTLA-4: from mechanism to autoimmune diseases. Front Immunol. 2023 Jul 11;14:1198365.

51. Ai L, Xu A, Xu J. Roles of PD-1/PD-L1 Pathway: Signaling, Cancer, and Beyond. Adv Exp Med Biol. 2020;1248:33–59.

52. Han Y, Liu D, Li L. PD-1/PD-L1 pathway: current researches in cancer. Am J Cancer Res. 2020 Mar 1;10(3):727–42.

53. Ortega MA, Boaru DL, De Leon-Oliva D, Fraile-Martinez O, García-Montero C, Rios L, et al. PD-1/PD-L1 axis: implications in immune regulation, cancer progression, and translational applications. J Mol Med (Berl). 2024 Aug;102(8):987–1000.

54. Opitz CA, Somarribas Patterson LF, Mohapatra SR, Dewi DL, Sadik A, Platten M, et al. The therapeutic potential of targeting tryptophan catabolism in cancer. Br J Cancer. 2020 Jan;122(1):30–44.

55. Sauer N, Janicka N, Szlasa W, Skinderowicz B, Kołodzińska K, Dwernicka W, et al. TIM-3 as a promising target for cancer immunotherapy in a wide range of tumors. Cancer Immunol Immunother. 2023 Aug 11;72(11):3405–25.

56. Lv Y, Ma X, Ma Y, Du Y, Feng J. A new emerging target in cancer immunotherapy: Galectin-9 (LGALS9). Genes & Diseases. 2023 Nov 1;10(6):2366–82.

57. Gonçalves Silva I, Yasinska IM, Sakhnevych SS, Fiedler W, Wellbrock J, Bardelli M, et al. The Tim-3-galectin-9 Secretory Pathway is Involved in the Immune Escape of Human Acute Myeloid Leukemia Cells. EBioMedicine. 2017 Aug 1;22:44–57.

58. Yan J, Zhang Y, Zhang JP, Liang J, Li L, Zheng L. Tim-3 Expression Defines Regulatory T Cells in Human Tumors. PLOS ONE. 2013 Mar 5;8(3):e58006.

59. Yang R, Sun L, Li CF, Wang YH, Yao J, Li H, et al. Galectin-9 interacts with PD-1 and TIM-3 to regulate T cell death and is a target for cancer immunotherapy. Nat Commun. 2021 Feb 5;12(1):832.

60. Yasinska IM, Sakhnevych SS, Pavlova L, Teo Hansen Selnø A, Teuscher Abeleira AM, Benlaouer O, et al. The Tim-3-Galectin-9 Pathway and Its Regulatory Mechanisms in Human Breast Cancer. Front Immunol. 2019;10:1594.

61. Zhai L, Ladomersky E, Lenzen A, Nguyen B, Patel R, Lauing KL, et al. IDO1 in cancer: a Gemini of immune checkpoints. Cell Mol Immunol. 2018 May;15(5):447–57.

62. Seo SK, Kwon B. Immune regulation through tryptophan metabolism. Exp Mol Med. 2023 Jul;55(7):1371–9.

63. Munn DH, Sharma MD, Baban B, Harding HP, Zhang Y, Ron D, et al. GCN2 Kinase in T Cells Mediates Proliferative Arrest and Anergy Induction in Response to Indoleamine 2,3-Dioxygenase. Immunity. 2005 May 1;22(5):633–42.

64. Fallarino F, Grohmann U, You S, McGrath BC, Cavener DR, Vacca C, et al. The Combined Effects of Tryptophan Starvation and Tryptophan Catabolites Down-Regulate T Cell Receptor ζ-Chain and Induce a Regulatory Phenotype in Naive T Cells1. The Journal of Immunology. 2006 Jun 1;176(11):6752–61.

65. Gandhi R, Kumar D, Burns EJ, Nadeau M, Dake B, Laroni A, et al. Activation of the aryl hydrocarbon receptor induces human type 1 regulatory T cell–like and Foxp3+ regulatory T cells. Nat Immunol. 2010 Sep;11(9):846–53.

66. Mezrich JD, Fechner JH, Zhang X, Johnson BP, Burlingham WJ, Bradfield CA. An Interaction between Kynurenine and the Aryl Hydrocarbon Receptor Can Generate Regulatory T Cells. The Journal of Immunology. 2010 Sep 15;185(6):3190–8.

67. Darvin P, Toor SM, Sasidharan Nair V, Elkord E. Immune checkpoint inhibitors: recent progress and potential biomarkers. Exp Mol Med. 2018 Dec;50(12):1–11.

68. Shiravand Y, Khodadadi F, Kashani SMA, Hosseini-Fard SR, Hosseini S, Sadeghirad H, et al. Immune Checkpoint Inhibitors in Cancer Therapy. Curr Oncol. 2022 Apr 24;29(5):3044–60.

69. Okazaki T, Honjo T. PD-1 and PD-1 ligands: from discovery to clinical application. Int Immunol. 2007 Jul;19(7):813–24.

70. Basudan AM. The Role of Immune Checkpoint Inhibitors in Cancer Therapy. Clin Pract. 2022 Dec 27;13(1):22–40.

71. Robert C. A decade of immune-checkpoint inhibitors in cancer therapy. Nat Commun. 2020 Jul 30;11(1):3801.

72. Hodi FS, O'Day SJ, McDermott DF, Weber RW, Sosman JA, Haanen JB, et al. Improved Survival with Ipilimumab in Patients with Metastatic Melanoma. New England Journal of Medicine. 2010 Aug 19;363(8):711–23.

73. Garon EB, Rizvi NA, Hui R, Leighl N, Balmanoukian AS, Eder JP, et al. Pembrolizumab for the Treatment of Non–Small-Cell Lung Cancer. New England Journal of Medicine. 2015 May 21;372(21):2018–28.

74. Cheng W, Fu D, Xu F, Zhang Z. Unwrapping the genomic characteristics of urothelial bladder cancer and successes with immune checkpoint blockade therapy. Oncogenesis. 2018 Jan 23;7(1):1–10.

75. Uson Junior PLS, Araujo RL. Immunotherapy in biliary tract cancers: Current evidence and future perspectives. World J Gastrointest Oncol. 2022 Aug 15;14(8):1446–55.

76. Piha-Paul SA, Oh DY, Ueno M, Malka D, Chung HC, Nagrial A, et al. Efficacy and safety of pembrolizumab for the treatment of advanced biliary cancer: Results from the KEYNOTE-158 and KEYNOTE-028 studies. International Journal of Cancer. 2020;147(8):2190–8.

77. Kim RD, Chung V, Alese OB, El-Rayes BF, Li D, Al-Toubah TE, et al. A Phase 2 Multi-institutional Study of Nivolumab for Patients With Advanced Refractory Biliary Tract Cancer. JAMA Oncology. 2020 Jun 1;6(6):888–94.

78. Doki Y, Ueno M, Hsu CH, Oh DY, Park K, Yamamoto N, et al. Tolerability and efficacy of durvalumab, either as monotherapy or in combination with tremelimumab, in patients

from Asia with advanced biliary tract, esophageal, or head-and-neck cancer. Cancer Medicine. 2022;11(13):2550–60.

79. Fabris L, Perugorria MJ, Mertens J, Björkström NK, Cramer T, Lleo A, et al. The tumour microenvironment and immune milieu of cholangiocarcinoma. Liver Int. 2019 May;39 Suppl 1(Suppl 1):63–78.

80. Fabris L, Sato K, Alpini G, Strazzabosco M. The Tumor Microenvironment in Cholangiocarcinoma Progression. Hepatology. 2021 Jan;73 Suppl 1(Suppl 1):75–85.

81. Job S, Rapoud D, Dos Santos A, Gonzalez P, Desterke C, Pascal G, et al. Identification of Four Immune Subtypes Characterized by Distinct Composition and Functions of Tumor Microenvironment in Intrahepatic Cholangiocarcinoma. Hepatology. 2020 Sep;72(3):965.

82. Yoon SB, Woo SM, Chun JW, Kim DU, Kim J, Park JK, et al. The predictive value of PD-L1 expression in response to anti-PD-1/PD-L1 therapy for biliary tract cancer: a systematic review and meta-analysis. Front Immunol. 2024;15:1321813.

83. Ahn S, Lee J chan, Shin DW, Kim J, Hwang JH. High PD-L1 expression is associated with therapeutic response to pembrolizumab in patients with advanced biliary tract cancer. Sci Rep. 2020 Jul 23;10(1):12348.

84. de Biasi AR, Villena-Vargas J, Adusumilli PS. Cisplatin-induced antitumor immunomodulation: a review of preclinical and clinical evidence. Clin Cancer Res. 2014 Nov 1;20(21):5384–91.

85. Li XM, Zhang XM, Li JY, Jiang N, Chen L, Tang LL, et al. The immune modulation effects of gemcitabine plus cisplatin induction chemotherapy in nasopharyngeal carcinoma. Cancer Medicine. 2022;11(18):3437–44.

86. Bailly C, Thuru X, Quesnel B. Combined cytotoxic chemotherapy and immunotherapy of cancer: modern times. NAR Cancer. 2020 Mar;2(1):zcaa002.

87. Grabosch S, Bulatovic M, Zeng F, Ma T, Zhang L, Ross M, et al. Cisplatin-induced immune modulation in ovarian cancer mouse models with distinct inflammation profiles. Oncogene. 2019 Mar;38(13):2380–93.

88. Tsai TF, Lin JF, Lin YC, Chou KY, Chen HE, Ho CY, et al. Cisplatin contributes to programmed death-ligand 1 expression in bladder cancer through ERK1/2-AP-1 signaling pathway. Bioscience Reports. 2019 Sep 6;39(9):BSR20190362.

89. Oh DY, Lee KH, Lee DW, Yoon J, Kim TY, Bang JH, et al. Gemcitabine and cisplatin plus durvalumab with or without tremelimumab in chemotherapy-naive patients with advanced biliary tract cancer: an open-label, single-centre, phase 2 study. Lancet Gastroenterol Hepatol. 2022 Jun;7(6):522–32.

90. Oh DY, Ruth He A, Qin S, Chen LT, Okusaka T, Vogel A, et al. Durvalumab plus Gemcitabine and Cisplatin in Advanced Biliary Tract Cancer. NEJM Evidence. 2022 Jul 26;1(8):EVIDoa2200015.

91. Kelley RK, Ueno M, Yoo C, Finn RS, Furuse J, Ren Z, et al. Pembrolizumab in combination with gemcitabine and cisplatin compared with gemcitabine and cisplatin alone for patients with advanced biliary tract cancer (KEYNOTE-966): a randomised, double-blind, placebo-controlled, phase 3 trial. The Lancet. 2023 Jun 3;401(10391):1853–65.

92. Friedrich M, Sankowski R, Bunse L, Kilian M, Green E, Ramallo Guevara C, et al. Tryptophan metabolism drives dynamic immunosuppressive myeloid states in IDH-mutant gliomas. Nat Cancer. 2021 Jul;2(7):723–40.

93. Bunse L, Pusch S, Bunse T, Sahm F, Sanghvi K, Friedrich M, et al. Suppression of antitumor T cell immunity by the oncometabolite (R)-2-hydroxyglutarate. Nat Med. 2018 Aug;24(8):1192–203.

94. Ruan R, Li L, Li X, Huang C, Zhang Z, Zhong H, et al. Unleashing the potential of combining FGFR inhibitor and immune checkpoint blockade for FGF/FGFR signaling in tumor microenvironment. Mol Cancer. 2023 Dec;22(1):1–22.

95. Li P, Huang T, Zou Q, Liu D, Wang Y, Tan X, et al. FGFR2 Promotes Expression of PD-L1 in Colorectal Cancer via the JAK/STAT3 Signaling Pathway. The Journal of Immunology. 2019 May 15;202(10):3065–75.

96. Sridharan V, Neyaz A, Chogule A, Baiev I, Reyes S, Barr Fritcher EG, et al. FGFR mRNA Expression in Cholangiocarcinoma and Its Correlation with FGFR2 Fusion Status and Immune Signatures. Clin Cancer Res. 2022 Dec 15;28(24):5431–9.

97. Frampton JE. Ivosidenib: A Review in Advanced Cholangiocarcinoma. Target Oncol. 2023 Nov;18(6):973–80.

98. Kelley RK, Cleary JM, Sahai V, Baretti M, Bridgewater JA, Hua Z, et al. A phase 1/2, safety lead-in and dose expansion, open-label, multicenter trial investigating the safety, tolerability, and preliminary activity of ivosidenib in combination with nivolumab and ipilimumab in previously treated subjects with IDH1-mutated nonresectable or metastatic cholangiocarcinoma. JCO. 2024 Jun;42(16_suppl):TPS4197–TPS4197.

99. Crick F. Central Dogma of Molecular Biology. Nature. 1970 Aug;227(5258):561–3.

100. Crick FH. On protein synthesis. Symp Soc Exp Biol. 1958;12:138–63.

101. Lee RC, Feinbaum RL, Ambros V. The C. elegans heterochronic gene lin-4 encodes small RNAs with antisense complementarity to lin-14. Cell. 1993 Dec 3;75(5):843–54.

102. Reinhart BJ, Slack FJ, Basson M, Pasquinelli AE, Bettinger JC, Rougvie AE, et al. The 21-nucleotide let-7 RNA regulates developmental timing in Caenorhabditis elegans. Nature. 2000 Feb 24;403(6772):901–6.

103. Djebali S, Davis CA, Merkel A, Dobin A, Lassmann T, Mortazavi A, et al. Landscape of transcription in human cells. Nature. 2012 Sep;489(7414):101–8.

104. Ling H, Vincent K, Pichler M, Fodde R, Berindan-Neagoe I, Slack FJ, et al. Junk DNA and the long non-coding RNA twist in cancer genetics. Oncogene. 2015 Sep 24;34(39):5003–11.

105. Fernandes JCR, Acuña SM, Aoki JI, Floeter-Winter LM, Muxel SM. Long Non-Coding RNAs in the Regulation of Gene Expression: Physiology and Disease. Noncoding RNA. 2019 Feb 17;5(1):17.

106. Oo JA, Brandes RP, Leisegang MS. Long non-coding RNAs: novel regulators of cellular physiology and function. Pflugers Arch. 2022;474(2):191–204.

107. Statello L, Guo CJ, Chen LL, Huarte M. Gene regulation by long non-coding RNAs and its biological functions. Nat Rev Mol Cell Biol. 2021 Feb;22(2):96–118.

108. Nemeth K, Bayraktar R, Ferracin M, Calin GA. Non-coding RNAs in disease: from mechanisms to therapeutics. Nat Rev Genet. 2024 Mar;25(3):211–32.

109. Laurent GS, Wahlestedt C, Kapranov P. The Landscape of long noncoding RNA classification. Trends in Genetics. 2015 May 1;31(5):239–51.

110. Kwok ZH, Ni K, Jin Y. Extracellular Vesicle Associated Non-Coding RNAs in Lung Infections and Injury. Cells. 2021 May;10(5):965.

111. Shi J, Zhou T, Chen Q. Exploring the expanding universe of small RNAs. Nat Cell Biol. 2022 Apr;24(4):415–23.

112. Lee Y, Kim M, Han J, Yeom KH, Lee S, Baek SH, et al. MicroRNA genes are transcribed by RNA polymerase II. EMBO J. 2004 Oct 13;23(20):4051–60.

113. Borchert GM, Lanier W, Davidson BL. RNA polymerase III transcribes human microRNAs. Nat Struct Mol Biol. 2006 Dec;13(12):1097–101.

114. Han J, Lee Y, Yeom KH, Kim YK, Jin H, Kim VN. The Drosha-DGCR8 complex in primary microRNA processing. Genes Dev. 2004 Dec 15;18(24):3016–27.

115. Rodriguez A, Griffiths-Jones S, Ashurst JL, Bradley A. Identification of mammalian microRNA host genes and transcription units. Genome Res. 2004 Oct;14(10A):1902–10.

116. Lin SL, Kim H, Ying SY. Intron-mediated RNA interference and microRNA (miRNA). Front Biosci. 2008 Jan 1;13:2216–30.

117. MacFarlane LA, Murphy PR. MicroRNA: Biogenesis, Function and Role in Cancer. Curr Genomics. 2010 Nov;11(7):537–61.

118. Ruby JG, Jan CH, Bartel DP. Intronic microRNA precursors that bypass Drosha processing. Nature. 2007 Jul;448(7149):83–6.

119. Lund E, Güttinger S, Calado A, Dahlberg JE, Kutay U. Nuclear export of microRNA precursors. Science. 2004 Jan 2;303(5654):95–8.

120. Song MS, Rossi JJ. Molecular mechanisms of Dicer: endonuclease and enzymatic activity. Biochem J. 2017 May 4;474(10):1603–18.

121. Ha M, Kim VN. Regulation of microRNA biogenesis. Nat Rev Mol Cell Biol. 2014 Aug;15(8):509–24.

122. Shang R, Lee S, Senavirathne G, Lai EC. microRNAs in action: biogenesis, function and regulation. Nat Rev Genet. 2023 Dec;24(12):816–33.

123. Broughton JP, Lovci MT, Huang JL, Yeo GW, Pasquinelli AE. Pairing beyond the Seed Supports MicroRNA Targeting Specificity. Molecular Cell. 2016 Oct 20;64(2):320–33.

124. Filipowicz W, Bhattacharyya SN, Sonenberg N. Mechanisms of post-transcriptional regulation by microRNAs: are the answers in sight? Nat Rev Genet. 2008 Feb;9(2):102–14.

125. Parker R, Song H. The enzymes and control of eukaryotic mRNA turnover. Nat Struct Mol Biol. 2004 Feb;11(2):121–7.

126. Pu M, Chen J, Tao Z, Miao L, Qi X, Wang Y, et al. Regulatory network of miRNA on its target: coordination between transcriptional and post-transcriptional regulation of gene expression. Cell Mol Life Sci. 2019 Feb;76(3):441–51.

127. Peng Y, Croce CM. The role of MicroRNAs in human cancer. Sig Transduct Target Ther. 2016 Jan 28;1(1):1–9.

128. Suzuki HI. Roles of MicroRNAs in Disease Biology. JMA J. 2023 Apr 14;6(2):104–13.

129. Vannini I, Fanini F, Fabbri M. Emerging roles of microRNAs in cancer. Curr Opin Genet Dev. 2018 Feb;48:128–33.

130. Ardekani AM, Naeini MM. The Role of MicroRNAs in Human Diseases. Avicenna J Med Biotechnol. 2010;2(4):161–79.

131. Vaghf A, Khansarinejad B, Ghaznavi-Rad E, Mondanizadeh M. The role of microRNAs in diseases and related signaling pathways. Mol Biol Rep. 2022 Jul 1;49(7):6789–801.

132. Croce CM, Calin GA. miRNAs, cancer, and stem cell division. Cell. 2005 Jul 15;122(1):6–7.

133. Calin GA, Dumitru CD, Shimizu M, Bichi R, Zupo S, Noch E, et al. Frequent deletions and down-regulation of micro- RNA genes miR15 and miR16 at 13q14 in chronic lymphocytic leukemia. Proc Natl Acad Sci U S A. 2002 Nov 26;99(24):15524–9.

134. Hayashita Y, Osada H, Tatematsu Y, Yamada H, Yanagisawa K, Tomida S, et al. A polycistronic microRNA cluster, miR-17-92, is overexpressed in human lung cancers and enhances cell proliferation. Cancer Res. 2005 Nov 1;65(21):9628–32.

135. Mavrakis KJ, Wolfe AL, Oricchio E, Palomero T, de Keersmaecker K, McJunkin K, et al. Genome-wide RNA-mediated interference screen identifies miR-19 targets in Notch-induced T-cell acute lymphoblastic leukaemia. Nat Cell Biol. 2010 Apr;12(4):372–9.

136. Tagawa H, Seto M. A microRNA cluster as a target of genomic amplification in malignant lymphoma. Leukemia. 2005 Nov;19(11):2013–6.

137. O'Donnell KA, Wentzel EA, Zeller KI, Dang CV, Mendell JT. c-Myc-regulated microRNAs modulate E2F1 expression. Nature. 2005 Jun 9;435(7043):839–43.

138. Chang TC, Yu D, Lee YS, Wentzel EA, Arking DE, West KM, et al. Widespread microRNA repression by Myc contributes to tumorigenesis. Nat Genet. 2008 Jan;40(1):43–50.

139. Wang X, Zhao X, Gao P, Wu M. c-Myc modulates microRNA processing via the transcriptional regulation of Drosha. Sci Rep. 2013;3:1942.

140. Karube Y, Tanaka H, Osada H, Tomida S, Tatematsu Y, Yanagisawa K, et al. Reduced expression of Dicer associated with poor prognosis in lung cancer patients. Cancer Sci. 2005 Feb;96(2):111–5.

141. Merritt WM, Lin YG, Han LY, Kamat AA, Spannuth WA, Schmandt R, et al. Dicer, Drosha, and outcomes in patients with ovarian cancer. N Engl J Med. 2008 Dec 18;359(25):2641–50.

142. Allegra D, Bilan V, Garding A, Döhner H, Stilgenbauer S, Kuchenbauer F, et al. Defective DROSHA processing contributes to downregulation of MiR-15/-16 in chronic lymphocytic leukemia. Leukemia. 2014 Jan;28(1):98–107.

143. Shen J, Xia W, Khotskaya YB, Huo L, Nakanishi K, Lim SO, et al. EGFR modulates microRNA maturation in response to hypoxia through phosphorylation of AGO2. Nature. 2013 May 16;497(7449):383–7.

144. Hanahan D, Weinberg RA. The Hallmarks of Cancer. Cell. 2000 Jan 7;100(1):57–70.

145. Hanahan D, Weinberg RA. Hallmarks of cancer: the next generation. Cell. 2011 Mar 4;144(5):646–74.

146. Hanahan D. Hallmarks of Cancer: New Dimensions. Cancer Discovery. 2022 Jan 12;12(1):31–46.

147. Otmani K, Lewalle P. Tumor Suppressor miRNA in Cancer Cells and the Tumor Microenvironment: Mechanism of Deregulation and Clinical Implications. Front Oncol. 2021 Oct 15;11:708765.

148. Svoronos AA, Engelman DM, Slack FJ. OncomiR or Tumor Suppressor? The Duplicity of MicroRNAs in Cancer. Cancer Research. 2016 Jun 30;76(13):3666–70.

149. Yi C, Wang Q, Wang L, Huang Y, Li L, Liu L, et al. MiR-663, a microRNA targeting p21(WAF1/CIP1), promotes the proliferation and tumorigenesis of nasopharyngeal carcinoma. Oncogene. 2012 Oct 11;31(41):4421–33.

150. Ding L, Lan Z, Xiong X, Ao H, Feng Y, Gu H, et al. The Dual Role of MicroRNAs in Colorectal Cancer Progression. Int J Mol Sci. 2018 Sep 17;19(9):2791.

151. Feng YH, Tsao CJ. Emerging role of microRNA-21 in cancer. Biomed Rep. 2016 Oct;5(4):395–402.

152. Xiong B, Cheng Y, Ma L, Zhang C. MiR-21 regulates biological behavior through the PTEN/PI-3 K/Akt signaling pathway in human colorectal cancer cells. Int J Oncol. 2013 Jan;42(1):219–28.

153. Asangani IA, Rasheed S a. K, Nikolova DA, Leupold JH, Colburn NH, Post S, et al. MicroRNA-21 (miR-21) post-transcriptionally downregulates tumor suppressor Pdcd4 and stimulates invasion, intravasation and metastasis in colorectal cancer. Oncogene. 2008 Apr 3;27(15):2128–36.

154. Chi LH, Cross RSN, Redvers RP, Davis M, Hediyeh-zadeh S, Mathivanan S, et al. MicroRNA-21 is immunosuppressive and pro-metastatic via separate mechanisms. Oncogenesis. 2022 Jul 11;11(1):1–12.

155. Pekarsky Y, Croce CM. Role of miR-15/16 in CLL. Cell Death Differ. 2015 Jan;22(1):6–11.

156. He L, He X, Lim LP, de Stanchina E, Xuan Z, Liang Y, et al. A microRNA component of the p53 tumour suppressor network. Nature. 2007 Jun 28;447(7148):1130–4.

157. Chang TC, Wentzel EA, Kent OA, Ramachandran K, Mullendore M, Lee KH, et al. Transactivation of miR-34a by p53 broadly influences gene expression and promotes apoptosis. Mol Cell. 2007 Jun 8;26(5):745–52.

158. Raver-Shapira N, Marciano E, Meiri E, Spector Y, Rosenfeld N, Moskovits N, et al. Transcriptional activation of miR-34a contributes to p53-mediated apoptosis. Mol Cell. 2007 Jun 8;26(5):731–43.

159. Bader AG. miR-34 – a microRNA replacement therapy is headed to the clinic. Front Genet. 2012 Jul 2;3:120.

160. Pei D, Shu X, Gassama-Diagne A, Thiery JP. Mesenchymal–epithelial transition in development and reprogramming. Nat Cell Biol. 2019 Jan;21(1):44–53.

161. Gonzalez DM, Medici D. Signaling mechanisms of the epithelial-mesenchymal transition. Science Signaling. 2014 Sep 23;7(344):re8–re8.

162. Thiery JP. Epithelial–mesenchymal transitions in tumour progression. Nat Rev Cancer. 2002 Jun;2(6):442–54.

163. Nieto MA, Huang RYJ, Jackson RA, Thiery JP. EMT: 2016. Cell. 2016 Jun 30;166(1):21–45.

164. Nieto MA. Epithelial Plasticity: A Common Theme in Embryonic and Cancer Cells. Science. 2013 Nov 8;342(6159):1234850.

165. Armstrong AJ, Marengo MS, Oltean S, Kemeny G, Bitting RL, Turnbull JD, et al. Circulating Tumor Cells from Patients with Advanced Prostate and Breast Cancer Display Both Epithelial and Mesenchymal Markers. Molecular Cancer Research. 2011 Aug 1;9(8):997–1007.

166. Yu M, Bardia A, Wittner BS, Stott SL, Smas ME, Ting DT, et al. Circulating Breast Tumor Cells Exhibit Dynamic Changes in Epithelial and Mesenchymal Composition. Science. 2013 Feb;339(6119):580–4.

167. Jolly MK, Boareto M, Huang B, Jia D, Lu M, Ben-Jacob E, et al. Implications of the Hybrid Epithelial/Mesenchymal Phenotype in Metastasis. Front Oncol. 2015;5:155.

168. Saitoh M. Involvement of partial EMT in cancer progression. J Biochem. 2018 Oct 1;164(4):257–64.

169. Sinha D, Saha P, Samanta A, Bishayee A. Emerging Concepts of Hybrid Epithelial-to-Mesenchymal Transition in Cancer Progression. Biomolecules. 2020 Nov 16;10(11):1561.

170. Pal A, Barrett TF, Paolini R, Parikh A, Puram SV. Partial EMT in head and neck cancer biology: a spectrum instead of a switch. Oncogene. 2021 Aug;40(32):5049–65.

171. Heldin CH, Vanlandewijck M, Moustakas A. Regulation of EMT by TGFβ in cancer. FEBS Letters. 2012;586(14):1959–70.

172. McCormack N, O'Dea S. Regulation of epithelial to mesenchymal transition by bone morphogenetic proteins. Cellular Signalling. 2013 Dec 1;25(12):2856–62.

173. Espinoza I, Miele L. Deadly crosstalk: Notch signaling at the intersection of EMT and cancer stem cells. Cancer Letters. 2013 Nov 28;341(1):41–5.

174. Nieto MA, Cano A. The epithelial–mesenchymal transition under control: Global programs to regulate epithelial plasticity. Seminars in Cancer Biology. 2012 Oct 1;22(5):361–8.

175. Thiery JP, Acloque H, Huang RYJ, Nieto MA. Epithelial-Mesenchymal Transitions in Development and Disease. Cell. 2009 Nov 25;139(5):871–90.

176. Batlle E, Sancho E, Francí C, Domínguez D, Monfar M, Baulida J, et al. The transcription factor Snail is a repressor of E-cadherin gene expression in epithelial tumour cells. Nat Cell Biol. 2000 Feb;2(2):84–9.

177. Cano A, Pérez-Moreno MA, Rodrigo I, Locascio A, Blanco MJ, del Barrio MG, et al. The transcription factor Snail controls epithelial–mesenchymal transitions by repressing E-cadherin expression. Nat Cell Biol. 2000 Feb;2(2):76–83.

178. Yang J, Mani SA, Donaher JL, Ramaswamy S, Itzykson RA, Come C, et al. Twist, a Master Regulator of Morphogenesis, Plays an Essential Role in Tumor Metastasis. Cell. 2004 Jun 25;117(7):927–39.

179. Zaravinos A. The Regulatory Role of MicroRNAs in EMT and Cancer. J Oncol. 2015;2015:865816.

180. Díaz-López A, Moreno-Bueno G, Cano A. Role of microRNA in epithelial to mesenchymal transition and metastasis and clinical perspectives. Cancer Management and Research. 2014 Apr 25;6:205–16.

181. Humphries B, Yang C. The microRNA-200 family: small molecules with novel roles in cancer development, progression and therapy. Oncotarget. 2015 Jan 30;6(9):6472–98.

182. Cavallari I, Ciccarese F, Sharova E, Urso L, Raimondi V, Silic-Benussi M, et al. The miR-200 Family of microRNAs: Fine Tuners of Epithelial-Mesenchymal Transition and Circulating Cancer Biomarkers. Cancers (Basel). 2021 Nov 23;13(23):5874.

183. Korpal M, Lee ES, Hu G, Kang Y. The miR-200 family inhibits epithelial-mesenchymal transition and cancer cell migration by direct targeting of E-cadherin transcriptional repressors ZEB1 and ZEB2. J Biol Chem. 2008 May 30;283(22):14910–4.

184. Gregory PA, Bert AG, Paterson EL, Barry SC, Tsykin A, Farshid G, et al. The miR-200 family and miR-205 regulate epithelial to mesenchymal transition by targeting ZEB1 and SIP1. Nat Cell Biol. 2008 May;10(5):593–601.

185. Park SM, Gaur AB, Lengyel E, Peter ME. The miR-200 family determines the epithelial phenotype of cancer cells by targeting the E-cadherin repressors ZEB1 and ZEB2. Genes Dev. 2008 Apr 1;22(7):894–907.

186. Bracken CP, Gregory PA, Kolesnikoff N, Bert AG, Wang J, Shannon MF, et al. A Double-Negative Feedback Loop between ZEB1-SIP1 and the microRNA-200 Family Regulates Epithelial-Mesenchymal Transition. Cancer Research. 2008 Sep 30;68(19):7846–54.

187. Hill L, Browne G, Tulchinsky E. ZEB/miR-200 feedback loop: at the crossroads of signal transduction in cancer. Int J Cancer. 2013 Feb 15;132(4):745–54.

188. Abba ML, Patil N, Leupold JH, Allgayer H. MicroRNA Regulation of Epithelial to Mesenchymal Transition. J Clin Med. 2016 Jan 14;5(1):8.

189. Perdigão-Henriques R, Petrocca F, Altschuler G, Thomas MP, Le MTN, Tan SM, et al. miR-200 promotes the mesenchymal to epithelial transition by suppressing multiple members of the Zeb2 and Snail1 transcriptional repressor complexes. Oncogene. 2016 Jan;35(2):158–72.

190. Urbas R, Mayr C, Klieser E, Fuereder J, Bach D, Stättner S, et al. Relevance of MicroRNA200 Family and MicroRNA205 for Epithelial to Mesenchymal Transition and Clinical Outcome in Biliary Tract Cancer Patients. International Journal of Molecular Sciences. 2016 Dec;17(12):2053.

191. Oishi N, Kumar MR, Roessler S, Ji J, Forgues M, Budhu A, et al. Transcriptomic profiling reveals hepatic stem-like gene signatures and interplay of miR-200c and epithelial-mesenchymal transition in intrahepatic cholangiocarcinoma. Hepatology. 2012 Nov;56(5):1792–803.

192. Peng F, Jiang J, Yu Y, Tian R, Guo X, Li X, et al. Direct targeting of SUZ12/ROCK2 by miR-200b/c inhibits cholangiocarcinoma tumourigenesis and metastasis. Br J Cancer. 2013 Dec 10;109(12):3092–104.

193. Taki M, Abiko K, Ukita M, Murakami R, Yamanoi K, Yamaguchi K, et al. Tumor Immune Microenvironment during Epithelial–Mesenchymal Transition. Clinical Cancer Research. 2021 Sep 1;27(17):4669–79.

194. Imodoye SO, Adedokun KA. EMT-induced immune evasion: connecting the dots from mechanisms to therapy. Clin Exp Med. 2023 Dec 1;23(8):4265–87.

195. Lou Y, Diao L, Cuentas ERP, Denning WL, Chen L, Fan YH, et al. Epithelial–Mesenchymal Transition Is Associated with a Distinct Tumor Microenvironment Including Elevation of Inflammatory Signals and Multiple Immune Checkpoints in Lung Adenocarcinoma. Clinical Cancer Research. 2016 Jul 14;22(14):3630–42.

196. Guo CC, Majewski T, Zhang L, Yao H, Bondaruk J, Wang Y, et al. Dysregulation of EMT Drives the Progression to Clinically Aggressive Sarcomatoid Bladder Cancer. Cell Reports. 2019 May 7;27(6):1781-1793.e4.

197. Hugo W, Zaretsky JM, Sun L, Song C, Moreno BH, Hu-Lieskovan S, et al. Genomic and Transcriptomic Features of Response to Anti-PD-1 Therapy in Metastatic Melanoma. Cell. 2016 Mar 24;165(1):35–44.

198. Dongre A, Rashidian M, Reinhardt F, Bagnato A, Keckesova Z, Ploegh HL, et al. Epithelial-to-Mesenchymal Transition Contributes to Immunosuppression in Breast Carcinomas. Cancer Research. 2017 Aug 1;77(15):3982–9.

199. Chen L, Gibbons DL, Goswami S, Cortez MA, Ahn YH, Byers LA, et al. Metastasis is regulated via microRNA-200/ZEB1 axis control of tumour cell PD-L1 expression and intratumoral immunosuppression. Nat Commun. 2014 Oct 28;5:5241.

200. Guo Y, Lu X, Chen Y, Rendon B, Mitchell RA, Cuatrecasas M, et al. Zeb1 induces immune checkpoints to form an immunosuppressive envelope around invading cancer cells. Sci Adv. 2021 May;7(21):eabd7455.

201. Noman MZ, Janji B, Abdou A, Hasmim M, Terry S, Tan TZ, et al. The immune checkpoint ligand PD-L1 is upregulated in EMT-activated human breast cancer cells by a mechanism involving ZEB-1 and miR-200. Oncoimmunology. 2017 Jan 23;6(1):e1263412.

202. Ricciardi M, Zanotto M, Malpeli G, Bassi G, Perbellini O, Chilosi M, et al. Epithelial-to-mesenchymal transition (EMT) induced by inflammatory priming elicits mesenchymal stromal cell-like immune-modulatory properties in cancer cells. Br J Cancer. 2015 Mar;112(6):1067–75.

203. Xu S, Zhan M, Wang J. Epithelial-to-mesenchymal transition in gallbladder cancer: from clinical evidence to cellular regulatory networks. Cell Death Discov. 2017 Nov 27;3(1):1–11.

204. Oh CR, Kim HD, Ryu YM, Lee S, Kim D, Lee DS, et al. Epithelial-Mesenchymal Transition Phenotype and Peritumoral Immune Cell Infiltration in Advanced Biliary Tract Cancer. Anticancer Res. 2023 Feb;43(2):645–52.

205. Hu A, Sun L, Lin H, Liao Y, Yang H, Mao Y. Harnessing innate immune pathways for therapeutic advancement in cancer. Sig Transduct Target Ther. 2024 Mar 25;9(1):1–59.

206. Demaria O, Cornen S, Daëron M, Morel Y, Medzhitov R, Vivier E. Harnessing innate immunity in cancer therapy. Nature. 2019 Oct;574(7776):45–56.

207. Medzhitov R, Janeway CA. Innate immune induction of the adaptive immune response. Cold Spring Harb Symp Quant Biol. 1999;64:429–35.

208. Vivier E, Artis D, Colonna M, Diefenbach A, Di Santo JP, Eberl G, et al. Innate Lymphoid Cells: 10 Years On. Cell. 2018 Aug 23;174(5):1054–66.

209. Galluzzi L, Buqué A, Kepp O, Zitvogel L, Kroemer G. Immunogenic cell death in cancer and infectious disease. Nat Rev Immunol. 2017 Feb;17(2):97–111.

210. Sadler AJ, Williams BRG. Interferon-inducible antiviral effectors. Nat Rev Immunol. 2008 Jul;8(7):559–68.

211. Liu X, Cen X, Wu R, Chen Z, Xie Y, Wang F, et al. ARIH1 activates STING-mediated T-cell activation and sensitizes tumors to immune checkpoint blockade. Nat Commun. 2023 Jul 10;14(1):4066.

212. Lemos H, Mohamed E, Huang L, Ou R, Pacholczyk G, Arbab AS, et al. STING Promotes the Growth of Tumors Characterized by Low Antigenicity via IDO Activation. Cancer Research. 2016 Apr 14;76(8):2076–81.

213. Heidegger S, Wintges A, Stritzke F, Bek S, Steiger K, Koenig PA, et al. RIG-I activation is critical for responsiveness to checkpoint blockade. Science Immunology. 2019 Sep 13;4(39):eaau8943.

214. Ribas A, Medina T, Kummar S, Amin A, Kalbasi A, Drabick JJ, et al. SD-101 in Combination with Pembrolizumab in Advanced Melanoma: Results of a Phase Ib, Multicenter Study. Cancer Discov. 2018 Oct;8(10):1250–7.

215. Koerner J, Horvath D, Herrmann VL, MacKerracher A, Gander B, Yagita H, et al. PLGA-particle vaccine carrying TLR3/RIG-I ligand Riboxxim synergizes with immune checkpoint blockade for effective anti-cancer immunotherapy. Nat Commun. 2021 May 18;12(1):2935.

216. Miyagiwa M, Ichida T, Tokiwa T, Sato J, Sasaki H. A new human cholangiocellular carcinoma cell line (HuCC-T1) producing carbohydrate antigen 19/9 in serum-free medium. In Vitro Cell Dev Biol. 1989 Jun;25(6):503–10.

217. Kusaka Y, Tokiwa T, Sato J. Establishment and characterization of a cell line from a human cholangiocellular carcinoma. Res Exp Med (Berl). 1988;188(5):367–75.

218. Homma S, Nagamori S, Fujise K, Yamazaki K, Hasumura S, Sujino H, et al. Human bile duct carcinoma cell line producing abundant mucin in vitro. Gastroenterol Jpn. 1987 Aug;22(4):474–9.

219. Yamada N, Chung Y, Ohtani H, Ikeda T, Onoda N, Sawada T, et al. Establishment and characterization of a new human gallbladder carcinoma cell line (OCUG-1) producing TA-4. International Journal of Oncology. 1997 Jun 1;10(6):1251–5.

220. Sripa B, Leungwattanawanit S, Nitta T, Wongkham C, Bhudhisawasdi V, Puapairoj A, et al. Establishment and characterization of an opisthorchiasis-associated cholangiocarcinoma cell line (KKU-100). World J Gastroenterol. 2005 Jun 14;11(22):3392–7.

221. Maruyama M, Kobayashi N, Westerman KA, Sakaguchi M, Allain JE, Totsugawa T, et al. Establishment of a highly differentiated immortalized human cholangiocyte cell line with SV40T and hTERT. Transplantation. 2004 Feb 15;77(3):446–51.

222. Saijyo S, Kudo T, Suzuki M, Katayose Y, Shinoda M, Muto T, et al. Establishment of a new extrahepatic bile duct carcinoma cell line, TFK-1. Tohoku J Exp Med. 1995 Sep;177(1):61–71.

223. De Winter JC. Using the Student's t-test with extremely small sample sizes. Practical Assessment, Research, and Evaluation. 2019;18(1):10.

224. Gu Z, Eils R, Schlesner M. Complex heatmaps reveal patterns and correlations in multidimensional genomic data. Bioinformatics. 2016 Sep 15;32(18):2847–9.

225. Gu Z. Complex heatmap visualization. iMeta. 2022;1(3):e43.

226. Ragaini S, Wagner S, Marconi G, Parisi S, Sartor C, Nanni J, et al. An IDO1-related immune gene signature predicts overall survival in acute myeloid leukemia. Blood Adv. 2022 Jan 11;6(1):87–99.

227. Muller AJ, DuHadaway JB, Donover PS, Sutanto-Ward E, Prendergast GC. Inhibition of indoleamine 2,3-dioxygenase, an immunoregulatory target of the cancer suppression gene Bin1, potentiates cancer chemotherapy. Nat Med. 2005 Mar;11(3):312–9.

228. Agarwal V, Bell GW, Nam JW, Bartel DP. Predicting effective microRNA target sites in mammalian mRNAs. Izaurralde E, editor. eLife. 2015 Aug 12;4:e05005.

229. Chen Y, Wang X. miRDB: an online database for prediction of functional microRNA targets. Nucleic Acids Res. 2020 Jan 8;48(D1):D127–31.

230. Sticht C, De La Torre C, Parveen A, Gretz N. miRWalk: An online resource for prediction of microRNA binding sites. PLoS One. 2018;13(10):e0206239.

231. Riera Romo M. Cell death as part of innate immunity: Cause or consequence? Immunology. 2021 Aug;163(4):399–415.

232. Morimoto Y, Kishida T, Kotani SI, Takayama K, Mazda O. Interferon-β signal may up-regulate PD-L1 expression through IRF9-dependent and independent pathways in lung cancer cells. Biochem Biophys Res Commun. 2018 Dec 9;507(1–4):330–6.

233. Chen YG, Hur S. Cellular origins of dsRNA, their recognition and consequences. Nat Rev Mol Cell Biol. 2022 Apr;23(4):286–301.

234. Murao A, Aziz M, Wang H, Brenner M, Wang P. Release mechanisms of major DAMPs. Apoptosis. 2021;26(3):152–62.

235. Sadik N, Cruz L, Gurtner A, Rodosthenous RS, Dusoswa SA, Ziegler O, et al. Extracellular RNAs: A New Awareness of Old Perspectives. Methods Mol Biol. 2018;1740:1–15.

236. O'Brien SJ, Carter JV, Burton JF, Oxford BG, Schmidt MN, Hallion JC, et al. The role of the miR-200 family in epithelial–mesenchymal transition in colorectal cancer: a systematic review. International Journal of Cancer. 2018;142(12):2501–11.

237. Mongroo PS, Rustgi AK. The role of the miR-200 family in epithelial-mesenchymal transition. Cancer Biol Ther. 2010 Aug 1;10(3):219–22.

238. Terry S, Savagner P, Ortiz-Cuaran S, Mahjoubi L, Saintigny P, Thiery J, et al. New insights into the role of EMT in tumor immune escape. Mol Oncol. 2017 Jul;11(7):824–46.

239. Jung AR, Jung CH, Noh JK, Lee YC, Eun YG. Epithelial-mesenchymal transition gene signature is associated with prognosis and tumor microenvironment in head and neck squamous cell carcinoma. Sci Rep. 2020 Feb 27;10(1):3652.

240. Wang G, Xu D, Zhang Z, Li X, Shi J, Sun J, et al. The pan-cancer landscape of crosstalk between epithelial-mesenchymal transition and immune evasion relevant to prognosis and immunotherapy response. npj Precis Onc. 2021 Jun 22;5(1):1–10.

241. Datar I, Schalper KA. Epithelial–Mesenchymal Transition and Immune Evasion during Lung Cancer Progression: The Chicken or the Egg? Clin Cancer Res. 2016 Jul 15;22(14):3422–4.

242. Mahmoudian RA, Mozhgani S, Abbaszadegan MR, Mokhlessi L, Montazer M, Gholamin M. Correlation between the immune checkpoints and EMT genes proposes potential prognostic and therapeutic targets in ESCC. J Mol Histol. 2021 Jun;52(3):597–609.

243. Shadbad MA, Asadzadeh Z, Derakhshani A, Hosseinkhani N, Mokhtarzadeh A, Baghbanzadeh A, et al. A scoping review on the potentiality of PD-L1-inhibiting microRNAs in treating colorectal cancer: Toward single-cell sequencing-guided biocompatible-based delivery. Biomed Pharmacother. 2021 Nov;143:112213.

244. Jo H, Shim K, Jeoung D. Potential of the miR-200 Family as a Target for Developing Anti-Cancer Therapeutics. Int J Mol Sci. 2022 May 24;23(11):5881.

245. Nam DY, Rhee JK. Identifying microRNAs associated with tumor immunotherapy response using an interpretable machine learning model. Sci Rep. 2024 Mar 14;14(1):6172.

246. Lv J, Guo T, Qu X, Che X, Li C, Wang S, et al. PD-L1 Under Regulation of miR-429 Influences the Sensitivity of Gastric Cancer Cells to TRAIL by Binding of EGFR. Front Oncol. 2020;10:1067.

247. Mu L, Wang Y, Su H, Lin Y, Sui W, Yu X, et al. HIF1A-AS2 Promotes the Proliferation and Metastasis of Gastric Cancer Cells Through miR-429/PD-L1 Axis. Dig Dis Sci. 2021 Dec;66(12):4314–25.

248. Wei S, Wang K, Huang X, Zhao Z, Zhao Z. LncRNA MALAT1 contributes to non-small cell lung cancer progression via modulating miR-200a-3p/programmed death-ligand 1 axis. Int J Immunopathol Pharmacol. 2019;33:2058738419859699.

249. Fischer C, Deutsch TM, Feisst M, Rippinger N, Riedel F, Hartkopf AD, et al. Circulating miR-200 family as predictive markers during systemic therapy of metastatic breast cancer. Arch Gynecol Obstet. 2022 Sep 1;306(3):875–85.

250. Shen L, Chen G, Xia Q, Shao S, Fang H. Exosomal miR-200 family as serum biomarkers for early detection and prognostic prediction of cholangiocarcinoma. Int J Clin Exp Pathol. 2019;12(10):3870–6.

251. Choi PW, Bahrampour A, Ng SK, Liu SK, Qiu W, Xie F, et al. Characterization of miR-200 family members as blood biomarkers for human and laying hen ovarian cancer. Sci Rep. 2020 Nov 18;10(1):20071.

252. Fontana A, Barbano R, Dama E, Pasculli B, Rendina M, Morritti MG, et al. Combined analysis of miR-200 family and its significance for breast cancer. Sci Rep. 2021 Feb 3;11(1):2980.

253. Kang E, Jung SC, Nam SK, Park Y, Seo SH, Park KU, et al. Tissue miR-200c-3p and circulating miR-1290 as potential prognostic biomarkers for colorectal cancer. Sci Rep. 2022 Feb 10;12(1):2295.

254. Brabletz S, Brabletz T. The ZEB/miR-200 feedback loop—a motor of cellular plasticity in development and cancer? EMBO reports. 2010 Sep;11(9):670–7.

255. Burk U, Schubert J, Wellner U, Schmalhofer O, Vincan E, Spaderna S, et al. A reciprocal repression between ZEB1 and members of the miR-200 family promotes EMT and invasion in cancer cells. EMBO reports. 2008 Jun;9(6):582–9.

256. Anastasiadou E, Messina E, Sanavia T, Mundo L, Farinella F, Lazzi S, et al. MiR-200c-3p Contrasts PD-L1 Induction by Combinatorial Therapies and Slows Proliferation of Epithelial Ovarian Cancer through Downregulation of β-Catenin and c-Myc. Cells. 2021 Mar 1;10(3):519.

257. Humphries B, Yang C. The microRNA-200 family: small molecules with novel roles in cancer development, progression and therapy. Oncotarget. 2015 Jan 30;6(9):6472–98.

258. Briskin D, Wang PY, Bartel DP. The biochemical basis for the cooperative action of microRNAs. Proceedings of the National Academy of Sciences. 2020 Jul 28;117(30):17764–74.

259. Zhou X, Wang Y, Shan B, Han J, Zhu H, Lv Y, et al. The downregulation of miR-200c/141 promotes ZEB1/2 expression and gastric cancer progression. Med Oncol. 2014 Dec 12;32(1):428.

260. Hu W, Coller J. What comes first: translational repression or mRNA degradation? The deepening mystery of microRNA function. Cell Res. 2012 Sep;22(9):1322–4.

261. Fabian MR, Sonenberg N. The mechanics of miRNA-mediated gene silencing: a look under the hood of miRISC. Nat Struct Mol Biol. 2012 Jun;19(6):586–93.

262. Oomizu S, Arikawa T, Niki T, Kadowaki T, Ueno M, Nishi N, et al. Cell surface galectin-9 expressing Th cells regulate Th17 and Foxp3+ Treg development by galectin-9 secretion. PLoS One. 2012;7(11):e48574.

263. Na YJ, Kim JH. Understanding cooperativity of microRNAs via microRNA association networks. BMC Genomics. 2013 Oct 16;14(Suppl 5):S17.

264. Bracken CP, Scott HS, Goodall GJ. A network-biology perspective of microRNA function and dysfunction in cancer. Nat Rev Genet. 2016 Dec;17(12):719–32.

265. Jorge AL, Pereira ER, de Oliveira CS, Ferreira E dos S, Menon ETN, Diniz SN, et al. MicroRNAs: understanding their role in gene expression and cancer. Einstein (Sao Paulo). 19:eRB5996.

266. Prelich G. Gene Overexpression: Uses, Mechanisms, and Interpretation. Genetics. 2012 Mar;190(3):841–54.

267. Gibson TJ, Seiler M, Veitia RA. The transience of transient overexpression. Nat Methods. 2013 Aug;10(8):715–21.

268. Anastasiadou E, Ceccarelli S, Messina E, Gerini G, Megiorni F, Pontecorvi P, et al. MiR-200c-3p maintains stemness and proliferative potential in adipose-derived stem cells by counteracting senescence mechanisms. PLoS One. 2021;16(9):e0257070.

269. Pyzer AR, Stroopinsky D, Rosenblatt J, Anastasiadou E, Rajabi H, Washington A, et al. MUC1 inhibition leads to decrease in PD-L1 levels via upregulation of miRNAs. Leukemia. 2017 Dec;31(12):2780–90.

270. Wang Z. The guideline of the design and validation of MiRNA mimics. Methods Mol Biol. 2011;676:211–23.

271. Fabbri M, Paone A, Calore F, Galli R, Croce CM. A new role for microRNAs, as ligands of Toll-like receptors. RNA Biology. 2013 Feb;10(2):169–74.

272. Fabbri M. MicroRNAs and miRceptors: a new mechanism of action for intercellular communication. Philos Trans R Soc Lond B Biol Sci. 2018 Jan 5;373(1737):20160486.

273. Goldgraben MA, Russell R, Rueda OM, Caldas C, Git A. Double-stranded microRNA mimics can induce length- and passenger strand-dependent effects in a cell type-specific manner. RNA. 2016 Feb;22(2):193–203.

274. Søkilde R, Newie I, Persson H, Borg Å, Rovira C. Passenger strand loading in overexpression experiments using microRNA mimics. RNA Biology. 2015 Aug 3;12(8):787–91.

275. Thomson DW, Bracken CP, Szubert JM, Goodall GJ. On Measuring miRNAs after Transient Transfection of Mimics or Antisense Inhibitors. PLoS One. 2013 Jan 24;8(1):e55214.

276. Jin HY, Gonzalez-Martin A, Miletic AV, Lai M, Knight S, Sabouri-Ghomi M, et al. Transfection of microRNA Mimics Should Be Used with Caution. Front Genet. 2015;6:340.

277. Kim T, Croce CM. MicroRNA: trends in clinical trials of cancer diagnosis and therapy strategies. Exp Mol Med. 2023 Jul;55(7):1314–21.

278. Ling H, Fabbri M, Calin GA. MicroRNAs and other non-coding RNAs as targets for anticancer drug development. Nat Rev Drug Discov. 2013 Nov;12(11):847–65.

279. Hong DS, Kang YK, Borad M, Sachdev J, Ejadi S, Lim HY, et al. Phase 1 study of MRX34, a liposomal miR-34a mimic, in patients with advanced solid tumours. Br J Cancer. 2020 May;122(11):1630–7.

280. Zhang S, Cheng Z, Wang Y, Han T. The Risks of miRNA Therapeutics: In a Drug Target Perspective. Drug Des Devel Ther. 2021;15:721–33.

281. Chakraborty C, Sharma AR, Sharma G, Lee SS. Therapeutic advances of miRNAs: A preclinical and clinical update. J Adv Res. 2021 Feb;28:127–38.

282. Hanna J, Hossain GS, Kocerha J. The Potential for microRNA Therapeutics and Clinical Research. Front Genet. 2019;10:478.

283. Man SM, Kanneganti TD. Innate immune sensing of cell death in disease and therapeutics. Nat Cell Biol. 2024 Sep 2;1–14.

284. Choudhury SM, Sarkar R, Karki R, Kanneganti TD. A comparative study of apoptosis, pyroptosis, necroptosis, and PANoptosis components in mouse and human cells. PLOS ONE. 2024 Feb 27;19(2):e0299577.

285. Rock KL, Kono H. The Inflammatory Response to Cell Death. Annual Review of Pathology: Mechanisms of Disease. 2008 Feb 28;3(Volume 3, 2008):99–126.

286. Schwartzman RA, Cidlowski JA. Apoptosis: The Biochemistry and Molecular Biology of Programmed Cell Death*. Endocrine Reviews. 1993 Apr 1;14(2):133–51.

287. Salvesen GS, Riedl SJ. Caspase mechanisms. Adv Exp Med Biol. 2008;615:13–23.

288. Yu P, Zhang X, Liu N, Tang L, Peng C, Chen X. Pyroptosis: mechanisms and diseases. Sig Transduct Target Ther. 2021 Mar 29;6(1):1–21.

289. Man SM, Karki R, Kanneganti TD. Molecular mechanisms and functions of pyroptosis, inflammatory caspases and inflammasomes in infectious diseases. Immunological Reviews. 2017 May;277(1):61–75.

290. Bertheloot D, Latz E, Franklin BS. Necroptosis, pyroptosis and apoptosis: an intricate game of cell death. Cell Mol Immunol. 2021 May;18(5):1106–21.

291. Choi ME, Price DR, Ryter SW, Choi AMK. Necroptosis: a crucial pathogenic mediator of human disease. JCI Insight. 2019 Aug 8;4(15):e128834, 128834.

292. Martens S, Bridelance J, Roelandt R, Vandenabeele P, Takahashi N. MLKL in cancer: more than a necroptosis regulator. Cell Death Differ. 2021 Jun;28(6):1757–72.

293. Christgen S, Zheng M, Kesavardhana S, Karki R, Malireddi RKS, Banoth B, et al. Identification of the PANoptosome: A Molecular Platform Triggering Pyroptosis, Apoptosis, and Necroptosis (PANoptosis). Front Cell Infect Microbiol. 2020;10:237.

294. Pandeya A, Kanneganti TD. Therapeutic potential of PANoptosis: innate sensors, inflammasomes, and RIPKs in PANoptosomes. Trends in Molecular Medicine. 2024 Jan 1;30(1):74–88.

295. Rogers C, Fernandes-Alnemri T, Mayes L, Alnemri D, Cingolani G, Alnemri ES. Cleavage of DFNA5 by caspase-3 during apoptosis mediates progression to secondary necrotic/pyroptotic cell death. Nat Commun. 2017 Jan 3;8(1):14128.

296. Wang Y, Gao W, Shi X, Ding J, Liu W, He H, et al. Chemotherapy drugs induce pyroptosis through caspase-3 cleavage of a gasdermin. Nature. 2017 Jul;547(7661):99–103.

297. Han JH, Karki R, Malireddi RKS, Mall R, Sarkar R, Sharma BR, et al. NINJ1 mediates inflammatory cell death, PANoptosis, and lethality during infection conditions and heat stress. Nat Commun. 2024 Feb 26;15(1):1739.

298. Miyake T, Kumagai Y, Kato H, Guo Z, Matsushita K, Satoh T, et al. Poly I:C-induced activation of NK cells by CD8 alpha+ dendritic cells via the IPS-1 and TRIF-dependent pathways. J Immunol. 2009 Aug 15;183(4):2522–8.

299. Dauletbaev N, Cammisano M, Herscovitch K, Lands LC. Stimulation of the RIG-I/MAVS Pathway by Polyinosinic:Polycytidylic Acid Upregulates IFN-β in Airway Epithelial Cells with Minimal Costimulation of IL-8. J Immunol. 2015 Sep 15;195(6):2829–41.

300. Lim CS, Jang YH, Lee GY, Han GM, Jeong HJ, Kim JW, et al. TLR3 forms a highly organized cluster when bound to a poly(I:C) RNA ligand. Nat Commun. 2022 Nov 12;13(1):6876.

301. Palchetti S, Starace D, De Cesaris P, Filippini A, Ziparo E, Riccioli A. Transfected poly(I:C) activates different dsRNA receptors, leading to apoptosis or immunoadjuvant response in androgen-independent prostate cancer cells. J Biol Chem. 2015 Feb 27;290(9):5470–83.

302. Nellimarla S, Mossman KL. Extracellular dsRNA: Its Function and Mechanism of Cellular Uptake. Journal of Interferon & Cytokine Research. 2014 Jun;34(6):419–26.

303. Itoh K, Watanabe A, Funami K, Seya T, Matsumoto M. The clathrin-mediated endocytic pathway participates in dsRNA-induced IFN-beta production. J Immunol. 2008 Oct 15;181(8):5522–9.

304. Dansako H, Yamane D, Welsch C, McGivern DR, Hu F, Kato N, et al. Class A scavenger receptor 1 (MSR1) restricts hepatitis C virus replication by mediating toll-like receptor 3 recognition of viral RNAs produced in neighboring cells. PLoS Pathog. 2013;9(5):e1003345.

305. DeWitte-Orr SJ, Collins SE, Bauer CMT, Bowdish DM, Mossman KL. An accessory to the “Trinity”: SR-As are essential pathogen sensors of extracellular dsRNA, mediating entry and leading to subsequent type I IFN responses. PLoS Pathog. 2010 Mar 26;6(3):e1000829.

306. Watanabe A, Tatematsu M, Saeki K, Shibata S, Shime H, Yoshimura A, et al. Raftlin is involved in the nucleocapture complex to induce poly(I:C)-mediated TLR3 activation. J Biol Chem. 2011 Mar 25;286(12):10702–11.

307. Nguyen TA, Smith BRC, Tate MD, Belz GT, Barrios MH, Elgass KD, et al. SIDT2 transports extracellular dsRNA into the cytoplasm for innate immune recognition. Immunity. 2017 Sep 9;47(3):498.

308. Sultan H, Wu J, Fesenkova VI, Fan AE, Addis D, Salazar AM, et al. Poly-IC enhances the effectiveness of cancer immunotherapy by promoting T cell tumor infiltration. J Immunother Cancer. 2020 Sep;8(2):e001224.

309. Anfray C, Mainini F, Digifico E, Maeda A, Sironi M, Erreni M, et al. Intratumoral combination therapy with poly(I:C) and resiquimod synergistically triggers tumor-associated macrophages for effective systemic antitumoral immunity. J Immunother Cancer. 2021 Sep;9(9):e002408.

310. De Waele J, Verhezen T, van der Heijden S, Berneman ZN, Peeters M, Lardon F, et al. A systematic review on poly(I:C) and poly-ICLC in glioblastoma: adjuvants coordinating the unlocking of immunotherapy. J Exp Clin Cancer Res. 2021 Jun 25;40:213.

311. Silginer M, Nagy S, Happold C, Schneider H, Weller M, Roth P. Autocrine activation of the IFN signaling pathway may promote immune escape in glioblastoma. Neuro-Oncology. 2017 Oct 1;19(10):1338–49.

312. Garcia-Diaz A, Shin DS, Moreno BH, Saco J, Escuin-Ordinas H, Rodriguez GA, et al. Interferon Receptor Signaling Pathways Regulating PD-L1 and PD-L2 Expression. Cell Rep. 2017 May 9;19(6):1189–201.

313. Benci JL, Xu B, Qiu Y, Wu TJ, Dada H, Twyman-Saint Victor C, et al. Tumor Interferon Signaling Regulates a Multigenic Resistance Program to Immune Checkpoint Blockade. Cell. 2016 Dec 1;167(6):1540-1554.e12.

314. Zak J, Pratumchai I, Marro BS, Marquardt KL, Zavareh RB, Lairson LL, et al. JAK inhibition enhances checkpoint blockade immunotherapy in patients with Hodgkin lymphoma. Science. 2024 Jun 21;384(6702):eade8520.

315. Mathew D, Marmarelis ME, Foley C, Bauml JM, Ye D, Ghinnagow R, et al. Combined JAK inhibition and PD-1 immunotherapy for non-small cell lung cancer patients. Science. 2024 Jun 21;384(6702):eadf1329.

316. Sistigu A, Yamazaki T, Vacchelli E, Chaba K, Enot DP, Adam J, et al. Cancer cell–autonomous contribution of type I interferon signaling to the efficacy of chemotherapy. Nat Med. 2014 Nov;20(11):1301–9.

317. Choi H, Kwon J, Cho MS, Sun Y, Zheng X, Wang J, et al. Targeting DDX3X Triggers Antitumor Immunity via a dsRNA-Mediated Tumor-Intrinsic Type I Interferon Response. Cancer Res. 2021 Jul 1;81(13):3607–20.

318. Sheng W, LaFleur MW, Nguyen TH, Chen S, Chakravarthy A, Conway JR, et al. LSD1 Ablation Stimulates Anti-tumor Immunity and Enables Checkpoint Blockade. Cell. 2018 Jul 26;174(3):549-563.e19.

319. Guirguis AA, Ofir-Rosenfeld Y, Knezevic K, Blackaby W, Hardick D, Chan YC, et al. Inhibition of METTL3 Results in a Cell-Intrinsic Interferon Response That Enhances Antitumor Immunity. Cancer Discovery. 2023 Oct 5;13(10):2228–47.

320. Brichkina A, Suezov R, Huber M. Methyltransferase-like 3 (METTL3) inhibition potentiates anti-tumor immunity: a novel strategy for improving anti-PD1 therapy. Sig Transduct Target Ther. 2023 Dec 11;8(1):1–2.

321. Sordo-Bahamonde C, Lorenzo-Herrero S, Gonzalez-Rodriguez AP, Martínez-Pérez A, Rodrigo JP, García-Pedrero JM, et al. Chemo-Immunotherapy: A New Trend in Cancer Treatment. Cancers (Basel). 2023 May 25;15(11):2912.

322. Mezencev R. Interactions of cisplatin with non-DNA targets and their influence on anticancer activity and drug toxicity: the complex world of the platinum complex. Curr Cancer Drug Targets. 2015;14(9):794–816.

323. Rose F, Köberle B, Honnen S, Bay C, Burhenne J, Weiss J, et al. RNA is a pro-apoptotic target of cisplatin in cancer cell lines and *C. elegans*. Biomedicine & Pharmacotherapy. 2024 Apr 1;173:116450.

324. Yang T, Wang G, Zhang M, Hu X, Li Q, Yun F, et al. Triggering endogenous Z-RNA sensing for anti-tumor therapy through ZBP1-dependent necroptosis. Cell Rep. 2023 Nov 28;42(11):113377.

325. Doke T, Mukherjee S, Mukhi D, Dhillon P, Abedini A, Davis JG, et al. NAD+ precursor supplementation prevents mtRNA/RIG-I-dependent inflammation during kidney injury. Nat Metab. 2023 Mar;5(3):414–30.

326. Zeng TM, Pan YF, Yuan ZG, Chen DS, Song YJ, Gao Y. Immune-related RNA signature predicts outcome of PD-1 inhibitor-combined GEMCIS therapy in advanced intrahepatic cholangiocarcinoma. Front Immunol. 2022;13:943066.

327. Chen J, Amoozgar Z, Liu X, Aoki S, Liu Z, Shin SM, et al. Reprogramming the Intrahepatic Cholangiocarcinoma Immune Microenvironment by Chemotherapy and CTLA-4 Blockade Enhances Anti–PD-1 Therapy. Cancer Immunology Research. 2024 Apr 2;12(4):400–12.

328. Wang J, Liu Q, Zhao Y, Fu J, Su J. Tumor Cells Transmit Drug Resistance via Cisplatin-Induced Extracellular Vesicles. Int J Mol Sci. 2023 Aug 2;24(15):12347.

329. Ogawa T, Ono K, Ryumon S, Kawai H, Nakamura T, Umemori K, et al. Novel mechanism of cisplatin resistance in head and neck squamous cell carcinoma involving extracellular vesicles and a copper transporter system. Head & Neck. 2024;46(3):636–50.

330. Samuel P, Mulcahy LA, Furlong F, McCarthy HO, Brooks SA, Fabbri M, et al. Cisplatin induces the release of extracellular vesicles from ovarian cancer cells that can induce invasiveness and drug resistance in bystander cells. Philos Trans R Soc Lond B Biol Sci. 2018 Jan 5;373(1737):20170065.

331. Liu Y, Gu Y, Cao X. The exosomes in tumor immunity. OncoImmunology. 2015 Sep 2;4(9):e1027472.

332. Beninson LA, Fleshner M. Exosomes: an emerging factor in stress-induced immunomodulation. Semin Immunol. 2014 Oct;26(5):394–401.

333. Gobbo J, Marcion G, Cordonnier M, Dias AMM, Pernet N, Hammann A, et al. Restoring Anticancer Immune Response by Targeting Tumor-Derived Exosomes With a HSP70 Peptide Aptamer. J Natl Cancer Inst. 2016 Mar;108(3).

334. Daßler-Plenker J, Reiners KS, van den Boorn JG, Hansen HP, Putschli B, Barnert S, et al. RIG-I activation induces the release of extracellular vesicles with antitumor activity. Oncoimmunology. 2016;5(10):e1219827.

335. Brägelmann J, Lorenz C, Borchmann S, Nishii K, Wegner J, Meder L, et al. MAPK-pathway inhibition mediates inflammatory reprogramming and sensitizes tumors to targeted activation of innate immunity sensor RIG-I. Nat Commun. 2021 Sep 17;12(1):5505.

336. Zhang Y, Zeng L, Wang M, Yang Z, Zhang H, Gao L, et al. RIG-I promotes immune evasion of colon cancer by modulating PD-L1 ubiquitination. J Immunother Cancer. 2023 Sep;11(9):e007313.